TRANSACTIONS

THE FOURTH INTERNATIONAL SYMPOSIUM ON
SOIL WATER MEASUREMENT USING
CAPACITANCE, IMPEDANCE AND TIME DOMAIN TRANSMISSION

MONTREAL, QUEBEC, CANADA

JULY 16 – 18, 2014

IOAN C. PALTINEANU, PH. D., - EDITOR

PALTIN INTERNATIONAL INC., WWW.PALTIN.COM

LAUREL, MARYLAND, USA

TRANSACTIONS

THE FOURTH INTERNATIONAL SYMPOSIUM ON SOIL WATER MEASUREMENT USING CAPACITANCE, IMPEDANCE AND TIME DOMAIN TRANSMISSION

MONTREAL, QUEBEC, CANADA

JULY 16 – 18, 2014

IOAN C. PALTINEANU, PH. D., - EDITOR

PALTIN INTERNATIONAL INC., WWW.PALTIN.COM

ISBN – 10: 0982796935

ISBN – 13: 978-0-9827969-3-1

PRINTED IN THE UNITED STATES OF AMERICA

LAUREL, MARYLAND, USA

EDITORIAL COMMITTEE

INTERNATIONAL AND LOCAL ORGANIZING COMMITTEES

INTERNATIONAL ORGANIZING COMMITTEE

Dr. Ioan C. Paltineanu
President
Paltin International Inc.
Laurel, Maryland, USA
ioan@paltin.com

Dr. Chandra A. Madramootoo
Professor and Dean
Faculty of Agricultural and Environmental Sciences
McGill University
Macdonald Campus
Sainte-Anne-de-Bellevue QC, Canada
chandra.madramootoo@mcgill.ca

Dr. James E. Ayars
Research Agricultural Engineer
Water Management Research Laboratory
USDA-ARS, Parlier, California, USA
James.Ayars@ARS.USDA.GOV

Dr. Vaclav Kuraz
Associate Professor
Faculty of Civil Engineering
Department of Irrigation, Drainage and Landscape
Czech Technical University, Prague, Czech Republic
kuraz@fsv.cvut.cz

Dr. Juan Vera Munoz
Scientist
Spanish Council Research
CEBAS - CSIC
Department of Irrigation
Campus Universitario
Espinando, Murcia, Spain
jvera@cebas.csic.es

Dr. Jeffrey E. Campbell
Senior Vice President
Sensor Development

UgMO Technologies
King of Prussia, PA, USA
jcampbell@ugmo.com

Dr. Ole Wendroth
Professor of Soil Physics
Department of Plant and Soil Sciences
College of Agriculture
University of Kentucky
Lexington, KY, USA
owendroth@uky.edu

Dr. Shiv Prasher
James McGill Professor and Chair
Department of Bioresource Engineering
McGill University
Macdonald Campus
Anne de Bellevue QC, Canada
shiv.prasher@mcgill.ca

Dr. Ali Madani
Affiliate Member
McGill University
Retired Professor
Faculty of Agriculture (NSAC)
Dalhousie University
Orleans, ON, Canada
amadani49@gmail.com

Mr. Eduardo Ganem Cuenca
McGill University
Project Manager
Faculty of Agricultural Engineering
Sainte-Anne-de-Bellevue, Quebec, Canada
eduardo.ganemcuenca@mcgill.ca

LOCAL ORGANIZING COMMITTEE:

Dr. Chandra A. Madramootoo (co-Chair)
James McGill Professor and Dean
Faculty of Agricultural and Environmental Sciences
McGill University
Macdonald Campus
Sainte-Anne-de-Bellevue
Quebec, Canada
chandra.madramootoo@mcgill.ca

Mr. Eduardo Ganem Cuenca (co-Chair)
Project Manager
McGill University
Faculty of Agricultural and Environmental Sciences
Sainte-Anne-de-Bellevue, Quebec, Canada
eduardo.ganemcuenca@mcgill.ca

Dr. Viacheslav Adamchuk
Associate Professor
Department of Bioresource Engineering
Faculty of Agricultural and Environmental Sciences
McGill University
Sainte-Anne-de-Bellevue, Quebec, Canada
viacheslav.adamchuk@mcgill.ca

Mr. Peter Enright
Director
Farm Management and Technology Program
McGill University
Faculty of Agricultural Engineering
Sainte-Anne-de-Bellevue
Quebec, Canada
peter.enright@mcgill.ca

SPONSORS

Symposium – 2014 is
endorsed by the ASABE

www.paltin.com

www.mcgill.ca/macdonald

www.irrometer.com

www.sentek.com.au

www.stevenswater.com

www.campbellsci.ca

www.decagon.com

www.specmeters.com

www.aquachecktech.com

www.geneq.com

TABLE OF CONTENTS

STATE of THE ART:

1.1 **"On the Importance of International Standardization of Methodologies and Techniques for Laboratory and Field Calibration of Soil Water Measurement Sensors Based on Capacitance, Impedance, and TDT"**

Ioan C. Paltineanu, PALTIN International Inc., Laurel, Maryland, USA, icpaltin@msn.com

1.2 **"Comparison of SMOS Level 2 and Level 3 Soil Moisture at the SMOSREX Site"**

Arnaud Mialon (1), F. Cabot (1), S. Guibert (2), A. Al bitar (1), P. Richaume(1), J.-P. Wigneron (3), T. Pellarin (4), S. Tarot (5), S. Bircher (1), J. Grant (6), Nemesio Rodriguez-Fernandez (1), Y. H. Kerr (1).
arnaud.mialon@cesbio.cnes.fr
1. CESBIO, 18 Av. Edouard Belin, BPI 2801, 31401 Toulouse, Cedex 9, France.
2. CNES, Av. Edouard Belin, 31401 Toulouse, France.
3. INRA EPHYSE, Bordeaux, France.
4. LTHE, Grenoble, France.
5. IFREMER, Brest, France.
6. Department of Physical Geography and Ecosystem Science, University of Lund, Sweden.

1.3 **"Soil Moisture and Dielectric Constant Measurements of Organic Soils in the Higher Northern Latitudes in Support of the SMOS Mission"**

Simone Bircher*(1), S. Razafindratsima (2) , F. Demontoux (2), M. Andreasen (3) , J. Vuollet (4), K. Rautiainen (4), F. Jonard (5), L. Weihermüller (5), P. Richaume (1) , A. Mialon (1), J.-P. Wigneron (6), Y. H. Kerr (1).
1. Centre d'Etudes Spatiales de la Biosphère, Toulouse, France.
2. Laboratoire de l'Intégration du Matériau au Système, Bordeaux University, Bordeaux, France.
3. Department of Geosciences and Natural Resource Management, University of Copenhagen, Denmark.
4. Finnish Meteorological Institute, Helsinki, Finland.
5. Institute of Bio- and Geosciences Agrosphere (IBG-3), Forschungszentrum Jülich GmbH, Germany.
6. Division Ecologie fonctionnelle et Physique de l'Environnement, INRA, Bordeaux-Aquitaine, France.
* Corresponding author: simone.bircher@cesbio.cnes.fr

APPLICATIONS:

2.1 "**Dynamic Visualization of Real-time Wetting Fronts in Soils Using Multi-sensor Capacitance Probe Arrays"**

Dalton, M.(1), Buss, P.(2), Stevens, S.(3) & Fuentes, S.(4)
(1,2 & 3) Sentek Pty. Ltd., South Australia, 5069, mdalton@sentek.com.au
(4) Dept. Agriculture and Food Systems, University of Melbourne, Victoria, 3010, Australia, sfuentes@unimelb.edu.au

POSTERS:

PARTICIPANTS:

TRANSACTIONS OF THE FOURTH INTERNATIONAL SYMPOSIUM ON SOIL WATER
MEASUREMENT USING CAPACITANCE, IMPEDANCE AND TDT
MONTREAL, CANADA, JULY 16 – 18, 2014

STATE OF THE ART, PAPER 1.1

On the Importance of International Standardization of Methodologies and Techniques for Laboratory and Field Calibration of Soil Water Measurement Sensors Based on Capacitance, Impedance, and TDT

Ioan C. Paltineanu, PALTIN International Inc., Laurel, Maryland, USA, icpaltin@msn.com

ABSTRACT

Most technologies evolve, normally, from their ‘infancy’ and ‘adolescence’ stages, toward ‘maturity’ and ‘fruition’. Technologies for designing, testing, manufacturing and promoting of real-time soil water measurement sensors based on capacitance, impedance and time domain transmission (TDT) make no exceptions to the general accepted trends. One of the most important facets of technological and research development trajectory, in a globalized world, is standardization of methodologies and techniques for both the manufacturers “bench testing” techniques, and for the more elaborate, independent, laboratory and field calibration methodologies of soil water measurement sensors in more diverse, but very well described conditions. This paper will introduce a global review and critique of past and current methods and techniques for direct correlations of sensors outputs to known dielectric constants of specific liquids, as well as correlations between apparent dielectric constant of soil matrix vs. volumetric water content determined experimentally in the main zone of influence of electromagnetic fields generated by sensors operating at different frequencies. Published and unpublished experimental data will be used to show the similarities and differences between some well known soil water measurement sensors and probes based on capacitance, impedance and TDT. A minimum of experimental protocols describing sensors and test requirements, as well as statistical analysis and interpretation, will be proposed such as: frequencies of operation; response of sensors in air and distilled water at room temperature (~22 deg. C); soil intrinsic characteristics (texture, clay mineralogy, EC, organic material, gravel content, etc..); method and uniformity of soil packing (dry and wet bulk density); axial and radial sensitivity of sensors in distilled water, in air – water and in air – soil interfaces, as well as in soil at different depths; rotational orientation response of cylindrical sensors inside access tubes; sensors response in controlled levels of temperature in air, water, and soil; sensors response at different soil EC and temperature conditions; scaled output(frequency, voltage, etc..) vs. volumetric water content; description of specific liquids of known dielectric constant, etc..

Keywords**:** soil water sensors, capacitance, impedance, TDT, calibration methods, standardization

INTRODUCTION

Real-time soil water profile measurement as well as data transmission over large areas at affordable prices has been made possible by using fundamental principles of electro-magnetism (EM) in an evolving world of basic electronics. Early laboratory studies on electrical properties of soil for alternating currents at radio frequencies were reported by Smith-Rose (1933, 1935) as well as by Aleksandrov (1935, 1936) and Petrovskii (1937), both cited by Chernyak (1964) in his book on “Dielectric methods for investigating moist soils”. In situ measurement of moisture in soil by ‘fringe capacitance’ using a bridge method, at operating frequency of 30 MHz, was reported by Thomas (1966). A ‘resonance – capacitance’ meter, with cylindrical type electrodes, was introduced by Kuraz et al., (1970), followed by reports on further testing presented by Kuraz et al, (1977) and Kuraz (1982).

New developments in electronics of the late 1980s as well as during the 1990s determined an increase in innovations originated by the private industry, and/or by various research institutions. Based on others previous experiences using capacitance based sensors at low frequencies, Dean et al., (1987) introduced the design and laboratory calibration of an improved, portable, capacitance probe (cylindrical sensors), operating at 150 MHz, for soil water profile measurement inside the pre-installed PVC access tubes. Also, Bell et al., (1987) presented the field techniques for installation, evaluation and field calibration of the same sensor. Experiments involving a commercial portable capacitance probe with a pair of cylindrical electrodes, operating at 50 MHz (Sentry 200AP), conducted in air, in water, and in a repacked soil model, were reported by Paltineanu et al., (1993) and by Mead et al., (1994), showing the importance of testing the axial and radial influence of a particular capacitance probe in controlled conditions before calibrating it directly in field conditions. A soil water profile monitoring system involving multi-sensor capacitance probes (pair of cylindrical electrodes/each sensor) semi-permanently installed in specific PVC access tubes at designed 10 cm incremental soil depths as well as probes being connected by underground wires to a central data acquisition logger and having the possibility of analyzing and interpreting the volumetric soil water profile dynamics directly in the field for irrigation scheduling decision making was introduced by Buss (1993).

A laboratory calibration of the commercial EnviroSCAN multisensor capacitance probe (three pairs of cylindrical electrodes operating at ~150 MHz) performed under controlled laboratory conditions in air, in water, and in an uniformly repacked Mattapex silt loam soil in a plywood box using a hydraulic press, and allowed the collection of five undisturbed core replicates taken at 2.5 mm distance from the PVC access tube around each capacitance sensor, was reported by Paltineanu and Starr (1997). Their experimental results showed: the extent of axial and radial sensitivity; the air and water temperature effects; and a highly significant, nonlinear, positive relationship between the soil volumetric water content (Θv) versus the dimensionless scaled frequency (SF). The authors made specific recommendations for EnviroSCAN multisensor capacitance probe to be further calibrated on special soils (eg., swelling 2:1 clays, high organic content soils) or for extreme soil temperature conditions. Data on the laboratory calibration of a commercial EnviroSCAN probe using different techniques (repacked soil columns), different soil texture soils (sandy to clay), imposed EC and temperature variations had been reported by Mead et al., (1995). Experimenting in large weighing soil columns, repacked with Olton and Pullman type soils (containing dominant 2:1 clay minerals, montmorillonite – smectite), Baumhardt et al., (2000) and Evett et al., (2006), revealed the possible impact of clay mineralogy on the relationship between the soil volumetric water content and the scaled frequency response of both EnviroSCAN and Diviner2000 commercial produced capacitance based sensors. Other laboratory calibration studies of commercial EnviroSCAN capacitance probe, conducted in plastic boxes with repacked soil (Typic Calciserept, silty clay loam texture, 2:1 clay mineral composition of 70-80% Illites and 10-20% smectites), at fixed bulk densities and varying soil volumetric water content, were reported by Gabriel et al., (2010), and Quemada et al., (2010). Initial field calibration studies on capacitance based sensors (Sentry 200AP, EnviroSCAN, Diviner2000, etc..) obtained by not knowing the intrinsic characteristics of each sensor (because of either protected and/or the lack of proper manufacturer's information as well as by using inadequate techniques for PVC access tube's installation in the field), along with the ill advised direct comparisons (ex. neutron thermalization method for soil water content vs. EM methods), generally yielded mixed and/or conflicting experimental results.

The introduction, in the last 10 – 15 years, of individual type sensors based on capacitance, impedance and TDT, designed by incorporating in one single unit both the electronics (head) and the electrodes (one plus more surrounding parallel rods or fork types, 5 – 10 cm long), for measuring soil water/ EC/ temperature, operating at one or two different frequencies, and reasonably priced, have opened a new window of opportunity for large scale research and application studies. Multi - parameter (soil water/EC/temperature) sensors based on measurement of complex impedance, using parallel metal electrodes and operating at fixed frequencies up to 50 MHz, were introduced by: Campbell (1990, 1995); Atkins et al., (1998); and Hilhorst (1998). The measurement of soil water content using "a simplified impedance measuring technique" was reported by Gaskin and Miller (1996), and a commercial soil water measurement impedance probe, with multi parallel rod type metal electrodes, operating at 100 MHz, was reported by Miller and Gaskin (1998).

Recent introduction of the so called low-cost, fork type (bi, or trifurcate) sensors, based on capacitance, and operating at 70 MHz frequency, increased the opportunity of developing large scale studies associated with wireless network applications. At the same time, their rapid introduction on large scale projects raised the awareness of the sensor - to - sensor variability and accuracy, as well as the importance of top bench testing in standard dielectric and of specific laboratory calibration on different soil type intrinsic characteristics: Rosenbaum et al., (2010), Bogena et al.,(2007). Individual, multi parameter (soil water/EC/ temperature) sensors based on Time Domain Transmission (TDT) method and techniques incorporating both the electronics (head) and the parallel wires loops for transmitting broad band (from 100 MHz to 1-2 GHz) frequencies and using digital interpretation of TDR signals have been introduced by Anderson (2003) and Anderson (2004). Generally, the usefulness of all TDT based sensors is restricted to the field applications close to soil surface, because of the in - field soil profile major installation difficulties. A reevaluation of the TDR propagation time determination in soils, including digital interpretation of signals, is under consideration, with opportunities for TDR/TDT new sensor designs: Schwartz et al., (2013a) and (2013b).

Procedures and experimental results for direct calibration of different commercially produced EM sensors in liquids with different permittivity values and their experimental results have been reported by: Seyfried and Murdock (2002) and (2004); Kelleners et al., (2004a); Blomquist et al., (2005a) and (2005b); Bogena et al., (2007); Regalado et al., (2010); Rosenbaum et al., (2010); Vaz et al., (2013).

Specific methods and techniques for laboratory calibration (in air, in water, and in repacked soils) of selected capacitance and impedance sensors and probes (commercially produced) versus sensor's Scaled Output (frequency, voltage, etc..), have been reported in the last 20 years by: Paltineanu et al., (1993); Mead et al., (1995); Paltineanu and Starr (1997); Baumhardt et al., (2000); Paltineanu (2000) and (2004); Starr and Paltineanu (2002); Groves and Rose (2004); Evett et al., (2006); Paltineanu and Paltineanu (2007); Inoue et al., (2008); Moroizumi and Sasaki., (2008); Kizito et al., (2008); Starr et al., (2009); Gabriel et al., (2010); Mounzer et al., (2010); Matula et al., (2010); Fares et al., (2011); Scudiero et al., (2012); Kargas and Soulis (2012); Rallo et al., (2012); Vaz et al., (2013); Rallo and Provenzano (2014); Visconti et al., (2014a) and (2014b).

Initial papers on the importance of specific calibration, accuracy and sensor - to - sensor variability of EM sensors when harmonizing the soil water content data obtained from different sources of monitoring networks (local, country, global levels) to be used as "ground-truth" in validation of remote sensing data (platforms, aircraft, satellites, etc..), have been published by Paltineanu and Starr (2000), Paltineanu (2002), Paltineanu and Paltineanu (2007), and recently by: Dorigo et al., (2011) and (2013); Guber et al., (2013); Paleki and Bell (2013). It is obvious that international standardization of both the manufacturer "bench top testing" procedures, and the laboratory and field testing methods and techniques, including tool-kits for proper installation of EM sensors and probes, become a necessity in the current and future integrated and globalized 21st century economy.

The objectives of this paper are: i) to search (data mining) both published papers and unpublished reports (in the last two decades) for methods and techniques used in both "manufacturer's bench testing", and in laboratory or field calibration studies of EM soil water measurement sensors and probes; ii) to critically analyze the available data, interpret, and find similarities and differences in characterizing the sensors direct output or scaled response (frequency, voltage, etc) in: standard dielectric liquids; air and distilled water (at room temperature ~22 deg C.); and in controlled repacked soils of known intrinsic characteristics (texture, clay mineralogy, organic content, etc..); iii) to discuss, comparatively, the obtained results and to recommend a minimal set of experimental protocols for mandatory description of a specific sensor's characteristics, its test requirements, and for statistical analysis and interpretation procedures, in order to be taken into consideration for future international standardization proposals.

Theory on dielectric properties of soils and practical applications for soil water measurement using capacitance, impedance and TDT

The correlation between the apparent dielectric constant of the soil-air-water mixture (Ka), and the volumetric soil water content (Ѳv), at different electromagnetic field frequencies, as well as a brief description of the Time Domain Reflectometry (TDR) and the Capacitance methods to measure this relationship, based on worldwide published reports, was described by Paltineanu and Starr (1997). Overall the apparent dielectric constant (Ka) is a function of many factors including: electromagnetic frequency (F); temperature (T); salinity (S); volumetric water content (Ѳv); ratio of the bound water (Ѳbw) to the free water (Ѳfw), which is related to the soil surface area per unit volume; bulk soil density (ρb); shape of soil particles; shape of the water inclusions. Electromagnetically, a soil medium can be represented as a four-component dielectric mixture of air, bulk soil, bound water and free water, according to Hallikainen et al., (1985).

In the case of "fixed frequency capacitance based sensors", operating in the lower part of the radiofrequency band (20 – 150 MHz), the dielectric constant of soils can be measured by capacitance. This method includes the soil as part of a capacitor, in which the permanent dipoles of water in the dielectric medium are aligned by an electric field and become polarized. In order to contribute to the dielectric constant, the electric dipoles, of any origin, must respond to the frequency of the electric field. A particular design of a portable soil water measurement sensor (one pair of cylindrical electrodes) "measures the capacitance of the electrode with dielectric comprising the in-situ moist soil surrounding the access tube"; and "the capacitor forms part of the feedback loop of a modified Clapp high-frequency transistor oscillator operating at about 150 MHz", was reported by Dean et al., (1987). Another design, introduced by Watson et al., (1995), uses multi capacitance sensors (pairs of two cylindrical electrodes) mounted on a plastic sensor body. Each individual probe is inserted (semi-permanently) in a special manufactured PVC access tube and is operating, alternatively, at two imposed frequencies: ~ 150 MHz for soil water content measurement; and <27 MHz for salinity measurement. In both designs, the conductive rings of the sensor form the plates of the capacitor. The capacitor is connected to the "LC oscillator", consisting of an inductor (L) and a capacitor (C) connected to circuitry that oscillates at a frequency depending on the values of (L) and (C). As the inductor is fixed (different turns of wire), the frequency of oscillation varies depending on variations of capacitance. The oscillating capacitance field generated between the two rings of the sensor extends beyond the PVC access pipe into the surrounding medium-soil (dielectric). As described by Paltineanu and Starr (1997) the resonant frequency (**F**) can be measured using a general formula:

$$F = [2\pi \sqrt{(LC)}]^{-1} \qquad [1]$$

where **L** is the circuit inductance and **C** is the total capacitance (which includes the soil components together with some constants).

According to Dean et al., (1987): "the relation between the measuring capacitance (**C**) and the dielectric constant (**ε**) is:

$$C = g\,\varepsilon \qquad [2]$$

where **g** is a geometrical constant that is difficult to calculate for other than simple electrode geometries". Also, these authors, based on previous information from Hasted, J. B. (1973), reported that "there is no simple relation between the dielectric constant and the volumetric water content":

$$F = f\,(\Theta v) \qquad [3]$$

"So, the overall relation must be determined empirically by calibration against a standard technique", Dean et al., (1987).

Data on the generalized relationship between the **Θv** (m3/m3) and the dimensionless **S**caled **O**utput of a specific sensor [ex.: frequency (SF); or voltage (SV)], for different EM sensors based on capacitance and impedance calibrated under laboratory conditions were presented by Paltineanu, I. C. and I. Paltineanu (2007):

$$\Theta v = aSO^{b} \qquad [4]$$

$$\mathbf{SO} = (Oair – Osoil)(Oair\text{-}Owater)^{-1} \qquad [5]$$

where: O is the specific sensor's output (ex. frequency - F, or voltage - V) measured in air, in distilled water, and in soil at room temperature (~22˚C). Coefficients (a) and (b) in formula [4] are obtained experimentally by laboratory calibration under controlled conditions.

According to Allmaras and Kempthorne (2002): "under some circumstances, a reasonable measure of accuracy would be the root-mean-square error: $RMSE = [1/n\sum (\text{measured} – \text{scientific true value})^{2}\ ]^{0.5}$.

For the soil water measurement sensors under consideration, it has been suggested to address "two levels of accuracy": 1) the raw dielectric measurement accuracy (repeatability, sensor to sensor variation) and; 2) the accuracy when used across soil textures. This information separates out the peculiarities of whatever 'average' soil was used to produce the volumetric water content levels from the possible accuracy, if the sensor was calibrated to a specific soil type" Campbell, J. E., (personal communication, 2014).

Correlating the experimentally measured volumetric soil water content Θv (m3/m3) data with the SF (dimensionless) data, obtained in the laboratory calibration of multisensor capacitance probes on different soils: Paltineanu and Starr (1997); Baumhardt et al., (2000); Evett et al., (2006); Gabriel et al., (2010); Quemada et al., (2010); among others, have used **RMSE** as a measure of accuracy between the experimental data sets (X, Y) and predicted values by the fitting power functions (with or without intercept).

MATERIALS, METHODS and TECHNIQUES

A large variety of methods, techniques and materials have been used over the years of experimentation: starting with simple "bench top testing techniques" and materials; and finishing with the more elaborate methods of laboratory calibration of sensors and probes based on capacitance, impedance and TDT. Detailed information, describing selected sensors and probes designs based on capacitance, impedance and TDT, which have been manufactured internationally and independently calibrated in laboratory conditions during the last 20 years, is presented in **Table 1A and Table 1B.**

Table 1A. Independent laboratory calibration (in air, water, std. liquids, soils) of selected commercial EM sensors and probes based on capacitance

Model name and type:	**Independent laboratory calibration**	**References**
Sentry 200-AP, Fringe Capacitance (50 MHz): portable probe for soil water content one pair of cylindrical stainless steel electrodes of unequal heights (63 mm and 47 mm); O.D. (51 mm) with separation space (19 mm) **Manufacturer:** Troxler Electronic Laboratories, Inc. Research Triangle Park, NC, USA (United States Patent - US5260666) Dishman, M. R., and A. W. Jordan, 1991	(in air, water, std. liquids, soils)	* unpublished data
	air, water, repacked soil	Paltineanu, I. C., et al., 1993*
	air, water, repacked soil	Mead, R. M., et al., 1994
	repacked soils	Yoder, R. E., et al., 1998
Model name and type:	**Independent laboratory calibration**	**References**
EnviroSCAN, Fringe Capacitance (100 - 150 MHz) semi permanent probe for soil water content, multiple pairs of cylindrical brass electrodes of equal heights (25 mm); O.D. (50.4 mm); with separation space (12.6 mm). **Manufacturer:** Sentek Sensor Technologies Pty. Stepney, SA, Australia (United States Patent - US5418466) Watson et al, 1995	air, water,	Paltineanu, I. C., et al., 1993*
	air, water, repacked soils, EC	Mead, R. M., et al., 1995
	air, water, repacked soil, temp.	Paltineanu, I. C., and J. L. Starr, 1997
	air, water, repacked soil, EC, temp.	Baumhardt, R.L., et al., 2000
	air, water, repacked soil	Williams, B., et al., 2003
	std. liquids	Kelleners et al., 2004a
	air, water, repacked soil, EC, temp.	Scobie, M., 2006
	air, water, repacked soil, temp.	Evett, S. R., et al., 2006
	air, water, std. liquids	Schwank, M., et al., 2006
	air, water, repacked soil, EC	Gabriel, L. J., et al., 2010.
	air, water, repacked soil	Mounzer, O., et al., 2010
	air, water, repacked soil	Rowland, R., et al., 2011
	air, water, std. liquids, EC, soil	Avanzi, F., et al., 2013

Model name and type:	**Independent laboratory calibration**	**References**
Diviner2000, Fringe Capacitance (100 - 150 MHz):	air, water, repacked soil	Williams, B., et al., 2003
portable probe for soil water content;	air, water, repacked soils	Groves, S. J., and S. C. Rose, 2004
one pair of two cylindrical brass electrodes	air, water, repacked soil, temp.	Evett, S. R., et al., 2006
of equal heights (25 mm); O.D. (47.0 mm);	air, water, repacked soil	Rallo, G., et al., 2012
with separation space (12.6 mm).		
Manufacturer:		
Sentek Sensor Technologies Pty.		
Stepney, SA, Australia		

Model name and type:	**Independent laboratory calibration**	**References**
EasyAG 50, Fringe Capacitance (100 - 150 MHz)	air, water, repacked soil, temp.	Polyakov, V., et al., 2005
semi permanent probe for soil water content	air, water, repacked soils, temp.	Fares, A., et al., 2007
multiple pairs of cylindrical brass electrodes		
of equal heights (25 mm); O.D. (26.5 mm)		
with separation space (11.6 mm).		
Manufacturer:		
Sentek Sensor Technologies Pty.		
Stepney, SA, Australia		

Model name and type:	**Independent laboratory calibration**	**References**
TriSCAN, Fringe Capacitance, dual frequency:	air, water, repacked soil, EC	Starr, J. L., et al., 2009
< 27 MHz for salinity, and > 100 MHz for soil water;		
semi permanent probe for soil water content and		
salinity multiple of two cylindrical brass electrodes;		
of equal heights (25 mm); O.D. (50.4 mm);		
with separation space (12.6 mm).		
Manufacturer:		
Sentek Sensor Technologies Pty.		
Stepney, SA, Australia		
(United States Patent - US5418466)		
Watson et al, 1995		

Model name and type:	**Independent laboratory calibration**	**References**
5TE, Capacitance (70 MHz) sensor:	standard liquid media	Bogena, H. R., et al., 2007
for soil water/EC/temperature measurement	air, water, soil, EC	Kizito, R., et al., 2008
trifurcate type, stainless steel electrodes;	air, water, soil, EC	Matula, S., et al., 2010

of the same length (50 mm). **Manufacturer:** Decagon Devices Inc. Pullman, WA, USA (United States Patent, US6904789 B2) Campbell, G. S., and W. C. Greenway, 2005	standard liquid media	Rosenbaum, U., et al., 2010
	air, water, soil, EC	Scudiero, E. et al., 2012
	soils, EC	Visconti, F., et al., 2014 a & b

Model name and type:	**Independent laboratory calibration**	**References**
10HS, Capacitance (70 MHz) sensor: for soil water content measurement, bifurcate type; stainless steel electrodes (80mm/each). **Manufacturer:** Decagon Devices Inc. Pullman, WA, USA	air, water, std. liquid, repacked soil, EC, temp.	Kargas, G., and K. X. Soulis, 2012
	soils, EC	Visconti, F., et al., 2014a

Model name and type:	**Independent laboratory calibration**	**References**
PH100WS, Capacitance, dual frequency: wireless digital sensor for soil water/EC/temperature dual frequency (1 MHz for EC, and 107.9 MHz for soil water); Internal battery and radio antenna; **Manufacturer:** UgMO Technologies Inc. King of Prussia, PA, USA. United States Patent - US7884620 B2 Campbell, J. E., 2011	air, water, soil, EC, temperature	Campbell, J. E., 2010a, and 2010b
	soils, EC, temperature	Irrigation Association, SWAT, 2013

Table 1B. Independent laboratory calibration (in air, water, std. liquids, soils) of selected commercial EM sensors and probes based on impedance and TDT

Model name and type	**Independent laboratory calibration** **(in air, water, std. liquids, soils)**	**References** *** unpublished data**
Hydra Probe, Impedance (50 MHz): portable and semi permanent probe for soil water/EC/temperature, permittivity, four parallel stainless steel electrodes, (1 in the center + 3 peripheral parallel shield rods) of (4 mm diameter X 58 mm length/each).	air, water, repacked soil	Paltineanu, I. C., 2000*
	soils, freeze-thaw	Hanek, L. G., et al., 2001
	air, water, repacked soil, std. liquids	Seyfried, M. S., and M. D. Murdock, 2002
	air, water	Loiskandl, W., et al., 2003
	air, water, repacked soil, std. liquids	Seyfried, M. S., and M. D. Murdock, 2004
	soils	Bosch, D. D., 2004

Manufacturer Vitel, Inc. Chantilly, VA, USA (United States Patent - US5479104 A) Campbell, J. E., 1995 Stevens Water Monitoring Systems, Inc. Beaverton, OR, USA	soils	Leao, T. P., and E. Perfect., 2007
	soils	Leao, T. P., at al., 2010
	air, std. liquids, undisturbed soil cores	Logsdon, S. D., et al., 2010
	soils(organic)	Mortl, A., et al., 2011
	air, water, repacked soil	Vaz, C. M. P., et al., 2013
Model name and type **Theta Probe ML2x,** Impedance (100 MHz): portable and semi permanent probe for soil water content: four parallel stainless steel electrodes, 1 in the center + 3 peripheral parallel shield rods, of (2 mm diameter X 60 mm length/each). **Manufacturer** Delta-T Devices Ltd. Burwell, Cambridge, UK (United States Patent - 5804976) Gaskin, G. J., 1998	**Independent laboratory calibration**	**References**
	(in air, water, std. liquids, soils)	*** unpublished data**
	repacked soils	Tsegaye, T. D., et al., 2002 and 2004
	air, water	Loiskandl, W., et al., 2003
	air, water, repacked soil	Paltineanu, I. C., 2004*
	repacked soils	Kaleita, A., et al., 2005
	air, water, soil, EC	Inoue, M., et al., 2008
	air, water, soil, (NAPLs)	Moroizumi, T., and Y. Sasaki., 2008
	standard liquid media	Regalado, C. M., et al., 2010
	air, water, repacked soil, EC	Matula, S., et al., 2010
	repacked soils	Fares, A., et al., 2011
	standard liquid media	Vaz, C. M. P., et al., 2013
Model name and type **PR 1/4 Profile Probe**, Impedance (100 MHz) portable and semi permanent probe for soil water content: multiple pairs of semi-cylindrical steel electrodes, of equal heights (8 mm) and O.D. (26 mm); with separation space (32 mm). **Manufacturer** Delta-T Devices Ltd. Burwell, Cambridge, UK (U.S. Patent - US 2008/0211521 A1) Lock, G., 2008	**Independent laboratory calibration**	**References**
	(in air, water, std. liquids, soils)	*** unpublished data**
	air, water	Paltineanu, I. C., 2002*
	air, repacked soil, temp.	Evett, S. R., et al., 2002
	air, water	Paltineanu, I. C., 2004*
	repacked soils, lysimeters	Irmak, S., and A. Irmak. 2005
	air, water, repacked soil, temp.	Evett, S. R., et al., 2006
	air, water, repacked soil, EC	Inoue, M., et al., 2008
	repacked soil, lysimeters	Qi, Z., and M. J. Helmers, 2010
Model name and type **ACC - SEN - TDT,** Digital TDT (100 MHz to 1-2 GHz) sensor: for soil water/EC/temperature measurement; two parallel stainless steel, semielliptical shaped wires; of the same diameter (3.5 mm) and different lengths.	**Independent laboratory calibration**	**References**
	(in air, water, std. liquids, soils)	*** unpublished data**
	standard liquid media	Blomquist, J. M. Jr., et al., 2005 a & b
	soils, EC, temperature	Irrigation Association, SWAT, 2013

Manufacturer		
Acclima Inc.		
Meridian, ID, USA		
(United States Patent - US6657443 B2)		
Anderson, S. K., 2003		

Departing from general and sometimes confusing descriptions (FDR, capacitance, impedance, TDT, etc..) when testing and calibrating EM sensors and probes, the focus in Table 1A and 1B is on the main physical characteristics of a particular, designed and patented model such as: fixed frequency(s) of operation; as well as the geometry and free space between different types of electrodes (cylindrical, rod, and fork); which will have determining impacts on the axial and radial influence in soils, and finally on the real comparison based on future internationally recognized standardization criteria. It should be noted that except for the TDT based sensors (using a broad EM spectrum) which are based on the Topps et al., (1980) reported presumption that "over the frequency range of 1 MHz to 1 GHz, the real part of the dielectric constant does not appear to be strongly frequency dependent", all other commercial models presented in Tables 1A and 1B, are designed and patented to perform on fixed frequency(s), under 150 MHz.

When performing simple "bench top testing" of EM sensors in the air and in water, it is important to specify the room temperature (deg. C), and characteristics of water (distilled, tap, EC), as well as what standard dielectric constant standard liquid(s) and their permittivity (**ε**) values have been used and any corrections to the DC dielectric constants that may need to be applied due to dielectric relaxation phenomena at the sensor operating frequency.

For more elaborate laboratory calibration under controlled conditions, intrinsic characteristics of original soils must be reported such as: classification type; texture, particular clay mineralogy (percentage of 1:1, 2:1 clay types); organic matter content; EC; gravel size and content. Also: a correct description of repacked soils in experimental calibration settings (wooden boxes, PVC or metal tubes, etc..); the method of the sieved soil compaction (manual, Proctor hammer, Hydraulic press, etc..), and its controlled bulk density uniformity verification; method and technique of the particular EM sensor or probe insertion (mimicking the future field installation; and the method, type of technique, and the number of inserted sample rings as close as possible to the EM sensor for soil volumetric water content measurement; method of statistical analysis and interpretation, will have specific roles on future comparisons of laboratory calibrated EM sensors using internationally recognized standard criteria.

In **Table 2A** and **Table 2B** a comparison is presented, based on the already published laboratory testing of two fringe capacitance models (EnviroSCAN and Diviner2000) in laboratory conditions using different techniques: 1) predetermined volumetric water content repacked and compacted sieved soil samples in wooden boxes, and PVC tubes using hydraulic presses reported by Paltineanu and Star, (1997), and Paltineanu, (2000), or Proctor hammer test - ASTM D698) reported by Rallo et al, (2012 and 2014); and 2) manually compacted sieved soils in large and water added in large weighing columns, drums, as reported by Baumhardt et al, (2000) and Evett et al., (2006) among others.

Picture 1, and Pictures 2A and 2B show details of technique 1, using large hydraulic presses: 50 T (39.7 kgf/cm2, or 3.89 MPa potential pressure for EnviroSCAN calibration); and 20 T (93.6 kgf/cm2, or 9.18 MPa potential pressure for Hydra Probe calibration).

Picture 1. Experimental setup, using a 50 T hydraulic press, and details of volumetric soil water content and bulk density sampling (5 brass rings around the sensor) for laboratory calibration of fringe capacitance probe EnviroSCAN (Sentek Technologies), as reported by Paltineanu and Starr, (1997).

Picture 2A. Experimental setup, using a 20 T hydraulic press, for laboratory calibration of impedance Hydra Probe (Vitel Inc., VA, USA) sensor, as reported by Paltineanu, I. C., (2000- unpublished data).

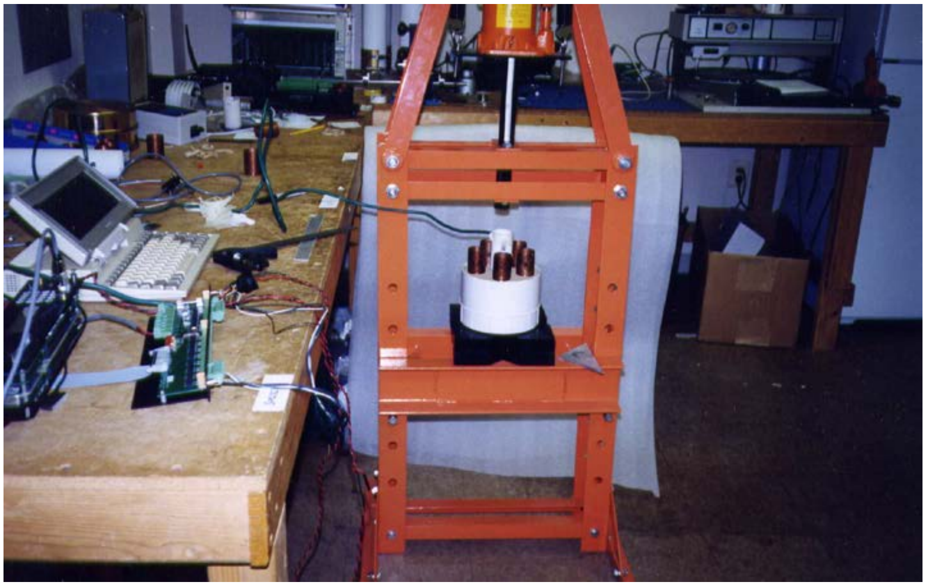

Picture 2B. Details of volumetric soil water content and bulk density sampling (5 small copper rings around the sensor), for laboratory calibration of impedance Hydra Probe(Vitel Inc.) sensor, as reported by Paltineanu, I. C., (2000 – unpublished data)

Uniform compaction of sieved soil samples in predetermined layers, as well as the locations of multiple soil sampling brass rings inserted in close vicinity and around the EM sensors are critical for obtaining credible and verifiable results that can be compared under future international standardization protocols.

RESULTS and DISCUSSION

At radio frequencies, the dielectric constant of pure water (**Kw**), at 20^0 C and atmospheric pressure is 80.4, that of solids is 3 to 7, and that of air is 1. The **Kw** is inversely related to temperature, (Weast, 1980, cited by Paltineanu and Starr, 1997). According to Topp and Ferre (2002) "the relative dielectric permittivity, sometimes called the dielectric constant, is not constant but varies with frequency, which must be taken into account when using electromagnetic methods". Indeed, by definition, the relative dielectric permittivity (**ε**) is the ratio between the dielectric permittivity of a substance (material) to the dielectric permittivity of free space (vacuum).

This is the main reason for testing the EM sensors in laboratory controlled conditions first, and later in the field under a multitude of soil water/EC/temperature conditions.

1. "Bench top testing" of EM sensors in air, in water, and in reference (standard) dielectric constant liquids:

1.1 Bench top testing in air, and in distilled water, at room temperature (~ 22^0 C):

Experimental results obtained by using simple bench top techniques for testing of different commercial EM sensors both in the air and with their rod type electrodes length immersed in distilled water (25%; 50%, 75% and 100%) at room temperature (~ 22 ^{0}C) are shown comparatively in **Figure 1.**

When using the ratio of their specific output **(O),** measured in mV, mA, water content, or permittivity, to the maximum output (**Omax.)** by immersion in distilled water, commercial sensors (HydraProbe and ML2x) based on impedance (operating at fixed frequencies of ~50 MHz, or ~ 100 MHz and having shorter rod type electrodes of 50 - 60 mm lengths) respond differently than the commercial sensors based on TDT (ACC-SEN) or TDR (Aqua-Tel) operating under broad spectrum frequencies (from MHz to GHz) and having longer electrodes 135 – 700 mm).

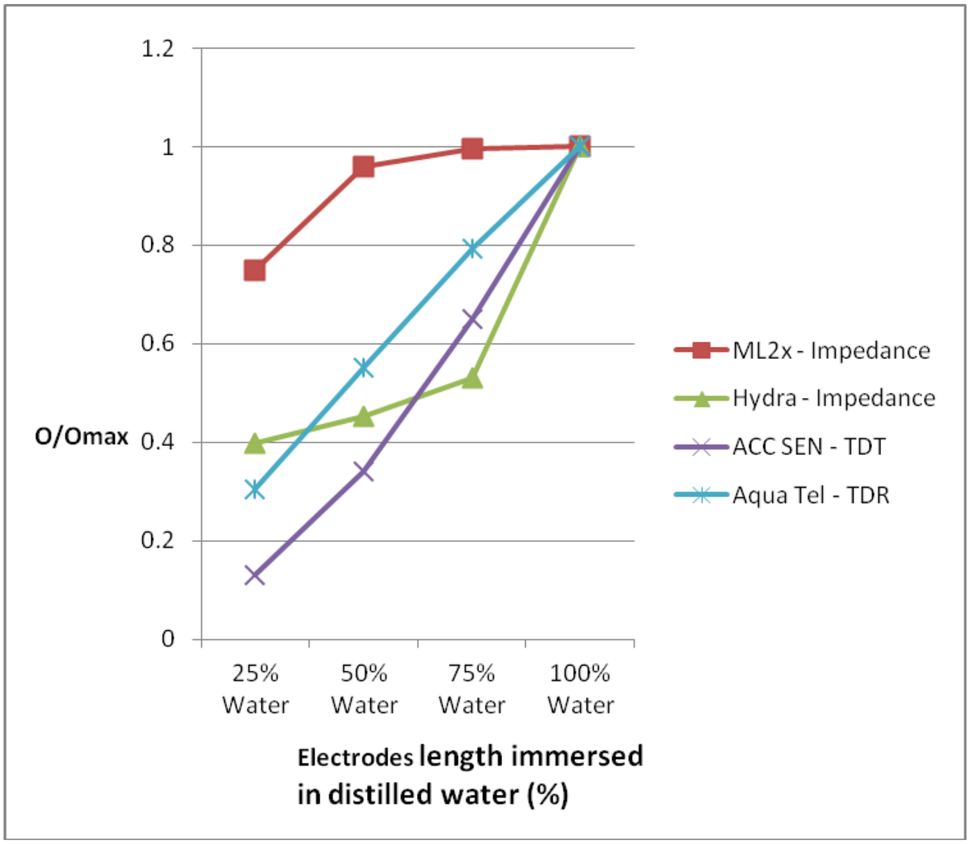

Fig. 1 Output (O/Omax) sensitivity response of different commercial EM sensors with rod type electrodes lengths immersed in distilled water (Paltineanu, unpublished data)

It is very important to know this specific response from the manufacturers published experimental data, before deciding to use any EM sensor for a particular research or practical application.

1.2 Bench top testing in reference (standard) dielectric constant liquids:

A large variety of “reference dielectric constant liquids”, from highly volatile, carcinogenic, to pure acetic acid – distilled water mixtures, used for independent testing of commercial EM sensors , are presented in Table 1A and Table 1B. Also, attempts of classification and standardizing reference dielectric constants liquids for bench top testing of EM sensors have been reported by: Blonquist et al., (2005b); Campbell et al., (2007); Regalado et al., (2010); Vaz et al., (2013); Vaz et al., (2014b). Unfortunately, manufacturers of EM sensors are reluctant to describe the methodologies, techniques and materials used for their internal testing, and to make their own results available for the general public. Also, it is important to take into consideration the uniqueness of the EM sensors based on capacitance and impedance which perform under imposed radio frequency (usually under 150 MHz) response, compared directly with the research results obtained by using broad spectrum frequencies sensors (TDR) for laboratory calibration on different soil samples in coaxial transmission lines, reported by Topp et all., (1980). It has been suggested that: “some of these references (including some common ones like acetic acid, ethanol, propanol, have Debye relaxation frequencies close enough to the sensor operating frequencies that the actual dielectric constant of the liquid needs to be adjusted to the appropriate value at the sensor frequency. This can be an even bigger problem for TDR, TDT, due to the broad spectral content of the pulses” Campbell, E. J. (personal communication, 2014).

1.3 Testing for Air and Water Temperature Effects on the EM sensors performance:

Temperature-controlled chambers have been used for testing the effects of air temperature (0 – 50^0 C) and 25-L insulated plastic (picnic) water coolers, with special PVC access tubes, temperature sensors and a recirculation water pump installed, for studying the effects of water temperature (8 – 54^0 C) on EnviroSCAN multi sensor capacitance probe and results reported by Paltineanu and Starr (1997). In the same paper, “stability of EnviroSCAN capacitance sensors with time was measured in air at ~ 11.0 degrees Celsius (° C) in the incubation chamber in which the air temperature decreased very slowly (0.00760 ^{0}C/day) showing slowly increasing frequency in air (Fa) with time. During a 3-d period 432 pairs of temperature (every 10 min) showed a coefficient of variation (CV) of external temperature of 0.0.768% while the CV for Fa was more than two orders of magnitude smaller, or 0.0042% (1.5 out of 36000)”. Other techniques for studying different multi sensor capacitance probes response to air and water temperature effects have been reported by Baumhardt et al., (2000); Schwank et al., (2006); Evett et al., 2006; and Fares et al., (2007) among others.

1.4 Testing for axial and radial sensitivity of EM cylindrical type sensors in air, in water and in soils:

Experimental results for determination of the axial and radial sensitivity of EM cylindrical type sensors in air, in water, and in soils, by using different techniques have been reported by: Paltineanu et al., (1993); Paltineanu and Starr (1997); Evett et al., 2006; Mounzer et al., (2010). Standardization of the methods and techniques for correct determination of the axial and radial sensitivity of EM sensors will have an important role in the establishment of the specific/maximum volume of influence in the soil surrounding the sensors.

1.5 Testing for rotational orientation response of EM cylindrical type sensors inside the access tubes:

It has been noticed that there is an orientation response of EM fringe capacitance cylindrical type sensors inside the access tube, and some manufacturers (Sentek Technologies, SA, Australia) introduced techniques to limit this effect by imposing one single position for both their multisensor probes (EnviroScan, EasyAG 50, etc..) as well as for single sensors (Diviner2000). Also, experimental results obtained by using the Delta-T Profile Probe(Delta-T Devices, Cambridge, UK) show that inserting the probe in the access tube and rotating it at 90, 180 and 270 deg., different soil water contents values have been obtained in both uniformed soil conditions and in the field (Paltineanu, I.C., to be published). By standardization, this rotational effect must be reported by the manufacturer and its influence on soil water measurement limited by using different techniques.

2. Laboratory calibration of EM sensors and probes on specific soils:

Experimental results obtained by independent laboratory calibration of two commercial fringe capacitance models (EnviroSCAN and Diviner2000) are presented in Table 2A and Table 2B. Two sieved soil repacking techniques have been used: predetermined volumetric water content soil samples compacted by hydraulic presses in wooden boxes, and PVC tubes; and sieved soil samples manually compacted in large weighing columns.

Also, **Table 2A and Table 2B** introduce details of the soil water content **Ѳv** (m3/m3) vs. Scaled frequency **SF** (dimensionless) mathematical relationship formula **$Ѳv = c + aSF^{b}$**, along with domain and codomain limits, number of replications (n) as well as statistical interpretation (**RMSE, R^2**) obtained by laboratory calibration of the same fringe capacitance models (EnviroSCAN and Diviner2000), performed on specific soils from different continents and reported by different authors in international literature.

Table 2A Soil volumetric water content(Ѳv) vs. scaled frequency(SF) response function of fringe capacitance probe EnviroSCAN calibrated in laboratory on specific soils from North America, Australia and Europe

Soils (location)	**coeff. C**	**coeff. A**	**coeff. B**	**Domain of SF** min. to max.	**Codomain of Ѳv** min. to max.	**RMSE**	**R^2**	**n**
Mattapex Silt Loam (Beltsville, MD, USA) **Reference: Paltineanu, and Starr, 1997**	0	0.49	2.167	0.39 → 0.89	0.07 → 0.38	0.009	1	15
Sand, Sandy Loam and Clay (Fresno, CA, USA) **Reference: Mead, R. M., et al., 1995**	0	0.522	2.046	0.30 → 0.95	0.05 → 0.45	0.031	0.9	38
Sandy Loam, Loamy Sand (Adelaide, SA, Australia) **Reference: Dighton, J. C., and P. J. Dillon., 1993 (unpublished data)**	0	0.5	2.231	0.35 → 0.90	0.04 → 0.42	0.016	1	24
Olton Soil, 2:1 clay mineralogy, dominant montmorillonite, pooled untransformed data (Lubbock, TX, USA) **Reference: Baumhardt, R. L., et al., 2000**	0	0.752	3.841	0.25 → 0.85	0.02 → 0.41	0.028	1	89
Pullman Soil, 2:1 clay dominant, illite and montmorillonite (smectite) Soil A (silty clay loam) + B (clay). (Bushland, TX, USA) **Reference: Evett, S. R., et al., 2006**	0.024	0.605	3.812	0.35 → 0.95		0.022	1	178

Pullman Soil, 2:1 clay dominant, illite and montmorillonite (smectite) Soil C, clay loam (containing 50% CaCO3) (Bushland, TX, USA) **Reference: Evett, S. R., et al., 2006**	0.041	0.781	4.981	0.35 → 0.95		0.018	1	90
Typic Xerochrept, Silty Clay Loam Soil illite and montmorillonite (Aranjuez, Madrid, Spain) **Reference: Gabriel, J. L., et al., 2010 & Quemada, M., et al., 2010**	0	0.482	3.097	0.27 → 0.95	0.015 → 0.455	0.027	1	672

Table 2 B. Soil volumetric water content (Ѳv) vs. scaled frequency (SF) response function of fringe capacitance sensor Diviner2000, calibrated in laboratory on specific soils from North America and Europe

Soils (location)	coeff. C	Coeff. A	Coeff. B	Domain of SF min. to max.	Codomain of Ѳv min. to max.	RMSE	R^2	n
Pullman Soil, 2:1 clay dominant, montmorillonite, Silty Clay Loam + Clay (Soil A + B), Bushland, TX, USA **Reference: Evett, et al., 2006**	0.034	0.457	5.421	0.35 → 0.95		0.024	0.992	336
Pullman Soil, 2:1 clay dominant, montmorillonite, Clay Loam with 50% CaCO3 (Soil C), Bushland, TX, USA **Reference: Evett, et al., 2006**	0.028	0.563	6.182	0.35 → 0.95		0.025	0.993	192
Partinico, Loamy Sand (sieved, repacked), Sicily, Italy **Referene: Rallo, et al., 2014**	0	0.5407	3.816	0.45 → 0.85	0.01 → 0.44	0.02	0.992	16
Partinico, Loamy Sand (undisturbed), Sicily, Italy **Referene: Rallo, et al., 2014**	0	0.5615	4.76	0.45 → 0.85	0.01 → 0.26	0.0196	0.935	29
Castelvetrano B, Clay Loam (sieved repacked), Sicily, Italy **Referene: Rallo, et al., 2014**	0	0.4387	4.396	0.35 → 0.95	0.05 → 0.45	0.0242	0.94	16

Castelvetrano B, Clay Loam (undisturbed), Sicily, Italy **Referene: Rallo, et al., 2014**	0	0.3407	5.181	0.45 → 0.95	0.025 → 0.37	0.0225	0.885	46

Monte Conca, Clay (sieved repacked), Sicily, Italy **Referene: Rallo, et al., 2012**	0	0.535	3.465	0.70 → 0.95	0.12 → 0.45	0.0376	0.9189	35

Monte Conca, Clay (undisturbed), Sicily, Italy **Referene: Rallo, et al., 2012**	0	0.572	2.646	0.45 → 0.90	0.05 → 0.90	0.0581	0.9095	56

2.1 Similarities and differences in the Ɵv (m3/m3) vs. SF response by laboratory and field calibration on different soils:

For consistency in analyzing and comparison of experimental data obtained by different authors using a variety of methods, materials and compaction techniques for laboratory calibration of EM sensors, only the soil volumetric water content **Ɵv (m3/m3)** relationship to the scaled frequency **SF** response of two models based on fringe capacitance: a multi-sensor probe (EnviroSCAN); and a single sensor ‘swipe and go’ (Diviner2000) is presented in Fig. 2A and 2B.

While the shape of the nonlinear relationship **$\Theta v = aSF^{b}$** hold true for both models, there are differences between results obtained on soils with 2:1 dominant type clay, montmorillonite, from Texas, USA (reported by Baumhardt et al., 2000; and Evett et al., 2006) as well as on soil from Aranjuez, Madrid, Spain, with lesser content of 2:1 clay, montmorilonite, (reported by Gabriel et al., 2010, and Quemada et al., 2010); versus data obtained from soils with 1:1 clay type, probably due to the ‘bound water’ effect.

There are few reported data when laboratory calibration is accompanied by laborious field calibration techniques on similar soils, validating the accuracy of laboratory calibration, as presented for EnviroSCAN in Fig. 2B.

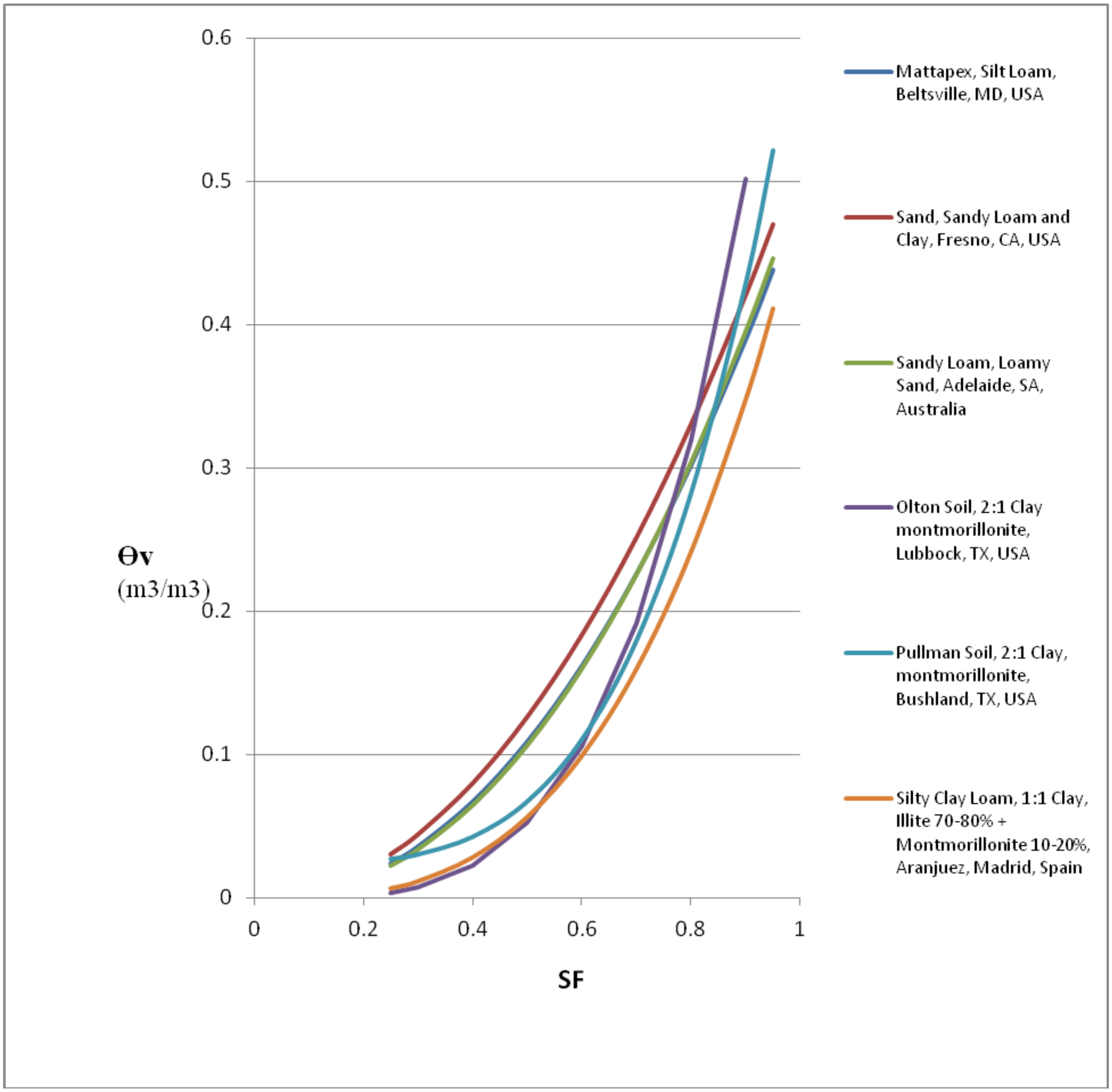

Fig.2A. Laboratory calibration of EnviroSCAN fringe capacitance probe studies performed on different soils from North America, Australia and Europe(adaptation from: Paltineanu and Star 1997; Baumhardt et al., 2000; Evett et al., 2006; Gabriel et al., 2010; and Quemada et al., 2010)

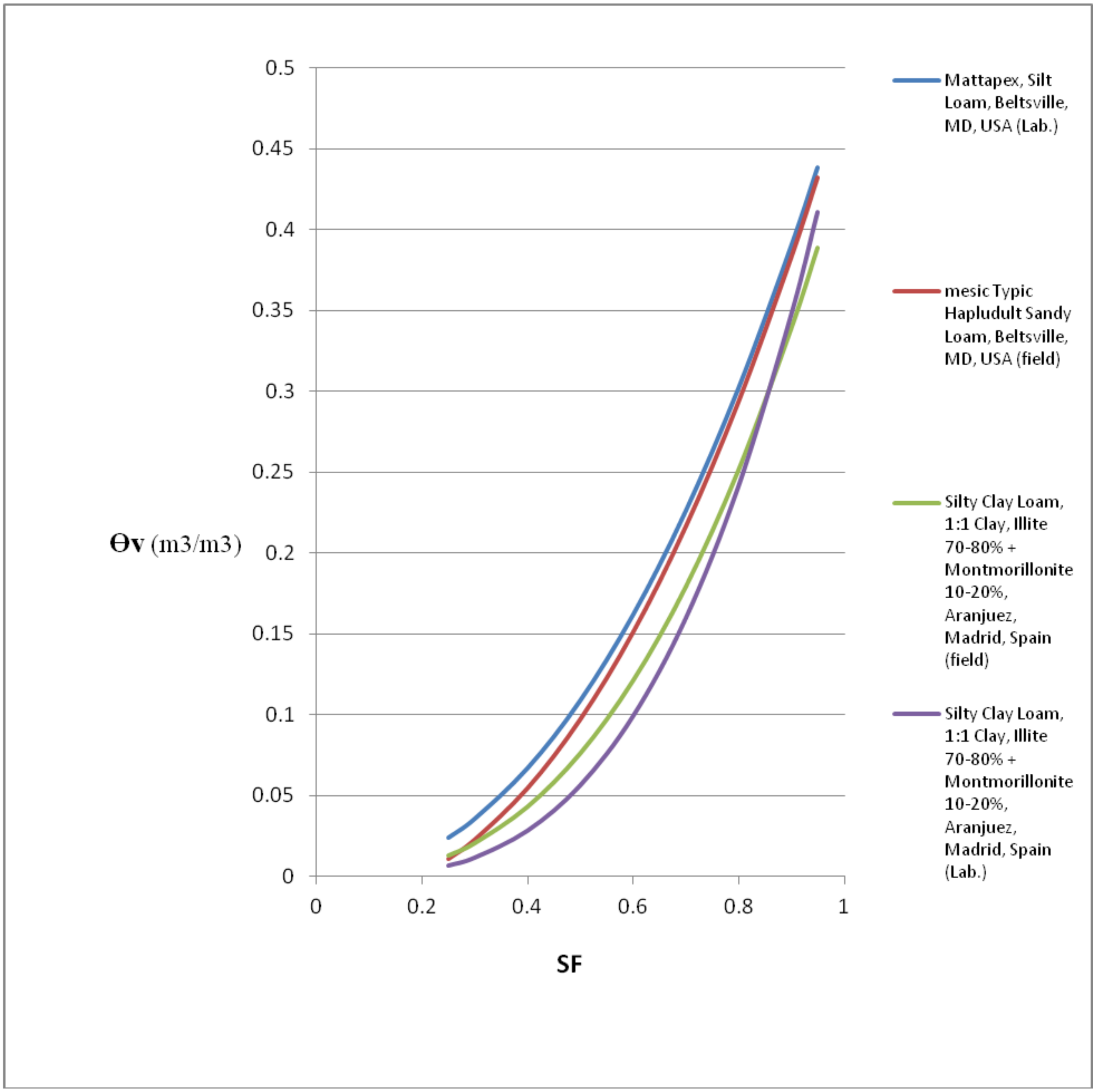

Fig. 2B. Comparison of laboratory and field calibration of EnviroSCAN performed on soils from North America and Europe (adaptation from: Paltineanu and Starr, 1997; Guber et al, 2010; Gabriel et al., 2010, and Quemada et al., 2010)

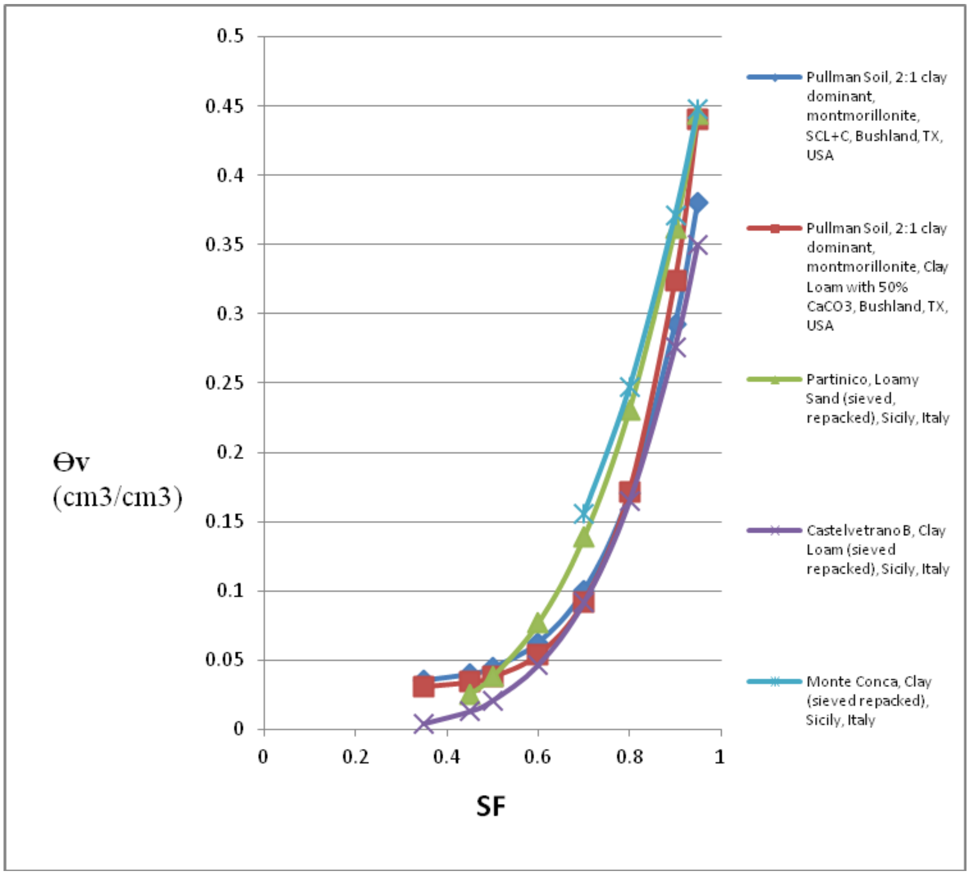

Fig. 3A. Laboratory calibration of Diviner2000 fringe capacitance sensor studies performed on different soils from North America and Europe (adaptation from: Evett et al., 2006; Rallo et al., 2012 and 2014)

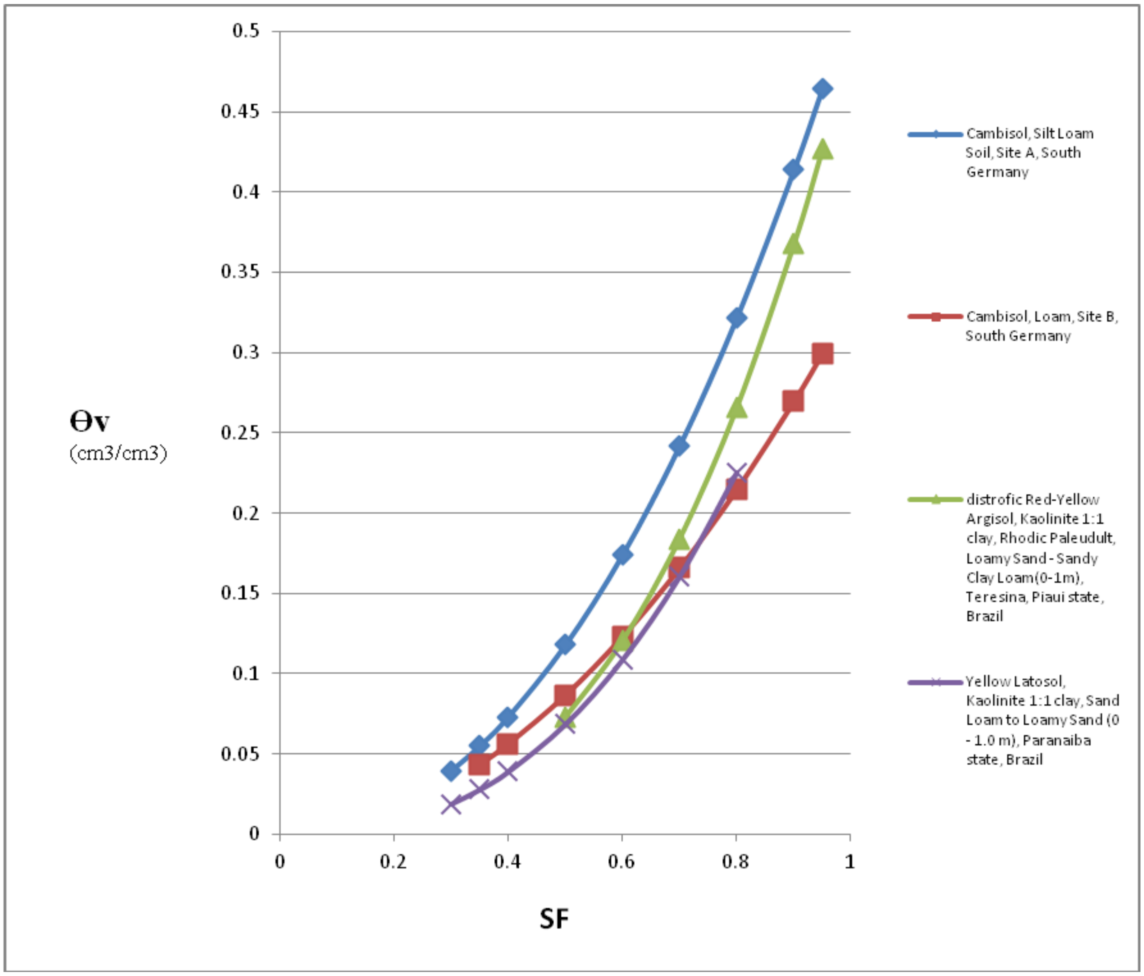

Fig. 3B. Field calibration of Diviner2000 fringe capacitance sensor studies performed on different soils from South America and Europe (adaptation from: Geesing et al., 2004; Silva et al., 2007; Andrade et al., 2010)

When starting with field calibration first, using different techniques, the results are more divergent as shown in Fig. 3B.

This is why standardization of methodologies and techniques for both laboratory and field calibration has become more stringent when more and more data are accumulated from different continents.

CONCLUSIONS and RECOMMENDATIONS:

After two decades of accumulated experience on using diverse methodologies, materials and techniques for both laboratory and field calibration methods, of commercial EM sensors based on capacitance, impedance and TDT, it is important to elaborate international agreed protocols and standards in order to guide the potential users in their research and practical application projects.

A minimal of experimental protocols describing sensors and test requirements as well as statistical analysis and interpretation should include: frequency(s) of operation; response of sensors in air and distilled water at room temperature (~22 deg. C); detailed description of soil intrinsic characteristics (texture, clay mineralogy, EC, organic material, gravel content, etc..); method and techniques for uniform soil repacking and compaction (coefficient of uniformity for dry and wet bulk density around the sensor); axial and radial sensitivity of sensors in distilled water, in air – water and in air – soil interfaces, as well as in soil at different depths; rotational orientation response of cylindrical sensors inside access tubes; sensors response in controlled levels of temperature in air, in distilled water, and in soil; sensors response at different soil EC and temperature conditions; soil volumetric water content **Ѳv (cm3/cm3)** versus **SO** scaled output(frequency, voltage, etc..); description of specific liquid of known dielectric constant, etc..
It is important that both the sensor output (voltage, SF, etc.) relationship with the apparent dielectric constant, along with the intrinsic apparent dielectric constant to the volumetric soil water content curve should be published.

Special experimentation criteria and reporting of results must be elaborated to better describe how soil salinity can distort the measurement of apparent soil volumetric water content.

REFERENCES

(*) Abbreviations:

Symposium - 2002, Beltsville, MD, USA = Transactions of the First International Symposium on Soil Water Measurement using Capacitance and Impedance. Ed. Ioan Caton Paltineanu, Publisher Paltin International Inc., Laurel, Maryland, USA. ISBN 0982796900

Symposium - 2007, Beltsville, MD, USA = Transactions of the Second International Symposium on Soil Water Measurement using Capacitance, Impedance and TDT. Ed. Ioan Caton Paltineanu, Publisher Paltin International Inc., Laurel, Maryland, USA.Maryland, USA. ISBN 0982796919

Symposium - 2010, Murcia, Spain = Transactions of The Third International Symposium on Soil Water Measurement using Capacitance, Impedance and TDT, Ed. Ioan Caton Paltineanu and Juan Vera Munoz, Publisher Paltin International Inc., Laurel, Maryland, ISBN 0982796927

Symposium - 2014, Montreal, Canada = Transactions of the Fourth International Symposium on Soil Water Measurement using Capacitance, Impedance and TDT, Ed. Ioan Caton Paltineanu, Publisher Paltin International Inc., Laurel, Maryland, ISBN

Allmaras, R. R., and O. Kempthorne, 2002. Errors, Variability, and Precision. Chapter 1.3. In: Dane, J. H., and G. C. Topp, Co-editors, Methods of Soil Analysis, Part 4 - Physical Methods. P. 15 - 44, SSSA Book Series No. 5, SSSA Inc., Madison Wisconsin, USA.

Anderson, S. K., 2003. Absolute - reading soil moisture and conductivity sensor. United States Patent, US6,657,443 B2

Anderson, S. K., and H. S. Anderson. 2004. Method and apparatus for determining moisture content and conductivity. US 6,831,468 B2

Andrade Junior, A. S., C. R. Silva, da., C. F. Souza. 2010. Calibration of Diviner 2000® capacitance probe in two soils of Piaui State, Brazil. Paper # 1.5. Symposium - 2010, Murcia, Spain

Atkins, R. T., T. Pangburn, R. T. Bates, and B. E. Brocket., 1998. Soil moisture determinations using capacitance probe methodology. US Army - CRREL, Report, Jan. 1998, 49pp

Avanzi, F., M. Caruso, and C. Jommi, 2013. Calibration in the laboratory of capacitance sensors for water content monitoring. Advances in Unsaturated Soils, Caiceo, et al. (eds), London, UK

Ayars, J. E., R. M. Mead, I. C. Paltineanu, and J. Liu. 1995. Radioactive versus capacitance techniques for measuring soil water. Proceedings Series, 17-21 Oct 1994 / IAEA, Vienna (Austria), 1995, p. 419-428

Baumhardt, R. L., R. J. Lascano, and S. R. Evett., 2000. Soil Material, Temperature, and Salinity Effects on Calibration of Multisensor Capacitance Probes. Soil Sci. Soc. Am. J. 64:1940–1946

Bell, J. P., T. J. Dean and M. G. Hodnett, 1987. Soil moisture measurement by an improved capacitance technique, Part II. Field techniques, evaluation and calibration. Journal of Hydrology, 93(1987) 79-90

Blonquist, J. M. Jr., S.B. Jones, and D.A. Robinson. 2005 a. A time domain transmission sensor with TDR performance characteristics. Journal of Hydrology 314: 235–245

Blonquist, J. M. Jr., S. B. Jones, and D. A. Robinson, 2005 b. Standardizing characterization of Electromagnetic Water Content Sensors, Part 2. Evaluation of Seven Sensing .Vadose Zone Journal 4:1059–1069 (on-line)

Bogena, H. R., J. A. Huisman, C. Oberdörster, and H. Vereecken. 2007. Evaluation of a low-cost soil water content sensor for wireless network applications. Journal of Hydrology, Volume 344, Issue 1-2, p. 32-42.

Bosch D. D., 2004. Comparison of Capacitance-Based Soil Water Probes in Coastal Plain Soils. Vadose Zone Journal 3:1380–1389

Buss, P., 1993. The use of capacitance based measurements of real-time soil water profile dynamics for irrigation scheduling. In Under pressure. Irrig. 93. Proc. Natl. Conf. Irrig. Assoc. Australia and the Natl. Committee on Irrig. and Drainage, Launceston, Tasmania.

Buss, P., M. Dalton, and S. Olden. 2002. EasyAG performance of a new slim line multisensor soil water capacitance probe. Paper 3.1. Symposium - 2002, Beltsville, MD, USA.

Campbell, J. E., 1990. Dielectric properties and influence of conductivity in soils at one to fifty Megahertz. Soil Sci. Soc. Am. J. 54:332-341

Campbell, J. E., 1993. Electrical sensor for determining the moisture content of soil. United States Patent, US5479104 A

Campbell, E. J., 2002. Salinity effects in capacitive soil moisture measurement. Paper 1.2., Symposium - 2002, Beltsville, MD, USA

Campbell, E. J., I. C. Paltineanu and J. L. Starr., 2007. An overview of the need for standardization and calibration protocols, methodology to implement them, and future directions. Abstract Paper 3.6 ., Symposium - 2007, Beltsville, MD, USA

Campbell, J. E., 2007. Interplay of soil moisture, conductivity and temperature in soil moisture sensors: A theoretical overwiew and practical implications. 2007. Paper 1.2., Symposium - 2007, Beltsville, MD, USA.

Campbell, J. E., 2010a. Soil moisture, temperature and salinity coupling and its impacts on sensor design and performance: A theoretical review and practical example. Paper 1.2. Symposium - 2010, Murcia, Spain.

Campbell, J. E., 2010b. A unique, self-contained, belowground wireless soil moisture sensor. Paper 3.1. Symposium - 2010, Murcia, Spain

Campbell, J. E., 2011. Sensor for measuring moisture and salinity. United States Patent - US 7884620 B2

Campbell, G. S., and R. Y. Anderson., 1998. Evaluation of simple transmission line oscillators for soil moisture measurements. Computers and Electronics in Agriculture, vol. 20, issue 1: 31-44.

Campbell, G. S., and W. C. Greenway., 2005. Moisture detection apparatus and method. United States Patent, US6,904,789 B2

Chernyak, G. Ya., 1964. Dielectric methods for inverstigating moist soils.In Ogil'vi, N. A., (ed), Works of the All-Union Research Institute of Hydrology and Engineering Geology(VSEGINGEO), Moskva, New Series, No. 5. Israel Program for Scientific Translations, Jerusalem 1967.

Dean, T. J., J. P. Bell and A. J. B. Baty. 1987. Soil moisture measurement by an improved capacitance technique, Part I. Sensor design and performance. Journal of Hydrology, 93(1987) 67-78

Dishman, M. R., and Jordan, A. W., 1991. Capacitance monitor for soil moisture. United States Patent, US5260666

Dorigo, W., et al., 2011. The International Soil Moisture Network: a data hosting facility for global in situ soil moisture measurements. Hydrol. Earth Syst. Sci., 15, 1675–1698

Dorigo, W. A. 2013. The International Soil Moisture Network: Background, experiences, outlook. (http://ismn.geo.tuwien.ac.at)

Evett, S. R., J. A. Tolk, and T. A. Howell., 2006. Soil profile water content determination: sensor accuracy, axial response, calibration, temperature dependence, and precision. Vadose Zone Journal 5:894-907

Evett, S., B. Ruthhardt, S. Kottkamp, T. Howwell, A. Schneider, and J. Talk. 2002. Accuracy and precision of soil water measurements by neutron, capacitance and TDR methods. Poster presentation, 17th WCSS, Thailand.

Fares, A., A. Farhat, M. Domingos, and A. Mair. 2011. Improved Calibration Functions of Three Capacitance Probes for the Measurement of Soil Moisture in Tropical Soils. Sensors (Basel). 2011; 11(5): 4858–4874.

Fares, A., H. Hamdahani, and D. M. Jenkins. 2007. Temperature-Dependent Scaled Frequency: Improved Accuracy of Multisensor Capacitance Probes. SSSAJ, Vol. 71 No. 3, p. 894-900

Gabriel, L. J., J. I. Lizaso, M. Quemada. 2010. Laboratory versus field calibration of capacitance probes. SSSAJ: vol. 74, no. 2, 593-601

Gaskin, G., and G. D. Miller. 1996. Measurement of Soil Water Content Using a Simplified Impedance Measuring Technique. J . agric . Engng Res . (1996) 63 , 153 – 160

Gaskin, G. J., 1998. Device for determining ratio of substances. United States Patent - US5804976

Geesing, D., M. Bachmaier, and U. Schmidhalter., 2004. Field calibration of a capacitance soil water probe in heterogeneous fields.CSIRO, Australian Journal of Soil Research, 42, 289-299.

Groves, S. J., and S. C. Rose,. 2004. Calibration equations for Diviner 2000 capacitance measurements of volumetric soil water content of six soils. Soil Use and Management, 20, 96-97

Gruber, A., W. A. Dorigo, S. Zwieback, A. Xaver, and W. Wagner. 2013. Characterizing coarse-scale representativeness of in situ soil moisture measurements from the International Soil Moisture Network. Vadose Zone J. vol. 12, No. 2.

Guber, A.K., Y. A. Pachepsky, R. Rowland, and T. J. Gish., 2010. Field correction of the multisensor capacitance probe calibration. International Agrophysics 24 (1), pp. 43-49.

Hallikainen, M. T., F. T. Ulaby, M. C. Dobson, M. A. El-Rayes, and and K. L.. Wu. 1985. Microwave dielectric behaviour of of wet-soil. Part I. : Empirical modeld and experimental observatios. IEEE Trans. Geosci. Remote Sens. 23:25-34.

Hanek, L. G., M. A. Truebe, and M. A. Kestler., 2001. Using TDR and Radio Frequency (RF) devices to monitor seasonal moisture variation in forest road subgrade and base materials. USDA - Forest Service, T&D Program, and US Army - CRREL, Report, July 2001, 88pp

Hasted, J. B., 1973. Aqueous Dielectrics. Chapman and Hall, London, 302 pp

Hilhorst, M. A., 1998. Dielectric characterisation of soil. Doctoral Thesis. Wageningen Agricultural University, IMAG-DLO, Wageningen, The Netherlands, 141p.

Inoue, M., B.A. Ould Ahmed, T. Saito and M. Irshad., 2008. Comparison of Twelve Dielectric Moisture Probes for Soil Water Measurement under Saline Conditions. AJES, 4 (4): 367-372,

Irmak, S., and A. Irmak. 2005. Performance of frequency-domain reflectometer, capacitance, and pseudo-transit time-based soil water content probes in four coarse-textured soils. Appl. Eng. in Agric, 21(6): 999−1008

Irrigation Association, SWAT. 2013. List of IA-SWAT calibration reports for soil moisture sensors: calibration summaries(www.irrigation.org/swat/control-sensor)

Irrigation Association, SWAT Commiitee. 2011. Soil moisture sensor-based controllers: laboratory and operational tests. Test Protocol-Version 3.0(www.irrigation.org/swat/control-sensor)

Kaleita, A., J. L. Heitman, and S. D. Logsdon. 2005. Field calibration of the Theta probe for Des Moines lobe soils. ASABE, Appl. Eng. Agric. 21:865-870

Kargas, G., and K. X. Soulis. 2012. Performance Analysis and Calibration of a New Low-Cost Capacitance Soil Moisture Sensor, J Irrig Drain E-Asce, 138(7), 632-641.

Kelleners, T. J., R. W. O. Soppe, D. A. Robinson, M. G. Schaap, J. E. Ayars, and T. H. Skaggs. 2004 a. Calibration of Capacitance Probe Sensors using Electric Circuit Theory. Soil Sci. Soc. Am. J. 68:430–439

Kelleners, T. J., R. W. O. Soppe, J. E. Ayars, and T. H. Skaggs. 2004 b. Calibration of Capacitance Probe Sensors in a Saline Silty Clay Soil. Soil Sci. Soc. Am. J. 68:770–778

Kizito, F., C.S. Campbell, G.S. Campbell, D.R. Cobos, B.L. Teare, B. Carter, and J.W. Hopmans. 2008. Frequency, electrical conductivity and temperature analysis of a low-cost capacitance soil moisture sensor. Journal of Hydrology 352, 367– 378

Kuraz, V. 1982. Testing of a field dielectric moisture meter. ASTM Geotech. Test. J. 4:111-116

Kuraz, V., and Matousek, J., 1977. A new dielectric soil moisture meter for field measurement of soil moisture. ICID., 26:76-79

Kuraz, V., M. Kutilek, and I. Kaspar., 1970. Resonance-capacitance soil moisture meter. Soil Sci. 110:278-279

Leao, T. P., and E. Perfect., 2007. Water content estimation from dielectric permittivity measured using the Hydra Probe in disturbed and undisturbed soil samples. Paper 1.3. Symposium - 2007, Beltsville, MD, USA

Leao T. P., E. Perfect, and J. S. Tyner., 2010. Estimation of soil water content using a 50 MHz impedance sensor: soil texture, structure, and salinity interactions. Transactions of the ASABE, Vol. 53(1): 163-170

Lock, G., 2008. Moisture content sensor and related methods. United States Patent - US 2008/0211521 A1

Loiskandl, W. R., R. Stangl, and W. Sokol. 2003. Comparison of calibration methods for electromagnetic soil water sensors. In Proc. ISEME, int. Conf. on Interaction of Electromagnetic Wave with Water and Moist Substances, New Zealand, p. 234-241.

Logsdon, S. D., 2002. Dielectrics - beyond water content. Paper 1.3. Symposium 2002, Beltsville, MD, MD, USA.

Logsdon, S. D., T. R. Green, M. Seyfried, S. R. Evett, and J. Bonta. 2010. Hydra Probe and Twelve-Wire Probe comparisons in fluids and soil cores. Soil Sci. Soc. Am. J. 74: 5-12

Matula, S., K. Špongrová, W. L. Lagese, A. Klik. 2010. Evaluation of selected FDR soil moisture sensors in the laboratory conditions: Theta Probe; ECH2O EC-5, EC-10, EC-20 and EC-5 TE. Poster 4.8, Symposium - 2010, Murcia, Spain

Mead, R. M., J. E. Ayars, and J. Liu, 1995. Evaluating the influence of soil texture, bulk density and soil water salinity on a capacitance probe calibration. ASAE Paper No. 95-3264. ASAE, St. Joseph, MI, USA.

Mead, R. M., I. C. Paltineanu, J. E. Ayars, and J. Liu., 1994. Capacitance Probe Use in Soil Moisture measurements. ASAE Paper No. 942122, Kansas City, MO, USA

Miller, J. D., and G. J. Gaskin, 1998. ThetaProbe ML2x Principles of operation and applications. MLURI Technical Note (2nd ed)
Moroizumi, T., and Y. Sasaki., 2008. Estimating the Nonaqueous-Phase Liquid Content in Saturated Sandy Soil Using Amplitude Domain Reflectometry. Soil Sci. Soc. Am. J. 72:1520-1526
Mortl, A., R. Muñoz-Carpena, D. Kaplan and Y. Li , 2011, Calibration of a combined dielectric probe for soil moisture and porewater salinity measurement in organic and mineral coastal wetland soils. Geoderma 161: 50–62 (online)
Mounzer, O., I. Abrisqueta, J. M. Abrisqueta, M. C. Ruiz-Sancez and J. Vera., 2010. Volume of influence of two FDR Capacitance sensors used to measure soil water content. Paper 1.10, Symposium - 2010, Murcia, Spain
Palecki, M. A., and J. E. Bell. 2013. U.S. Climate Reference Network Soil Moisture Observations with Triple Redundancy: Measurement Variability. Vadose Zone J., Vol. 12 No. 2.
Paltineanu, I. C. 2010. Real-time soil water dynamics using capacitance, impedance and TDT - A global view. Paper 1.1. Symposium - 2010, Murcia, Spain.
Paltineanu, I. C., and I. Paltineanu, 2007. Real-time soil water dynamics monitoring using capacitance, impedance and TDT - A global view and critique. Paper 1.1, Symposium - 2007, Beltsville, MD, USA.
Paltineanu, I. C., 2004. Laboratory calibration of Delta-T ML2x soil moisture sensor on sandy soil. Paltin International Inc., Internal Report to US Army, NVSD, Fort Belvoir, VA, USA.(unpublished data)
Paltineanu, I. C. 2002. Real-time soil water dynamics monitoring using capacitance and impedance - A global view. Paper 1.1, Symposium - 2002, Beltsville, MD, USA. (www.paltin.com)
Paltineanu, I. C., and J. L. Starr. 2000. Real-time soil water dynamics. Ch. 4 Hydrology(S.4.6),in Jay H. Lehr, Ed., Standard handbook of environmental science, health and technology.McGraw-Hill, Standard Handbooks, New York, NY, USA.
Paltineanu, I. C., 2000. Laboratory calibration of Vitel - Hydra soil moisture probe on a Mattapex silt - loam soil. Paltin International Inc., Internal Report to Vitel Inc., Chantily, VA, USA(unpublished)
Paltineanu, I. C., and J. L. Starr. 1997. Real-time soil water dynamics using multisensor capacitance probes: laboratory calibration. Soil Sci. Soc. Am. J. 61:1576-1585
Paltineanu, I.C., et al., 1993. Radioactive vs. nonradioactive calibration methods for real-time measurement of soil-water-plant-atmosphere interrelationships under high evaporative demands. Final Report, pp. 203, USDA-ARS, W. M. R., Fresno, CA, USA(unpublished)
Polyakov, V., A. Fares, and M. H. Ryder. 2005. Calibration of a Capacitance System for Measuring Water Content of Tropical Soil. Vadose Zone Journal 4:1004–1010
Qi, Z., and M. J. Helmers. 2010. Soil water dynamics under winter rye cover crop in Central Iowa. Vadose Zone J. 9:53-60
Quemada, M., J. L. Gabriel, and J. Lizaso., 2010. Calibration of Capacitance Probes: Laboratory versus field procedures. Paper 1.9. Symposium - 2010, Murcia, Spain
Rallo, G., G. Giordano, and G. Provenzano. 2012. Assesing a calibration procedure to estimate soil water content with Sentek 2000 capacitance probe. EGU2012-8727(presentation.ppt)
Rallo, G., and G. Provenzano., 2014. Indirect estimation of calibration equation parameters for Sentek Diviner2000 capacitance probe by means of soil physical properties. EGU2014-2494 (poster).
Regalado, M. C., A. Ritter, and O. Garcia. 2010, Dielectric response of commercial capacitance, impedance and TDR electromagnetic sensors in standard liquid media. Paper 1.3., Symposium - 2010, Murcia, Spain.
Rosenbaum, U., J.A. Huisman, A. Weuthen, H. Vereecken, and H.R. Bogena. 2010. Sensor-to-Sensor Variability of the ECH2O EC-5, TE, and 5TE Sensors in Dielectric Liquids. Vadose Zone J. Vol. 9 No. 1, p.181–186.
Robinson, D. A., et al., 2005. Evaluation of a Capacitance Probe Frequency Response Model Accounting for Bulk Electrical Conductivity: Comparison with TDR and Network Analyzer Measurements. Vadose Zone Journal 4:992–1003
Rowland, R., A. Guber, Y. Pachepsky, and T. Gish. 2007. Comparison of plot-scale average soil water contents with data from calibrated multisensor capacitance probes. Paper 1.6., Symposium - 2007, Beltsville, MD, USA.
Rowland, R., Y. A. Pachepsky, and A. K. Guber,. 2011. Sensitivity of a capacitance sensor to artificial macropores. Soil Science, Vol. 176, No. 1, 9 - 14
Schwank, M., T. R. Green, C. Matzler, H. Benedickter, and H. Fluhler. 2006. Laboratory Characterization of a Commercial Capacitance Sensor for Estimating Permittivity and Inferring Soil Water Content. Vadose Zone J. 5:1048-1064
Schwartz, R. C., J.J. Casanova, M.G. Pelletier, S.R. Evett and R.L. Baumhardt. 2013a. Soil Permittivity Response to Bulk Electrical Conductivity for Selected Soil Water Sensors. VZJ, Vol. 12 No. 2
Schwartz, R. C., J.J. Casanova, J. M. Bell, and S. R. Evett. 2013b. A Reevaluation of Time Domain Reflectometry Propagation Time Determination in Soils. VZJ, Vol. 13 No. 1.
Scobie, M., 2006. Sensitivity of Capacitance Probes to Soil Cracks. Disertation - Research Project for Bachelor of Engineering (Environmental), Faculty of Engineering and Surveying, University of Southern Queensland, Australia, 67pp
Scudiero, E., A. Berti, P. Teatini, and F. Morari., 2012. Simultaneous Monitoring of Soil Water Content and Salinity with a Low-Cost Capacitance-Resistance Probe. Sensors 2012, 12, 17588-17607;
Seyfried S. M., and M. D. Murdock., 2002. Effects of soil type and temperature on soil water content measurement using a soil dielectric sensor. Paper 1.6., Symposium - 2002, Beltsville, MD, USA
Seyfried M. S., and Mark D. Murdock., 2004. Measurement of Soil Water Content with a 50-MHz Soil Dielectric Sensor. Soil Sci. Soc. Am. J. 68:394–403
Silva, C. R. da., A. S. Andrade Junior, J. Alvez Junior, A. B. Sousa, de., F. B. Melo, de., and M. A. Coelho Filho. 2007. Calibration of Diviner 2000® capacitance probe in a Rhodic Paleudult. Scientia Agricola, v. 64, p. 636-640
Smith-Rose, R. L., 1935. The electrical properties of soil at frequencies up to 100 megacycles per second; with a note on the resistivity of ground in the United Kingdom. Proc. Phys. Soc. 47 923
Smith-Rose, R. L., 1933. The electrical properties of soil for alternating currents at radio frequencies. Proc. Royal Society of London, Volume 140, Issue 841, pp. 359-377
Starr, J. L., and I. C. Paltineanu, 2002. Capacitance devices. The soil solution phase, 3.1.3.6, In: Dane, J. H., and G. C. Topp, Co-editors, Methods of Soil Analysis, Part 4 - Physical Methods. P. 463-474, SSSA Book Series No. 5, SSSA Inc., Madison Wisconsin, USA.

Starr, J. L., D. J. Timlin, P. M. Downey, and I. R. McCann,. 2009. Laboratory evaluation of dual-frequency multisensor capacitance probes to monitor soil water and salinity. Irrig Sci (2009) 27:393–400

Thomas, A. M., 1966. In-situ measurement of moisture in soil and similar substances by 'fringe capacitance'. J. Sci. Instrum. 43:21-27

Topp, C. G., and P.A. (Ty) Ferre., 2002. Sub-chapter: 3.1.3.3.c., In: Dane and Topp, Co-editors, Methods of Soil Analysis, Part 4 - Physical Methods. P. 432-433, SSSA Book Series No. 5, SSSA Inc., Madison, WI, USA.

Topp, C. G., J. L. Davis, and A. P. Annan, 1980. Electromagnetic determination of soil water content: Measurements in coaxial transmission lines. Water Resources Research, Vol. 16, No. 3, Pages 574-582.

Tsegaye, T. D., W. Tadese, T. L. Coleman, T.J. Jackson. 2002. A modified technique to measure near surface soil moisture using an impedance probe. Paper 3.3. Symposium - 2002, Beltsville, MD, USA.

Tsegaye, T. D., W. Tadesse, T. L. Colman, T. J. Jackson, and H. Tewolde. 2004. Calibration and modification of impedance probe for near surface soil moisture measurements. Canadian Journal of Soil Science, 84:237-243

Vaz, C. M. P., S. Jones, M. Meding and M. Tuller. 2013. Evaluation of Standard Calibration Functions for Eight Electromagnetic Soil Moisture Sensors. Vadose Zone J., Vol. 12 No. 2

Vaz, C. M. P., S. B. Jones, M. Meding, and M. Tuller., 2014a. Evaluation of Eight Electromagnetic Sensors for Measuring Water Content and Electrical Conductivity in Mineral, Organic and Saline Soils. Poster 4.1, Symposium - 2014, Montreal, Canada

Vaz, C. M. P., S. Jones, and M. Tuller., 2014b. Calibration of EM sensors using acetic acid-water mixtures. Poster 4.2, Symposium - 2014, Montreal, Canada

Visconti, F., et al., 2014a. Laboratory and field assessment of the capacitance sensors Decagon 10HS and 5TE for estimating the water content of irrigated soils. Agricultural Water Management, 2014, vol. 132, issue C, pages 111-119

Watson, K., R. Gatto, P. Weir, and P. Buss. 1995. Moisture and salinity sensor and method of use, United States Patent, US005418466A

Weast, R. C., (ed). 1980. Handbook of chemistry and physics. 61st ed., CRC Press, Boca Raton, Florida, USA.

Williams, B., et al.,. 2003. Laboratory Calibration and Initial Results of a Soil Moisture Monitoring System at the Mt Leyshon Tailings Dam and Waste Rock Cover System. 6th ICARD, Cairns, QLD, 12 - 18 July 2003, 411-417.

Yoder, R. E., D. L. Johnson, J. B. Wilkerson, and D. C. Yoder. 1998. Soil water sensor performance. Appl. Eng. Agric. 14: 121-133.

TRANSACTIONS OF THE FOURTH INTERNATIONAL SYMPOSIUM ON SOIL WATER
MEASUREMENT USING CAPACITANCE, IMPEDANCE AND TDT
MONTREAL, CANADA, JULY 16 – 18, 2014

STATE OF THE ART, PAPER 1.2

Comparison of SMOS Level 2 and Level 3 Soil Moisture at the SMOSREX Site

Arnaud Mialon (1), F. Cabot (1), S. Guibert (2), A. Al bitar (1), P. Richaume(1), J.-P. Wigneron (3), T. Pellarin (4), S. Tarot (5), S. Bircher (1), J. Grant (6), Nemesio Rodriguez-Fernandez (1), Y. H. Kerr (1).
arnaud.mialon@cesbio.cnes.fr

(1) CESBIO, 18 Av. Edouard Belin, BPI 2801, 31401 Toulouse, Cedex 9, France.
(2) CNES, Av. Edouard Belin, 31401 Toulouse, France.
(3) INRA EPHYSE, Bordeaux, France
(4) LTHE, Grenoble, France.
(5) IFREMER, Brest, France.
(6) Department of Physical Geography and Ecosystem Science, University of Lund, Sweden.

Abstract

The ESA (European Space Agency) satellite mission SMOS (Soil Moisture and Ocean Salinity) was launched in November 2009 and has been providing data on ocean salinity and soil moisture over continental surfaces for the last 4 years. SMOS satellite is a passive L-band (1.4 GHz) interferometer that measures the surface soil moisture (top 5cm) with an overpass time at 6 am and 6 pm (local time) and a radiometric resolution of ~ 43 km in average. With a quasi polar orbit, it covers the entire Earth surface in 3 days.

The CATDS (Centre Aval de Traitements des Données SMOS) ground segment developed by the French space agency CNES, provides so called “level 3” soil moisture products that are time aggregated products, on the EASE (Equal Area Scalable Earth) Grid with a ~25 km spatial resolution. The retrieval algorithm is based on the radiative model L-MEB (L-band Microwave Emission of the Biosphere).

The aim of this paper is to present the different soil moisture products that are delivered by the CATDS such as daily products, 3-day and 10-day composites, monthly averages, discuss different features of the product contents, and also presenting the validation of the SMOS data. Several in-situ sites are equipped with various soil moisture sensors providing soil moisture measurements for different climate areas. For instance, the SMOSREX (Surface Monitoring of the Soil Reservoir Experiment) site was developed to test the SMOS soil moisture retrieval algorithm.

Two fields (bare soil and grassland) were monitored with Delta-T theta probes and a cosmic ray neutrons probe that measures the soil moisture over a large area (~ 700m). This site was stopped in 2012 which provides us with more than two years of data that can be compared to SMOS derived soil moisture values.

I - INTRODUCTION

The ESA (European Space Agency) SMOS satellite mission (Soil Moisture and Ocean Salinity) was launched in November 2009 and has been providing data on ocean salinity and soil moisture for the last 4 years. SMOS is a passive L-band (1.4 GHz) interferometer measuring the surface soil moisture (top 5cm) with an overpass time at 6 am and 6 pm (solar time). With a quasi polar orbit, it covers the entire Earth surface in 3 days (Mecklenburg et al., 2012).

Three ground segments have been producing and delivering SMOS data. The focus here is put on ESA level 2 soil moisture (Mecklenburg et al., 2012) and CNES (Centre Nationales d'Etudes Spatiales, France) level 3 products from the CATDS (Centre Aval de Traitement des Données SMOS) (Guibert et al., 2013). The main differences are: i) the level 3 algorithm takes advantage of three SMOS overpasses and uses a correlation function (Al Bitar et al., 2010) for the vegetation components; ii) ESA level 2 is on the isea4h9 grid with a spatial resolution of 15 km (Kerr et al., 2012) whereas the CATDS level 3 products are on the EASE Grid (Equal Area Scalable Earth Grid) defined at ~ 25 km ; iii) level3 products use the NETCDF (Network Common Data Form) format, commonly used and for which many tools exist to read the data, whereas the level 2 is using the binX format.

Validation efforts have been established for the SMOS soil moisture level 2 products at different sites such as Australia, the US (Al Bitar et al. 2012, Leroux et al. 2014), in Denmark (Bircher et al. 2012), in Spain (Wigneron et al. 2012). The aim of this study is to present the SMOS level 2 and level 3 over the experimental site SMOSREX (Surface Monitoring Of the Soil Reservoir EXperiment, de Rosnay et al. 2006) located in the South of France.

II - SMOS DATA

SMOS ESA level 2 soil moisture data are produced per half-orbit and separate the ascending (~ 6 am, local solar time) from the descending (~ 6 pm, local solar time) overpasses. The complete description of the algorithm is available in Kerr et al. (2012). Data that are used in this paper are obtained using the version 5.51 of the processor. The CATDS level3 products are time composite products (Jacquette et al. 2010), aggregated over several time windows: 1 day, 3 days to have a complete coverage of the Earth Surface; 10 days containing the minimum, the median and the maximum of soil moisture values observed during that period; monthly averages. These products have different applications from weather forecast (level 3 1-day product) to water management (level 3 10-day product) and contain the derived parameters such as the soil moisture and the optical thickness among other useful information (such as quality flags). A complete description of the content of the products is available in Berthon et al. (2012) and the data are obtained using version 2.5 of the level 3 processor. These versions of level 2 and level 3 are also different for the computation of the dielectric model (Kerr et al. 2011, Kerr et al. 2012) of soil. The dielectric constant depends on soil properties (texture, soil temperature) and on soil moisture especially at L-band. The dielectric constant controls the soil emission and so the brightness temperatures monitored by passive instruments like radiometers and SMOS interferometer. The SMOS level 2 data uses the Dobson model (Dobson et al. 1985, Hallikainen et al. 1985, Peplinski et al. 1995) whereas the level 3 uses the Mironov model (Mironov et al. 2009), which can lead to a slight difference in terms of derived soil moisture values. Globally, the use of the Mironov dielectric model tends to retrieve higher soil moisture values compared to the Dobson model (Mialon et al. 2012).

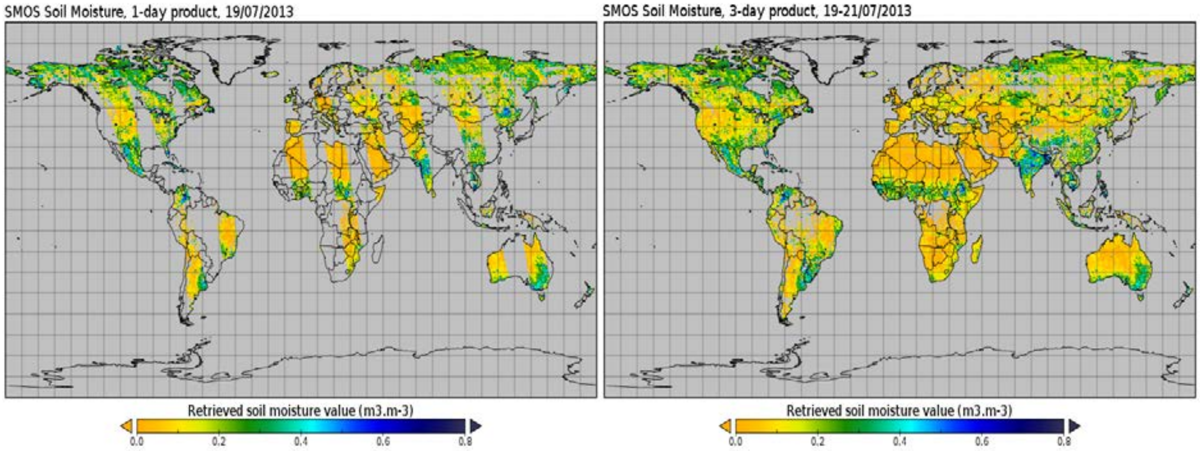

Figure 1 : Example of SMOS level 3 soil moisture map, from 1-day product (left figure) and from 3-day product (right figure)

Figure 1 shows an example of the soil moisture values as provided in a 1-day product for the ascending orbits of July 19, 2013 (left Figure), where the overpasses do not cover the entire Earth surface. Right Figure 1 presents a 3-day product obtained by selecting the best estimation of the soil moisture over a 3 day window, July 19-21, 2013. This selection is based on a data quality index (Kerr et al. 2013) associated with each retrieved parameter. Using a 3-day window allows a better surface cover compared to the 1-day product. The low values of soil moisture over Europe are consistent with the dry and hot weather conditions observed in mid-July 2013. On the other hand, Eastern Australia reported rain events[1] that lead to an increase in the surface soil moisture.

Although SMOS is operating in a protected band it is facing the important problem of man-made RFI (Radio Frequences Interferences) (Oliva et al. 2012, Richaume et al. 2010) increasing the brightness temperatures and so hampering the retrieval of soil moisture. It is thus necessary to filter out the data affected by these interferences based on indicators provided in the SMOS product. Generally it was found that SMOS derived soil moisture values associated with data quality index values lower than 0.07 m^3/m^3 and a RFI probability lower than 10 % (less than 10% of brightness temperatures affected by RFI) can be used with confidence.

III-SMOSREX site

SMOSREX was an experimental site near Toulouse in the South West of France. This site was developed to improve the SMOS algorithm over bare soil and grassland and was operational from 2003 and 2012, with the last 2 years in common with SMOS.

The soil is characterized by a clay content of 17%, a sand content of 36% and a silt content of 47% (de Rosnay et al. 2006). A set of soil moisture probes monitors the soil moisture content every 30 minutes at different depths, from surface (top 0-6 cm) down to 90 cm. For this study we focus on the bare field soil. As SMOS measures the soil moisture content of the top 5 cm or even less (Escorihuela et al. 2010), only the top surface probes are considered

---

[1] Australian Bureau of Meteorology, see http://www.bom.gov.au/jsp/awap/rain/archive.jsp?colour=colour&map=totals&year=2013&month=7&day=21&period=week&area=nat

for this study. Five Delta-T theta probes (ML2X) [2] were installed at the surface covering an area of ~ 2 m^2 and calibrated individually with the following protocol : at sixty occasions during the experiment time, soil samples were collected (6 samples each time), weighed and dried to obtain the soil moisture content (Schmugge et al .1980). The corresponding probe outputs (in Volt) and the measured soil moisture contents allowed us to define a linear relationship (as recommended by the manufacturer) between the probe measurements and the soil moisture. For the present study, we consider the average of the ML2X theta probe soil moisture as our reference. Since February 2011, a cosmic-ray probe was installed, also referred to as COSMOS (COsmic-ray Soil Moisture Observing System, Zreda et al. 2008). This probe measures soil moisture over a footprint with a diameter of ~ 670 m (86% of the signal) on an hourly basis. This encompasses the bare soil field but also the grassland part. The influencing soil depth depends on the soil moisture content from the top layer (~12 cm) for wet conditions to deeper layers (~ 76 cm) for dry conditions (Zreda et al. 2012). The monitored layer is different from the one that SMOS is sensitive to, but the probe presents the advantage of integrating the signal over a large footprint contrary to the Delta-T theta probes measuring the soil moisture content at a single location. This probe has also been calibrated for site specific conditions using ground samples (more than 100) so that the associated error is ~ 0.01 m^3/ m^3. A complete description of the procedure for cosmos probes calibration is detailed in Zreda et al. (2012) and the following parameters have been found for the SMOSREX site to convert the cosmic-ray outputs to soil moisture values: cutoff rigidity of 5.34 GV, mean pressure of 990 mB, lattice water of 3%, soil organic carbon content of 0.76% and maximum count rate of 2575 per hour.

IV- RESULTS

IV-A- Soil Moisture Calibration

The theta probe devices are commonly used to monitor soil moisture (Wigneron et al. 2012). A calibration function is given to convert the measured signal in volts into a soil moisture value (m^3/m^3). It is recommended to perform a site specific calibration using soil samples collected on site which is presented in Figure 2.

---

[2] Mention of manufacturers is for the convenience of the reader only and implies no endorsement on the part of the authors

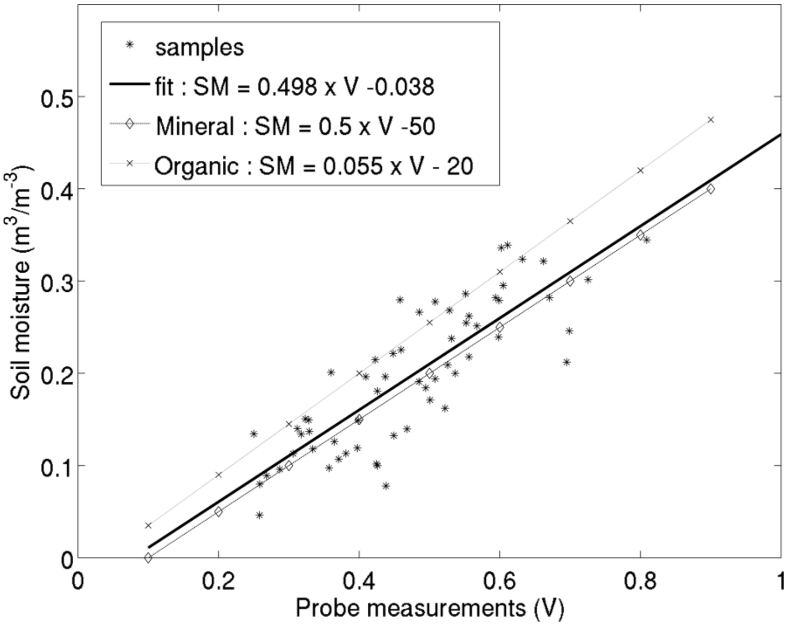

Figure 2: Relationship between soil moisture and theta probe output. Stars are the soil samples; black line is the best fit; light grey line with crosses is the manufacturer's relationship for organic soils and grey line with diamonds is the manufacturer's relationship for mineral soils.

Figure 2 shows the relationship SM = 0.0498 x V - 0.038 derived from 60 collected points (RMSE=0.043, R=0.83) spanning a wide range of soil moisture conditions. The manufacturer provides the users with two fitting curves for mineral and organic soils (light grey lines in Figure 2). The fitted curve is very close to the default one for mineral soil, the difference being within the accuracy of the probe, which is of +/- 0.05 m^3/m^3 according to the manufacturer. It was still decided to use the fitted relationship.

IV-B- Soil Moisture Comparison

Figure 3 presents time series of soil moisture values measured by theta probes (average of the 5 probes) and derived from SMOS observations (level2 and level3 products). Due to technical issues, some in-situ data are missing in October, November 2010 and January 2011.

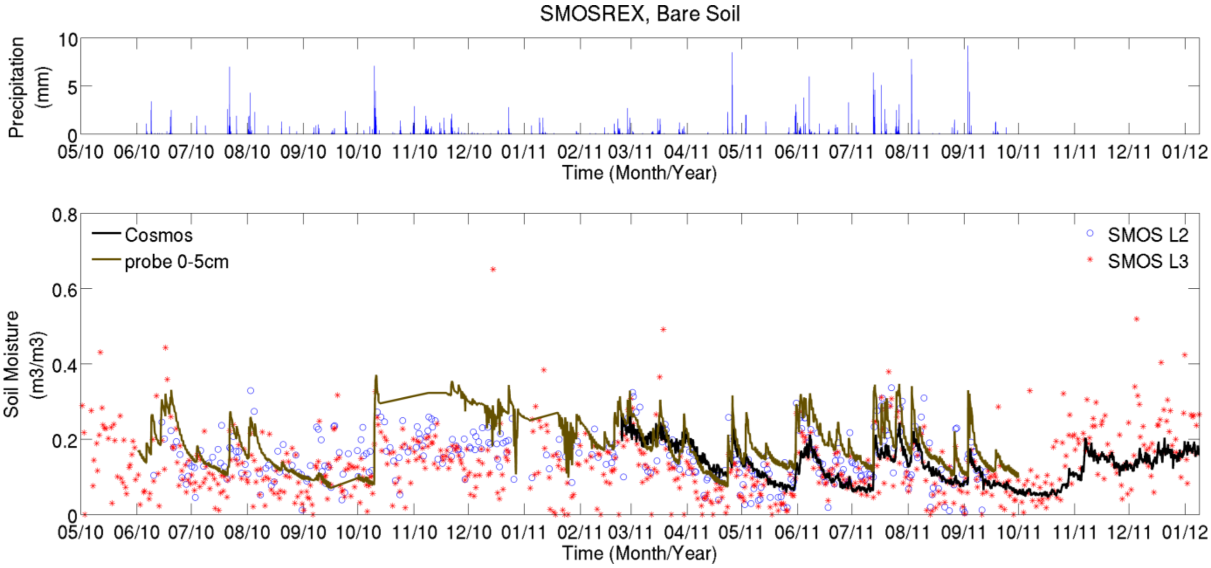

Figure 3: Measures at the SMOSREX site. Top is the precipitation, bottom is the soil moisture from : delta T theta probe sensors (average) in brown, cosmic ray in black, SMOS level 2 as blue circles and SMOS level 3 as red stars.

Both SMOS products perform relatively well catching all the precipitation events (red and blue in Figure 3) but they underestimate the soil moisture measured by the ML2X theta probe (brown in Figure 3) with a negative bias of 3% for the level 2 and 6% for the level 3 (Figure 4). SMOS level 3 data show lower values (higher absolute bias) compared to SMOS level 2 as the latter uses the Mironov dielectric constant model (Mironov et al. 2009) whereas the level 3 uses Dobson (Dobson et al., 1985). Since January 2014, both levels 2 and 3 of SMOS products are using the same dielectric model that is the Mironov one. The cosmic-ray measurements show similar results to SMOS level 3 (Figure 4) but agree better in terms of statistics (R=0.68 and a negative bias of 4.5%) with the theta probe measurements. Figure 4 presents the different soil moistures series (SMOS and Cosmos) as a function of delta-T theta probe data. SMOS level 3 (red in Figure 4) and cosmos (black circles in Figure 4) underestimate the ML2X theta probe soil moisture values, whereas the cosmos probe presents a better correlation coefficient. This result is expected as SMOS measurements cover a larger (radiometric resolution of ~ 40 km average, Kerr et al. 2012) and heterogeneous area (in terms of land cover) whereas the cosmos probe is representative of the field monitored by the probe even though the measurement depth is different.

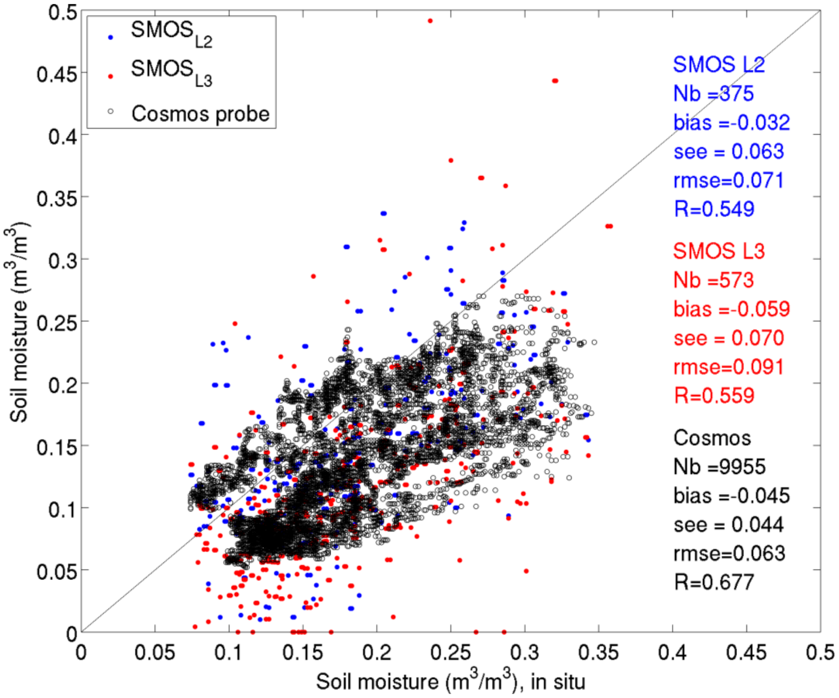

Figure 4: Soil moisture measured by the cosmic-ray probe (empty black squares), SMOS level 2 (blue dots) SMOS level 3 (red dots) as a function of delta-T theta probe soil moisture values (surface probes) at the SMOSREX site.

V- DISCUSSION AND CONCLUSION

This paper compares the SMOS products ESA level 2 and CATDS level3 for the SMOSREX experimental site in France. Two sorts of probe are used at this site to monitor soil moisture: Delta T Theta probes and a cosmic-ray probe. Both probes were calibrated by collecting soil samples to derive fitting curves to convert the probe output to soil moisture values based on site-specific soil characteristics. Some more work has to be done to derive a surface soil moisture value from the cosmic-ray probe to be comparable to SMOS data, but its spatial resolution is of real interest to validate satellite observations. One has to be careful when comparing data obtained at different scales (Wigneron et al. 2012), but SMOS level 2 and 3 agree relatively well with the Delta-T probe measurements and catch the rain events. Even though the probes give soil moisture values that are different from what is derived from SMOS due to the different scales, the good agreement between the dataset proves the interest of the SMOSREX site. The site provides us with a reference for the validation of SMOS data to evaluate the mission performance (Al Bitar et al. 2010, Leroux et al. 2014, Wigneron et al. 2012). Once the RFI are filtered out from SMOS dataset, the in situ measurements can be used to test and check the consistency of the different releases of the SMOS products (different versions of level 2 and level 3).

VI- REFERENCES

Al Bitar, A., E. Jacquette, O. Merlin, Y. Kerr, A. Mialon, A. Quesney, F. Cabot, P. Richaume, 2010. Multi-orbit inversion of SMOS surface soil moisture, IGARSS, 25-30 July 2010, Honolulu, USA, 2010.

Al Bitar, A., D. Leroux, Y. Kerr, O. Merlin, P. Richaume, A. Sahoo, and E. Wood, 2012. Evaluation of SMOS Soil Moisture Products Over Continental U.S. Using the SCAN/SNOTEL Network, Geoscience and Remote Sensing, IEEE Transactions on, vol. 50, no. 5, pp. 1572 –1586, DOI:10.1109/TGRS.2012.2186581.

Berthon, L., A. Mialon, F. Cabot, A. Al Bitar, P. Richaume, Y. Kerr, D. Leroux, S. Bircher, H. Lawrence, A. Quesney, and E. Jacquette, 2012. CATDS LEVEL 3 Data Product Description - Soil Moisture and Brightness Temperature part, CBSA, Tech. Rep. SO-TN-CB-CA-0001, Issue 1.b, 2012, 36 p., http://www.cesbio.ups-tlse.fr/SMOS_blog/wp-content/uploads/DOCS/SO-TN-CB-CA-0001.1b.pdf

Bircher, S., N. Skou, K. Jensen, J. Walker, and L. Rasmussen, 2012. A soil moisture and temperature network for smos validation in western denmark, Hydrology and Earth System Sciences, vol. 16, pp. 1445–1463, DOI:10.5194/hess-16-1445-2012.

de Rosnay, P., J. Calvet, Y. Kerr, J. Wigneron, F. Lemaître, M. Escorihuela, J. Sabater, K. Saleh, J. Barrié, G. Bouhours et al., 2006. SMOSREX: A long term field campaign experiment for soil moisture and land surface processes remote sensing, Remote Sens. Environ., vol. 102 (n 3-4), p377–389.

Dobson, F. Ulaby, M. Hallikainen, and M. El-Rayes, 1985. Microwave dielectric behavior of wet soil-part ii: dielectric mixing models, Geosci. Remote Sens.,vol GE-23 (no.1), pp.35–46, DOI:10.1109/TGRS.1985.289498.

Escorihuela, M.J., A. Chanzy, J. Wigneron, and Y. H. Kerr, 2010. Effective soil moisture sampling depth of l-band radiometry: A case study, Remote Sensing of Environment, vol. 114, no. 5, pp. 995 – 1001, DOI:10.1016/j.rse.2009.12.011.

Guibert, S., Tarot, S., Cabot, F., Hourcastagnou, J-N., Larigauderie, C., Kerr, Y.H., Reul, N., Boutin, J., 2013. Presentation of the CATDS Description of the SMOS L3 Products Generation and Dissemination, ESA living planet Symposium 9-13 Sept. 2013, Edinburgh (UK).

Hallikainen, M., F. Ulaby, M. Dobson, M. El-Rayes, and L.-K. Wu, 1985. Microwave dielectric behavior of wet Soil-part 1: Empirical models and experimental observations, IEEE T Geosci Remote, vol. GE-23, pp. 25–34, DOI:10.1109/TGRS.1985.289497.

Jacquette, E., A. Al Bitar, A. Mialon, Y. Kerr, A. Quesney, F. Cabot, and P. Richaume, 2010. SMOS CATDS level 3 global products over land, in Proc. SPIE 7824, 78240K(2010).

Kerr, Y.H, P. Waldteufel, P. Richaume, J.-P. Wigneron, P. Ferrazzoli, and R. Gurney, 2011. SMOS level 2 processor for soil moisture - Algorithm Theoretical Based Document (ATBD), CBSA, Tech. Rep. SO-TN-ESL-SM-GS-0001, Issue 3.e, 121 p., http://www.cesbio.ups-tlse.fr/fr/indexsmos.html.

Kerr, Y.H., P. Waldteufel, P. Richaume, J. P. Wigneron, P. Ferrazzoli, A. Mahmoodi, A. Al Bitar, F. Cabot, C. Gruhier, S. E. Juglea, D. Leroux, A. Mialon, and S. Delwart, 2012. The SMOS Soil Moisture Retrieval Algorithm, Geoscience and Remote Sensing, IEEE Transactions on, vol. 50, no. 5, pp. 1384 –1403, DOI:10.1109/TGRS.2012.2184548.

Leroux, D., Y. H. Kerr, A. Al Bitar, R. Bindlish, T. Jackson, B. Berthelot, G. Portet, 2014. Comparison Between SMOS, VUA, ASCAT, and ECMWF Soil Moisture Products Over Four Watersheds in U.S., Trans. Geosc. Remote Sens., vol. 52, no. 3, pp. 393–405. DOI:10.1109/TGRS.2013.2240691.

Mecklenburg, S, M. Drusch, Y. H. Kerr, J. Font, M. Martin-Neira, S. Delwart, G. Buenadicha, N. Reul, E. Daganzo-Eusebio, R. Oliva, and R. Crapolicchio, 2012. ESA's Soil Moisture and Ocean Salinity Mission: Mission Performance and Operations, Geoscience and Remote Sensing, IEEE Transactions on, vol. 50, no. 5, pp. 1354 – 1366, DOI:10.1109/TGRS.2012.2187666.

Mialon, A., P. Richaume, D. Leroux, K. Y. Al Bitar, A., F. Cabot, and J.-P. Wigneron, 2012. Comparison of dielectric models in SMOS soil moisture retrieval, in IGARSS 2012, July 22-27, Munich, Germany, 2012.

Mironov, V.L., S. V. Fomin, 2009. Temperature and Mineralogy Dependable Model for Microwave dielectric spectra of Moist Soils, PIERS Online, vol. Vol. 5, N. 5, pp. 411–415, DOI:10.2529/PIERS090220054025.

Oliva, R., E. Daganzo Eusebio, Y. H. Kerr, S. Mecklenburg, S. Nieto, P. Richaume, and C. Gruhier, 2012. SMOS Radio frequency Interference Scenario: Status and Actions Taken to Improve the RFI Environment in the 1400-1427 MHz Passive Band, IEEE T. Geosc. Remote, vol. 50 (no 5), pp. 1427–1439, DOI:10.1109/TGRS.2012.2182775.

Peplinski, F. Ulaby, and M. Dobson, 1985. Dielectric properties of soils in the 0.3-1.3-GHz range, IEEE T. Geosci. Remote, vol. 33, no. 3, pp. 803–807.

Richaume, P., C. Gruhier, Y. Kerr, F. Cabot, A. Mialon, J. Pla, E. Daganzo, R. Oliva, 2010. Characterization of SMOS RF inteferences in the 1400-1427 MHz band as detected during the comissioning phase, in RAQRS, 27 September- 1 October 2010, Valencia, Spain.

Schmugge, T.J., T. J. Jackson, and H. McKim, 1980. Survey of methods for soil moisture determination, Water Resour. Res., vol. 16(6), pp. 961–979, DOI:10.1029/WR016i006p00961.

Wigneron, J.-P., M. Schwank, E. Lopez Baeza, Y. H. Kerr, N. Novello, C. Millan, C. Moisy, P. Richaume, A. Mialon, A. Al Bitar, F. Cabot, H. Lawrence, D. Guyon, J. C. Calvet, J. P. Grant, T. Casal, P. de Rosnay, K. Saleh, A. Mahmoodi, S. Delwart, and S. Mecklenburg, 2012. First evaluation of the simultaneous SMOS and elbara-II observations in the mediterranean region, Remote Sensing of Environment, vol. 124, pp. 26 – 37 DOI:10.1016/j.rse.2012.04.014.

Zreda, M., D. Desilets, T. Ferre, and R. L. Scott, 2008. Measuring soil moisture content non-invasively at intermediate spatial scale using cosmic-ray neutrons, Geophys. Res. Letters, 35, L21402, DOI = 10.1029/2008GL035655.

Zreda, M., W. J. Shuttleworth, X. Zeng, C. Zweck, D. Desilets, T. Franz, and R. Rosolem, 2012. COSMOS: the COsmic-ray Soil Moisture Observing System, Hydrol. Earth Syst. Sci., vol. 16, pp. 4079–4099, DOI:10.5194/hess-16-4079-2012.

STATE OF THE ART, PAPER 1.3

Soil Moisture and Dielectric Constant Measurements of Organic Soils in the Higher Northern Latitudes in Support of the SMOS Mission

Simone Bircher[1], S. Razafindratsima[2] , F. Demontoux[2], M. Andreasen[3] , J. Vuollet[4], K. Rautiainen[4], F. Jonard[5], L. Weihermüller[5], P. Richaume[1] , A. Mialon[1], J.-P. Wigneron[6], Y. H. Kerr[1]*

1. Centre d'Etudes Spatiales de la Biosphère, Toulouse, France
2. Laboratoire de l'Intégration du Matériau au Système, Bordeaux University, Bordeaux, France
3. Department of Geosciences and Natural Resource Management, University of Copenhagen, Denmark
4. Finnish Meteorological Institute, Helsinki, Finland
5. Institute of Bio- and Geosciences Agrosphere (IBG-3), Forschungszentrum Jülich GmbH, Germany
6. Division Ecologie fonctionelle et Physique de l'Environnement, INRA, Bordeaux-Aquitaine, France

* Corresponding author: simone.bircher@cesbio.cnes.fr

ABSTRACT

The SMOSHiLat project aims at increasing our insufficient understanding of L-band (1.4 GHz) emission behaviour of organic soils in the higher northern latitudes in order to support soil moisture product generation from the Soil Moisture and Ocean Salinity (SMOS) satellite over these regions. Evaluation of two soil moisture sensors (Decagon 5TE and Delta-T ThetaProbe) for organic horizons and L-band dielectric constant measurements are being carried out on samples collected in Denmark, Finland, Scotland and Siberia. Here, focus is on the presentation of the material, applied methods and first results that show consistent trends, in agreement with other studies using TDR sensors. The observed dielectric constants of the organic substrate at a given water content are decreased compared to sandy mineral soils due to high water binding capabilities of the former. The current ongoing data analyses including the derivation of organic calibration functions shall be presented at the symposium.

I - INTRODUCTION

Organic-rich soils are typical for the circumpolar northern cold climate zone (boreal forest/tundra). Due to above-average rising temperatures in the higher northern latitudes, a large amount of these important carbon sinks might be released, possibly causing a significant positive feedback on global warming (e.g. Stokstad 2004). Hydrology plays a key role, but the overall response of these soils remains currently highly uncertain. Thus, there is a strong need to monitor hydrologic states and water redistribution processes in these regions.

The only means to acquire such observations at high temporal resolution and with complete spatial coverage are by spaceborne remote sensing techniques. The European Space Agency's (ESA) Soil Moisture and Ocean Salinity (SMOS) mission (Kerr et al. 2001) carries the first space-borne passive L-band microwave (1.4 GHz) radiometer on board. It acquires global brightness temperatures (TB) from which surface soil moisture is retrieved, taking advantage of the very large difference between the dielectric constant (also referred to as relative permittivity, ε) of dry soil and liquid water. The retrieval algorithm is based on the inversion of the L-band Microwave Emission of the Biosphere (L-MEB) radiative transfer model (Wigneron et al. 2007) using tuning parameters derived from study sites in dry and warm temperate climate zones

In order to improve our understanding of L-band emission of organic soil surface layers and thus, enhance the quality of SMOS soil moisture data in the higher northern latitudes, the ESA project "SMOSHiLat" has been initiated (http://due.esrin.esa.int/stse/projects/stse_project.php?id=179). Its aim is to adapt and calibrate the L-MEB model for organic soils encountered in Northern regions and test it in the SMOS soil moisture prototype retrieval algorithm in view of its implementation in the operational one. In a first step, a database is created including measured and modelled key parameters of the radiative transfer chain from Northern study sites, i.e. L-band TBs and soil dielectric constants, in situ soil moisture, temperature and soil characteristics. In this context, an important issue is soil moisture sensor calibration for organic-rich material to relate the acquired sensor response (a function of ε) to soil moisture. While several studies have investigated the influence of organic matter content on the Time Domain Reflectometry (TDR) sensors (e.g. Topp et al. 1980, Schaap et al. 1996, Jones et al. 2002, Vaz et al. 2013), such analyses are sparse for impedance and capacitance sensors, though the latter are widely used due to their significantly lower costs. Therefore, two sensors, Delta-T ThetaProbe ML2x (impedance) and Decagon 5TE (capacitance)[1,] are being calibrated for variable organic matter content using both field and lab measurements from mainly two study sites in Northern Finland and Denmark. While these sensors measure at 100 and 70 MHz, respectively, dielectric constant measurements are also being carried out at the L-band frequency using two complementary approaches (rectangular wave-guide and resonant cavity techniques).

In this paper, the sensor calibration and L-band dielectric constant measurements are presented and discussed. As analyses are still ongoing, here focus is on the presentation of the study sites, material and applied methods. Some preliminary results are shown and an outlook is given on the work that will be presented during the symposium.

II – STUDY SITES

An overview over the study locations is given in Figure 1. This experiment includes primarily the two main SMOSHiLat test sites in Finland (Finnish Meteorological Institute, FMI), and Denmark (Hydrologic Observatory, HOBE). The FMI's Arctic Research Centre is situated in Sodankylä in the boreal (coniferous forest) zone of Northern Finland. The prevailing soil type is podsol of mainly very sandy texture and overlying organic surface layers. Samples were collected from a heathland area within a forest clearing as well as under spruce. At both locations, a Decagon 5TE soil moisture and soil temperature station with sensors at 5, 10, 20, 40, and 80 cm depths, respectively, is placed.

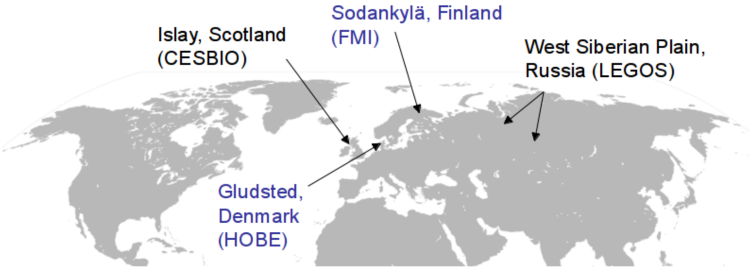

Figure 1: Overview over all sampling locations

---

[1] Mention of manufacturers is for the convenience of the reader only and implies no endorsement on the part of the authors

In Denmark, the selected HOBE test site is situated within the Gludsted spruce plantation in the Skjern River Catchment. Soil samples were mainly collected in the forested parts and to a small amount in a heathland area. The naturally occurring soil type is again podsol of coarse sandy texture with pronounced organic surface layers. Several soil moisture and soil temperature stations are distributed in the forest, including Decagon 5TE sensors at 5, 25 and 55 cm depths of the mineral soil as well as in the organic surface layer.

Furthermore**,** organic samples were collected in two peatlands on the Island Islay in Western Scotland, GB, (Centre d'Etudes Spatiales de la Biosphère, Toulouse), and on the West Siberian Plain, Russia, from a tundra area and a bog as well as a forest farther south (Laboratoire d'Etudes en Géophysique et Océanographie Spatiales, Toulouse).

III – MATERIAL AND METHODS

III - A - Soil Moisture Calibration

Calibration of the electromagnetic sensors, Delta-T ThetaProbe ML2x (impedance) and Decagon 5TE (capacitance), is being carried out. The ThetaProbe ML2x is a soil moisture sensor with four 6-cm long rods building an array whose impedance varies with a medium's water content (Delta-T Devices Ltd., 1999). The voltage output is proportional to the soil's dielectric constant and related to water content using the manufacturer's calibration curves for mineral and organic substrates. The probe has been widely evaluated and some calibration functions for organic material were derived (see Vaz et al. 2013). The Decagon ECH2O 5TE uses the capacitance method to measure around three 5.2 cm long prongs (Decagon Devices Inc., 2014). From the raw sensor output the dielectric constant is estimated dividing by 50. By default, the Topp equation for mineral soils (1980) is used to calculate soil moisture. Thus far, calibration for organic material has only been conducted by Vaz et al. (2013) for a plant potting mix. Curves for natural organic soils are lacking. The dielectric constants observed by 5TE sensors and ThetaProbes correspond mainly to the real part (ε'), but as the measurements are sensitive to the imaginary part (ε'') to some extent (e.g. Blonquist et al., 2005), the term “apparent dielectric constant” (ε_a) is used.

Most calibration measurements on different mineral and organic soil horizons were conducted at the Finish and Danish sites in the lab. At the HOBE forest site a field experiment was also carried out in order to validate the lab approach. To avoid increasing water content underestimation towards the dry end due to shrinkage effects of the organic matter (e.g. Schaap et al., 1996) the material was previously saturated. Subsequently, it was allowed to undergo a natural dry down in order to consider the changing volume during the sampling process. In case of lab calibration, saturated bulk densities were estimated in the field and the collected material packed accordingly in large buckets. In the center of each bucket one 5TE sensor was installed horizontally with the blade in vertical direction to avoid pounding of water. These measurements were logged continuously, while ThetaProbe readings and gravimetric samples were taken sporadically. The latter were oven-dried at 105 ºC during 24 hours and at 85 ºC during 48 hours for the mineral and organic material, respectively. The chosen organic drying temperature was estimated as the point around which mass loss due to charring balanced the effects of residual water due to the strong water binding capabilities of organic matter (O'Kelly, 2004). The estimated gravimetric water content was converted into the volumetric. Texture and organic content data were obtained using standard procedures. At the Finish sites and the Danish forest site, calibration samples were taken close to 5TE network stations at the respective sensor depths. The field experiment took place at one of the latter. Three Decagon 5TE sensors were installed in the organic horizon and logged permanently. The soil was saturated and during the dry-down ThetaProbe readings and gravimetric samples kept being taken. These field data include some further 5TE-ThetaProbe-gravimetric sample couples available from organic layers around other network stations within the plantation.

In order to increase the number of calibration points and thus, the scope of validity, some additional measurements were added: Few data were acquired during a radiometer experiment for which purpose a large soil patch (organic and A-horizon) from heathland within the Gludsted plantation was transported to the Research Center Jülich, Germany (Jonard et al. 2014). Furthermore, some ThetaProbe measurements together with gravimetric sampling were taken from the Scottish and Siberian samples in the lab.

An Overview of all calibration samples and their characteristics is given in Table 1. Layers with soil organic matter content (SOM) greater than around 34 % (e.g. Zanella et al. 2011) are considered organic horizons. Dry bulk densities range from 0.05-0.4 and 1.0-1.5 g/cm3 for the organic and mineral samples, respectively. Sand fractions always constitute more than 80 % of the total soil mass. Couples of sensor output and sample volumetric water content of all data are plotted for the two sensor types in order to evaluate the manufacturer's calibration curves and if required derive new ones.

III - B - L-band Dielectric Constant Measurements

L-band dielectric constant measurements are being carried out at the Laboratoire de l'Intégration du Matériau au Système (Bordeaux, France) using two complementary approaches: The resonant cavity is based on the small perturbation method (Boudouris, G., 1964) and measures sample-induced changes of resonance parameters of the transmission coefficient curve (resonance frequency and quality factor). The Nicolson, Ross and Weir rectangular waveguide technique (Weir 1974) estimates the complex coefficients of transmission and reflection. In both cases the real and imaginary parts of the dielectric constant (ε', ε'') are computed. The former method is more precise but restricted to fixed frequencies, while the latter can measure over a wider range and uses larger samples, better

Table 1: Overview of the calibration samples collected from organic and mineral horizons. N=Number of readings.

		Location	Land cover	Type	Layer depth [cm]	SOM [%]	N 5TE	N ThetaProbe
Organic	HOBE_Forest_O_F	Gludsted, DK	Forest	Field	0-5	69-93	19	13
	HOBE_Forest_O1_L			Lab	0-5	69	11	11
	HOBE_Forest_O2_L			Lab	0-5	31	11	11
	HOBE_Heath_O_F		Heath	Field	0-5	NaN	2	8
	FMI_Forest_O_L	Sodankylä, FI	Forest	Lab	0-5	36.6	7	7
	SIB_O_L	Siberia, RU	Tundra/bog	Lab	0-10	NaN	0	3
	ISL_O_L	Islay, GB	Bog	Lab	0-10	NaN	0	17
Mineral	HOBE_Forest_M_L	Gludsted, DK	Forest	Lab	10-15	8	11	11
	HOBE_Heath_M_F		Heath	Field	10-15	NaN	4	7
	FMI_Forest_M_L	Sodankylä, FI	Forest	Lab	10-15	15	6	6
	FMI_Heath_M1_L		Heath	Lab	0-5	7	5	5
	FMI_Heath_M2_L			Lab	10-15	5	4	4

accounting for the material's heterogeneity. Classification of the measured organic samples was undertaken according to Zanella et al. (2011, Table 2). A range of different humus types of both terrestrial and semi-terrestrial regimes (rarely/frequently water-saturated, respectively) were sampled. For comparison, the underlying mineral A-horizons and overlying vegetation layers were also acquired at the Danish and Finish sites.

In case of the resonant cavity, glass tubes were filled with air dried material (5.2 cm^3) using pre-defined in situ bulk densities. Different water contents were added to span the entire wetness range. Two tubes per step were prepared and each was measured three times at room temperature and frozen conditions, respectively. For the wave-guide measurements, Teflon containers (60 and 125 cm^3 depending on material's composition) were used. The samples having different soil water contents were measured twice at room temperature and under frozen conditions, respectively, turned 180 degrees between the two measurements to account for heterogeneity effects. Due to labor-intensity, the ideal preparation from the wet-end was only undertaken in case of semi-terrestrial samples exhibiting the strongest shrinkage effects. For both methods a calibrated vector network analyzer was used. The measurements in different substrates, using the two complementary methods, are currently being analyzed and compared.

Table 2: Overview over organic samples collected for L-band dielectric constant measurements

Location	Land cover	Water regime	Type	Horizons
Gludsted, Denmark	Coniferous forest (spruce)	Terrestrial	Mor	OL-OF-OH
	Heathland	Terrestrial	Moder	OL-(OF)-OH
Sodankylä, Finland	Coniferous forest (spruce)	Terrestrial	Mor	OL-OF-OH
	Heathland	Terrestrial	Mor	OL-OF-OH
West Siberia, Russia	Tundra	Semi-terrestrial	Hydromor	(OLg)-OFg-(OHg)
	Bog	Semi-terrestrial	Histomor	hf
	Forest	Terrestrial	Mor	OL-OF-OH
Islay, Scotland, GB	Peat	Semi-terrestrial	Histomor	hf-hm

IV – RESULTS/DISCUSSION

IV - A - Soil Moisture Calibration

Figure 2 shows Decagon 5TE and ThetaProbe output plotted against the sample water content, separately for organic and mineral horizons (listed in Table 1), together with the manufacturer's default curves. For the 5TE sensor, ϵ_a is used as the raw output is only logged by Decagon-fabricated devices. Color codes go from highest to lowest SOM content. Despite a significant dispersion, a clear and consistent trend is visible in the organic data from all locations. For both sensor types, there is good agreement between the field and lab measurements from the HOBE forest site. The 5TE sensor response at a given water content is significantly lower for organic material than indicated by the default mineral function. This behavior was likewise observed in respective TDR studies (e.g. Topp et al. 1980, Jones et al. 2002). It has been explained by the substantial bound water fraction in high surface-area porous organic matter where interfacial forces render water molecules rotationally hindered, leading to reduced ϵ_a. In contrast, and opposite to the manufacturer curve's trend, our organic ThetaProbe measurements consistently show an increased sensor output at a given water content, and the response seems to saturate around 1000 mV. The mineral data with SOM < 10% scatters around the default curves. While the ThetaProbe data of SOM > 10% follow this pattern, the 5TE sensor shows a tendency towards decreased ϵ_a but with weaker shape than for organic horizons.

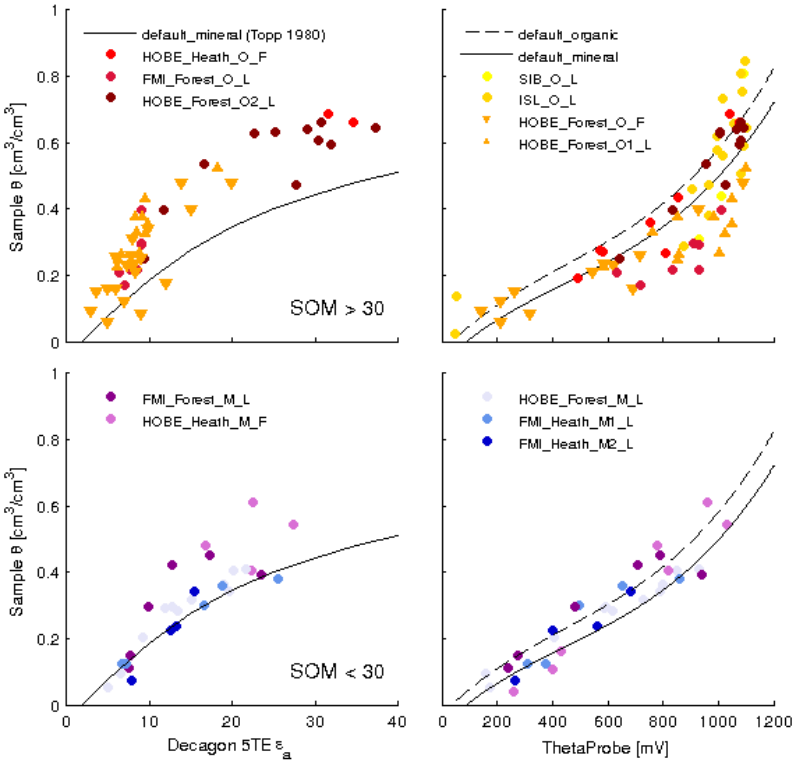

Figure 2: 5TE apparent dielectric constant ε_a (left) and ThetaProbe output [mV] (right column) against volumetric water content ϴ (gravimetric samples) for organic (top) and mineral horizons (bottom row) with color codes from highest to lowest SOM content (yellow – dark red and purple - dark blue, respectively). For SOM% see Table 1.

IV - B - L-band Dielectric Constant Measurements

Figure 3 illustrates an example of the first L-band dielectric constant measurements (real/imaginary parts) using an

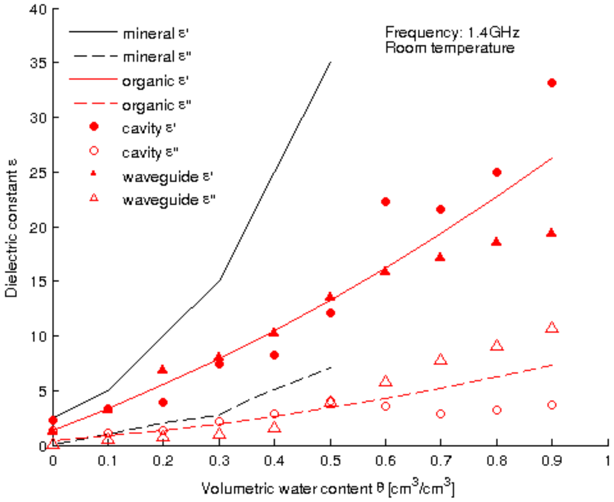

Figure 3: L-band dielectric constants (ε'/ε''), for an average mineral soil (Hallikainen et al., 1985) and fitted through preliminary wave-guide and cavity measurements of organic soil from the Sodankylä forest site.

organic sample from the Sodankylä forest site. Data is depicted over the entire wetness range including corresponding estimates for an average mineral soil after Hallikainen et al. (1985). Resonant cavity (1.48 GHz), and wave-guide (1.4 GHz) observations are in reasonable agreement. Consistent with the calibration data, lower values are observed for the organic material compared to the mineral soil.

V – CONCLUSIONS/OUTLOOK

Measurements of the two soil moisture sensors Decagon 5TE and Delta-T ThetaProbe for organic surface layers as well as sandy A-horizons from different sites in Denmark, Finland, Scotland and Russia show consistent trends. While the data from mineral horizons with low soil organic matter content are in good agreement with the manufacturer's default functions, adapted organic calibration functions are currently being derived. At the same time, other organic calibration curves, mainly derived for TDR sensors, are being tested. L-band dielectric constant measurements spanning a variety of humus types and water regimes, and using wave-guide as well as resonant cavity techniques are currently being analyzed. Existing work such as TDR observations in similar frequency domains will be considered. Also, the sensitivity of the organic matter's dielectric constant to varying frequency, notably between L-band and standard measurement frequencies of capacitance and impedance soil moisture probes (~50-100 MHz) shall be studied. These investigations will be presented during the Fourth International Symposium on Soil Water Measurements. In a next step, new SMOS soil moisture products will be retrieved over Northern regions using L-band dielectric constants adapted to measured values, and compared to re-calibrated in situ data.

REFERENCES

Blonquist, J. M., S. B. Jones, and D. A. Robinson, 2005. Standardizing Characterization of Electromagnetic Water Content Sensors: Part 2. Evaluation of Seven Sensing Systems. Vadose Zone Journal, 4, pp. 1059-1069.

Boudouris, G., 1964. Validité de la méthode de perturbation appliquée aux cavités résonnantes pour la mésure de la perméabilité et de la permittivité des petits échantillons. Annales des Télécommunications, 19(3-4), pp. 63-80.

Delta-T Devices Ltd., 1999. ThetaProbe Soil Moisture Sensor Type ML2x User Manual. ML2x-UM-1.21. Delta-T Devices Ltd., 128 Low Road, Burwell, Cambridge CB5 0EJ, GB.

Decagon Devices Inc., 2014. ECH2O soil moisture sensor. Operator's manual for model 5TE. Decagon Devices Inc., 2365 NE Hopkins Court, Pullman, WA 99163, USA.

Hallikainen, M., F. Ulaby, M. Dobson, M., et al. 1985. Microwave dielectric behavior of wet soil–part 1: Empirical models and experimental observations. IEEE Trans. on Geoscience and Remote Sens., 23(1), pp. 25-34.

Jonard, F., F. Demontoux, S. Bircher, et al., 2014. Electromagnetic characterization of organic-rich soils at the microwave L-band with ground-penetrating radar, radiometry and laboratory measurements. In proc. of the 15th Int. Conference on GPR, Burssels, Belgium, June 30 – July 4.

Jones, S., J. M. Wraith, and D. Or, 2002. Time domain reflectometry measurement principles and applications. Hydrological Processes, 16, pp. 141-153.

Kerr, Y., P. Waldteufel, J.-P. Wigneron, et al. 2001. Soil moisture retrieval from space: The Soil Moisture and Ocean Salinity (SMOS) mission. IEEE Trans. on Geoscience and Remote Sens., vol. 39(8), pp. 1729-1735.

O'Kelly, B., 2004. Accurate determination of moisture content of organic soils using the oven drying method. Drying Technology, 22(7), pp. 1767-1776.

Schaap, M. G., L. de Lange, and T. J. Heimovaara, 1996. TDR calibration of organic forest floor media. Soil Technology, 11, pp. 205-217.

Erik Stokstad (2004). Defrosting the carbon freezer of the north. Science, 304 (5677), pp. 1618–1620.

Topp, G. C., J. L. Davis, and A. P. Annan, 1980. Electromagnetic determination of soil water content: measurement in coaxial transmission lines. Water Resources Research, 16(3), pp. 574-582.

Vaz, C. M. P., S. Jones, M. Meding, et al., 2013. Evaluation of standard calibration functions for eight electromagentic soil moisture sensors. Vadose Zone Journal, 12(2), pp. 1-16.

Wigneron, J.-P., Y. Kerr, P. Waldteufel, et al. 2007. L-band microwave emission of the biosphere (L-MEB) model: Description and calibration against experimental data sets over crop fields. Remote Sens. of Env., 107, pp. 639-655.

Weir, W. B., 1974. Automatic measurement of complex dielectric constant and permeability at microwave frequencies. In proc. of the IEEE, 62(1), pp. 33-36

Zanella, A., B. Jabiol, J. F. Ponge, et al., 2011. European Humus Forms Reference Base. http://hal.archives-ouvertes.fr/hal-00541496/. Accessed April 4, 2014.

TRANSACTIONS OF THE FOURTH INTERNATIONAL SYMPOSIUM ON SOIL WATER
MEASUREMENT USING CAPACITANCE, IMPEDANCE AND TDT
MONTREAL, CANADA, JULY 16 – 18, 2014

APPLICATIONS, PAPER 2.1

Dynamic Visualization of Real-Time Wetting Fronts in Soils Using Multi-Sensor Capacitance Probe Arrays.

Dalton, M.(1), Buss, P.(2), Stevens, S.(3) & Fuentes, S.(4)

(1,2 & 3) Sentek Pty. Ltd., South Australia, 5069, mdalton@sentek.com.au
(4) Dept. Agriculture and Food Systems, University of Melbourne, Victoria, 3010, Australia,
sfuentes@unimelb.edu.au

Abstract

The use of small-site intensive soil water monitoring with multiple depth sensor arrays in representative soil volumes can indicate plant water usage rates in the broader scale. Multiple numbers of Sentek soil moisture monitoring probes were installed into sites within a range of different crops (including: grapevine, almond, cotton and watermelon) and irrigated with a range of different methods (drip, sprinkler and sub-surface drip). The probes were arranged within the plant root zones in transect lines extending from the water emitters. Soil water data was collected on a near-continuous basis simultaneously across the probe array. This was analysed using a new wetting pattern analysis software called IrriMAX™ 2D Imager to visualise the water distribution in the soil in 2-dimensions. This software uses automated cubic spline interpolation techniques to generate contour maps and video animation of water dynamics according to different levels of soil water. The soil water scale is obtained from the whole dataset and painted with false colours to visualise the dynamics of water movement throughout the soil profile. This method allows the visualisation of the spatial distribution of water in the soil and the duration of time over which such a distribution persists. This gave insights into the plant water uptake dynamics and soil drainage characteristics that could be extrapolated to the whole field for irrigation management purposes. Careful consideration of the data showed that root architecture and the passage of mobile salts could also be assessed at the root-zone scale. This visualization technique was shown to be a valuable adjunct to understanding the movement of water and nutrients throughout the root zone.

Keywords: capacitance, 2-D animation, soil moisture, wetting pattern analysis, salinity.

Introduction

For many years researchers have used modelling tools such as HYDRUS (Skaggs *et al.,* 2004) and SWIMS (Ross, 1990) to estimate and quantify the movement of water within the soil profile. These tools take inputs of varying importance to model the expected infiltration rates based on both known and unknown parameters considered important from the field of soil physics. The results obtained are therefore only as good as the accuracy of the inputs. Detailed knowledge of the soil hydraulic properties is needed to make the results relevant to the manager. It is also difficult in these models to introduce appropriate corrections for the variations in soil texture and transition zones, so-called heterogeneity. Additionally not easily anticipated in these models are factors such as irrigation water quality (which can affect infiltration rate), plant uptake and root density at various depths. In the commercial context, the gathering of these types of information is not often practical or cost-effective.

The Sentek 2D Imager software uses only one of these modelling principles (the cubic spline approximation) as it draws together empirical data collected from an array of sensors into a visualisation of the potential wetting pattern within chosen transects (Ross, 1992, Fuentes *et al.,* 2004; 2007). By recording the water and solute contents in such a comprehensive manner on a near-continuous basis, this visualisation can be performed for each timestamp and compiled together to make a dynamic video. In this way, the manager can more easily understand the rate of movement of both water and solutes throughout the soil profile, from a “whole-of-season” condensed time video to an expanded “minute-by-minute” shorter event demonstration. It is also possible to identify heterogeneity within the soil profile and to estimate the root exploration according to water uptake patterns.

Objectives:

The objectives of this study were to demonstrate how the new Sentek 2D Imager software could be used to enhance the understanding of the complex movement of water and salts within the soil profile in a range of different crops in real time, through the use of empirical site-specific data.

Methods and Materials

Multiple installations of Sentek capacitance probes were made into commercial crops of wine grapes, almonds, cotton and watermelons using the standard direct installation methodology (Sentek, 2014). These probes can have sensors every 10cm of depth of soil set up to record Volumetric Water Content (**VWC**) and Volumetric Ion Content (**VIC**) automatically every 20 seconds. All VWC data collected was calculated using the Sentek default calibration equation, so is indicative only. To obtain more accurate results, on-site soil calibrations are needed. The units used for VWC are millimetres (mm) of water. One millimetre defines a height of water spread over $1m^2$, and is hence equivalent to one litre. Each sensor reads the water content within a depth of soil of approximately 100mm.

The VIC value is a proprietary-defined index derived from capacitance readings taken at a lower frequency than normal (<50MHz). At this frequency, the sensor becomes sensitive to (among other things) charged particles. The manufacturers have calibrated the lower frequency sensor for various saline sand environments. The sensor loses resolution with increasing clay content, but can be used as a trending device for salt and ionic nutrient content in sandy soils. The VIC quantity is proprietary to Sentek Pty. Ltd. and is dimensionless (has no units).

Data was downloaded regularly to a web site for viewing. For convenience, all data sampling rates were set to 15 minutes except for the almond trial which was set to 60 minutes. The probes were configured such that sensors were spaced at the same depths down the probe and at consistent distances along each transect, although the software is not restricted by these conditions. Probes were positioned parallel to each other between 20 to 30cm apart along the transect lines.

Wine Grapes

The type of irrigation used was surface drip with 150cm emitter spacing. Applications of 4mm to 16mm were made 2 – 3 times per week, depending upon considered optimal plant requirement. The wine grape variety was *Vitis Vinifera* cv. Shiraz, grown in McLaren Vale, South Australia, in a rocky clay loam soil. The 1.5m length capacitance probes were placed in a simple two probe array 30cm apart along the planted row with the first probe being within 10cm of the emitter. Soil moisture sensors were placed at 10, 20, 40, 60, 80 and 110cm depths in each probe.

Almonds

The trial was conducted on 11 year old almond trees (*Prunus dulcis* (Mill.) Webb) at a commercial orchard (Clark Taylor farms) located in Berri, South Australia (34°200' S and 140°350' E), during the 2009–2010 season. The orchard was drip irrigated into a clay loam textured soil. Each row of trees had two laterals, one on either side at 1 m offset from the tree trunk. The laterals had 4 Lh^{-1} pressure-compensated button drippers spaced at 1m intervals. The laterals were buried at 10 cm below ground level and water was delivered to the ground surface via a small tube attached to the outlet of each dripper. Each tree had approximately 12 drippers in total. Irrigation events occurred daily, commencing at 8 a.m. with alternate on and off pulse cycles. The average flow rate of each dripper was 3.87 Lh^{-1}. Six EnviroSCAN® soil moisture probes were installed at 20cm intervals laterally out from the drippers at distances between 0 and 100 cm. Each probe had five sensors positioned at 20, 40, 60, 80 and 120cm depths. All probes were wired to a Sentek RT6 data logger, and soil moisture data were recorded every hour.

Cotton

No irrigation was used in this crop which was planted in Texas, USA. Four replicates of three genetically distinct varieties of *Gossypium hirsutum* (commercial in-confidence) were trialled. Two of these were intensively monitored with identical sensor arrays for a single growing season. The sensor arrays consisted of 3 x 1m length probes with sensors placed at every 10cm depth in a simple transect, the first of which was placed into the plant row. Subsequent probes were spaced 20cm away from each other into the inter-row. The soil type was deep clay loam.

Watermelons

The type of irrigation used was sub-surface drip tape, with some of the applications being fertigations. The *Citrullus lanatus* plants were grown for one season in sandy loam in Delaware, Georgetown, USA in 1m wide raised beds (15cm), protected with black plastic mulch. The probe transect consisted of 2 x 1m length probes with sensors placed at 10, 20, 30, 50 and 70cm depths. The first probe was installed within 10cm of an active plant, the other being 25cm away in the direction of the inter-row. The authors wish to gratefully acknowledge Dr. Jim Starr of the USDA for the provision of this as yet unpublished data.

Data analysis and 2D Imager

A new feature in IrriMAX™ software, called 2D Imager, allows for the 2-dimensional visualisation of water content throughout the soil profile over any selected time period. This software uses automated cubic spline interpolation techniques (Press *et al.*, 2002) to generate contour maps and video animations of water dynamics according to different levels of soil water content. The soil texture is assumed to be consistent between proximal data points. The soil water scale is obtained from the whole dataset and painted with false colours to visualise the dynamics of water movement throughout the soil profile. Colour palettes can be customised by the user to represent VWC (colour palette) or salinity levels (black and white). This method allows the visualisation of the spatial and temporal distribution of water in the soil and the duration of time over which such a distribution persists. The operator can set a series of conditions within the software before generating a time series of images, forming a video sequence which can be viewed at a convenient speed.

Also supplied in 2D Imager is the ability to express the overall percentage of data points within a transect between various VWC or VIC thresholds. This allows for objective comparisons to be made between replicated sites regarding the water and nutrient usage of plants with different treatments or genetic aetiologies on an individual depth basis. The implications of this for researchers as a comparative tool are immense.

Results and Discussion

Wine Grapes

The colorimetric video produced (example screen captures only shown in figure 1) showed that at various times during the growth cycle, water stress was experienced. Examples were found of shallow irrigations and rainfall events which did not travel more than 40cm into the soil profile. At lower depths below 95cm, however, the vine was supplied with plentiful water from a combination of a heavier soil texture and the sloping topography. No doubt, these 2 bands of water separated by a comparatively drier zone between 40cm to 95cm governed the final root distribution of the plants.

Additional rainfall events were observed to penetrate intermittently to replenish the middle zone. The combination of lower salinity contents and lower air temperatures during these rainfall events generally facilitated greater depth penetration than irrigation alone. This is a common observation in this type of continuous data.

On the basis of these data analyses and subsequent plant cell density (PCD) aerial scans of the vineyard, adjustments were made to the inadequate irrigation system to improve the overall plant vigour consistency in later vintages. This improvement was achieved by doubling the number of emitters, increasing the number of irrigations at peak agronomic times and covering the soil with organic mulch.

Almonds

The video produced (example screen captures only shown in figure 2) showed that water applied closer to the tree stem travelled downward in a non-uniform wetting pattern. There appeared to be a barrier to water infiltration closest to the plant at 70cm depth. This was probably due to differences in soil texture and may indicate the position of soil disruption caused by deep ripping at the time of orchard establishment.

The inter-row remained fairly dry except after high rainfall events. Moderate rainfall events were generally used quickly by the sward roots, keeping the inter-row at depth relatively dry. Higher water uptake dynamics were observed within a 40cm radius of the drip emitter, indicating a possible greater root density adjacent to them. This is a common feature often observed in this type of irrigation system.

Cotton

The colorimetric video that was produced (example screen captures only shown in figure 3) showed greater root infiltration depth for variety B when compared to variety A at the same chronological growth stage. This may simply be due to soil textural variation, but serves to demonstrate that these differences are detectable with this equipment. The root graphic was added purely as a demonstration of where the greater root densities may occur based solely on the observed water removal, and is not a feature of the 2D Imager software. More research needs to be conducted here involving the intensive monitoring of more treatment replicates with a greater number of both sensors and probes. Averages over the replicates could then be imported into fresh databases and comparisons made. This has been done in other unpublished test programs (Ghaffarzadeh, M, personal communication). Such observations could have a profound impact on the selection of future plant varieties of any species.

Watermelons

The colorimetric video produced (example screen capture only shown in figure 4) showed that the applied water at 20cm depth was being drawn rapidly downward to a heavier-textured soil at 50cm where it was being retained. This water reserve was also being added to by lateral flow from the inter-row, which acted like a catchment. This pooling water could have deleterious effects on the plants or it could be of great benefit in times of drought. Active root extraction could be seen down to 40cm, but less activity was noted below this due to the higher water contents. Plant roots need free oxygen for active water transport across their membranes. Figure 4 also shows the relative percentages of water ranges chosen by the setting of “Full Point” and “Onset of Stress” thresholds. These values can be used by the crop manager as an index for how any part of the soil profile is being stressed. For example, a management critical control point which sets a threshold of 2% for the percentage in the red zone (dry) would have been exceeded at the surface, as seen in the figure.

Also demonstrated, within the limitations of the equipment described above, was the movement of salts within the soil profile, added as four applications of 28 Kg N ha^{-1} via the drip tape irrigation system (example screen capture only shown in figure 5). Shown here is a salinity bubble as high as 2500 VIC extending from the drip tape. Over a period of a single week this dissipated, and presumably entered the plant, returning to normal levels around 1200 VIC (not shown). Salinity thresholds can be set as a management tool for operators to track the passage of salts at peak times such as fertigations. The percentages displayed on the graphs can be used to optimise the fertiliser dosage and application rate.

Data analysis and 2D Imager

All VWC data used here were calculated using the Sentek default calibration coefficients which describe a standard power function derived from a sandy organic soil. This means that the VWC values calculated here may have been underestimated for the heavier textured soils within the different site profiles. This would not affect the conclusions drawn here, as the trending would be similar. Only the range of values would change, increasing the number of available contour lines and thus resolution. Overall, the presentation of this data would be enhanced with recalculation using site-specific soil calibration parameters.

No corrections were made for temperature changes as none of the sensors used had the ability to perform this function. Temperature is known to have a small effect on capacitance measurements (Starr *et al.,* 2011).

Conclusions

The new 2D Imager feature of IrriMAX™ was shown to be a powerful tool that could be used to visually track the passage of water and salts (nutrients) throughout the soil profile over time. This gave insights into the plant water uptake dynamics and soil drainage characteristics that, when sited in a representative location, could be extrapolated to the whole field for irrigation management purposes.

The software uses empirical data collected in the field, rather than estimated parameters, to build up a 2-dimensional representation of the possible water and salinity spatial dynamics. This approach therefore takes into account some of the heterogeneity inherent in soil.

Also indicated were root architecture and root density characteristics, properties which could be used comparatively in plant variety trials.

Further work

More intensive monitoring of soil moisture dynamics in transects placed at right angles to each other in a grid should be conducted to extend the demonstration of water dynamics to 3-dimensions.

The temperature gradients throughout the soil profile could also be performed using the same software, providing a useful tool for agronomic managers to gain insight into the potential plant absorption of applied nutrients. In this way the operator could optimise the timing of fertiliser applications to maximise nutrient uptake at ideal root temperatures.

It would seem an interesting task in the future to compare empirical (Sentek) and modelled (HYDRUS) soil water distributions in both homogeneous and heterogeneous soil profiles with and without plant roots.

References

Fuentes, S., Camus, C., Rogers, G. and Conroy, J. (2004). "Precision irrigation in grapevines under RDI and PRD: Wetting pattern analysis (WPA(c)), a novel software tool to visualise real time soil wetting patterns". The Australian and New Zealand Grapegrower and Winemaker (Annual Technical Issue): 120-125.

Fuentes, S., Rogers, G., Conroy, J., Jobling, J., Camus, C. and Mercenaro, L. (2007). “A soil-plant-atmosphere approach to evaluate the effect of irrigation strategy on Grapevine (cv. Shiraz) water and nutrient uptake, grape quality and yield”. Acta Horticulturae (ISHS), 792: 297-304.

Press, W.H., Teukolsky, S.A., Vetterling, W.T. and Flannery, B.P. (2002). “Numerical Recipes in C; The art of Scientific Computing” in: Chapter 3, “Interpolation and Extrapolation: 3.3 Cubic Spline Interpolation”, 2nd Edition, Cambridge University Press (Publ.), The Pitt Building, Trumpington Street, Cambridge CB2 1RP, 113-116.

Ross, P. J. (1990). “SWIM: A simulation model for soil water infiltration and movement”. Reference Manual to SWIMv1. CSIRO Division of Soils, Canberra, New South Wales, Australia.

Ross, P. J. (1992). “Cubic approximation of hydraulic properties for simulations of unsaturated flow”. Water Resources Research, 28(10): 2617-2620.

Sentek Pty. Ltd. (2014). “Access Tube Installation Guide”. Website accessed 15/6/2014: http://www.sentek.com.au/downloads/downloadform.asp?ItemID=14.

Skaggs, T., Trout, T., Šimůnek, J., and Shouse, P. (2004). ”Comparison of HYDRUS-2D simulations of drip irrigation with experimental observations”. Journal of Irrigation and Drain Engineering, 130(4): 304–310.

Starr, J.L., Timlin, D.J., Downey, P.M. and McCann, I.R. (2011). “Laboratory evaluation of dual-frequency multisensory capacitance probes to monitor soil water and salinity”. Irrigation Science, DOI 10.1007/s00271-009-0154-3.

Figures

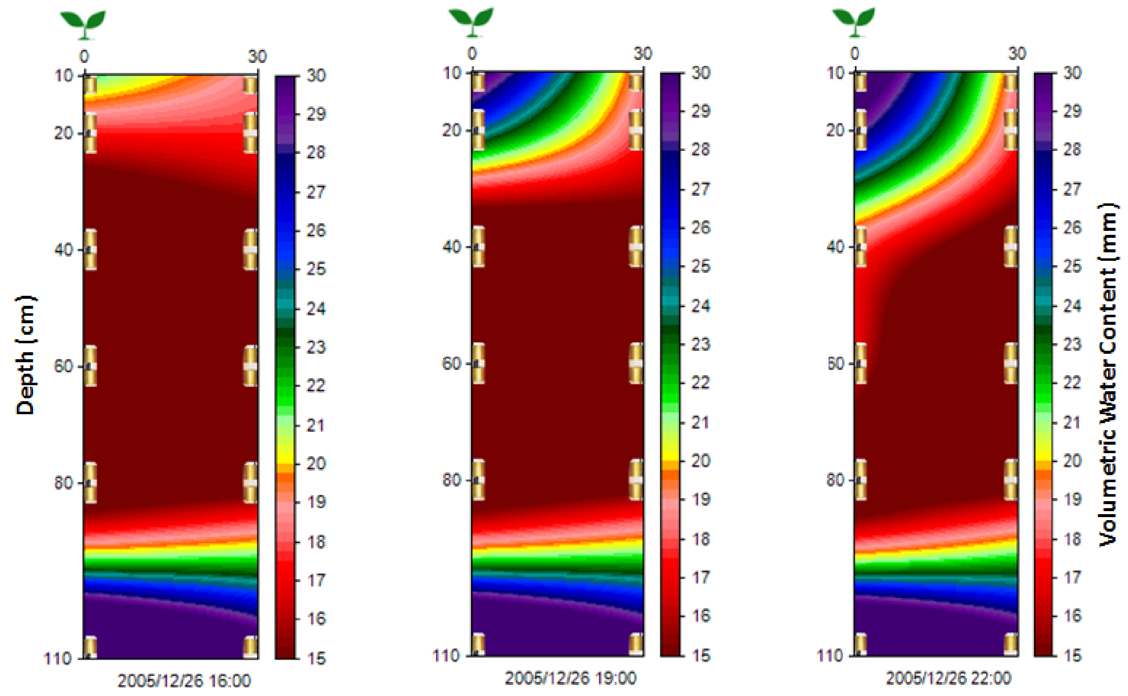

Figure 1: Shiraz vineyard: Application of irrigation at 0 infiltrates to as much as 60cm depth over 6 hours.

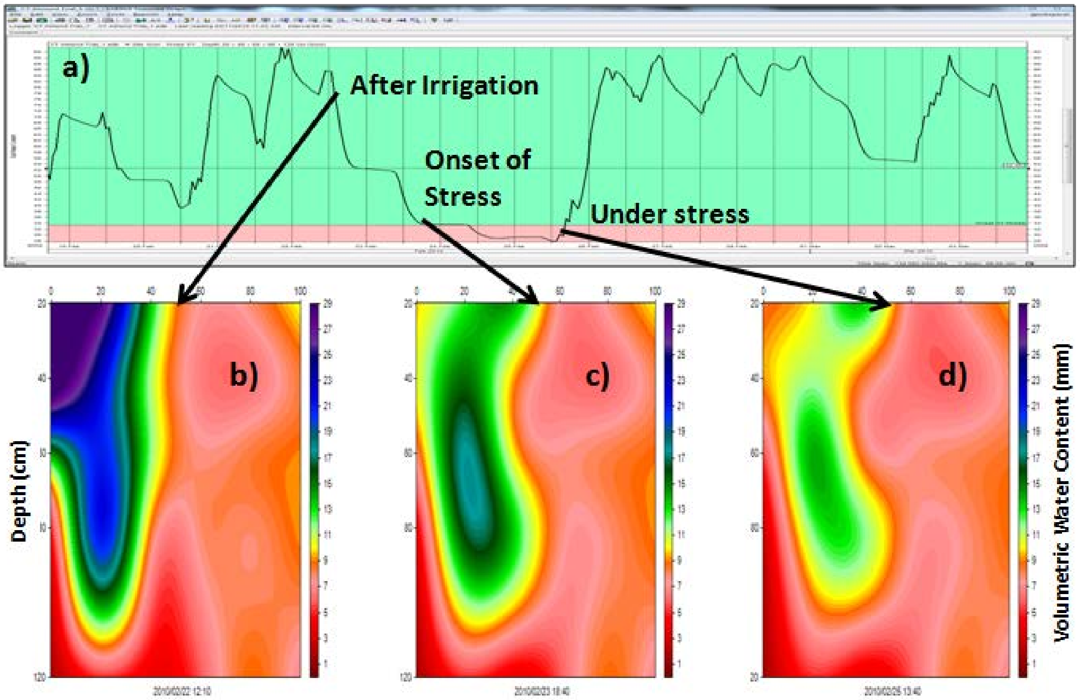

Figure 2: Almond orchard: Top graph (a) showing the summed soil moisture data from sensors to 1.2m depth; below: (b) transect directly after irrigation, (c) at Onset of Stress and (d) after 2 days of water stress.

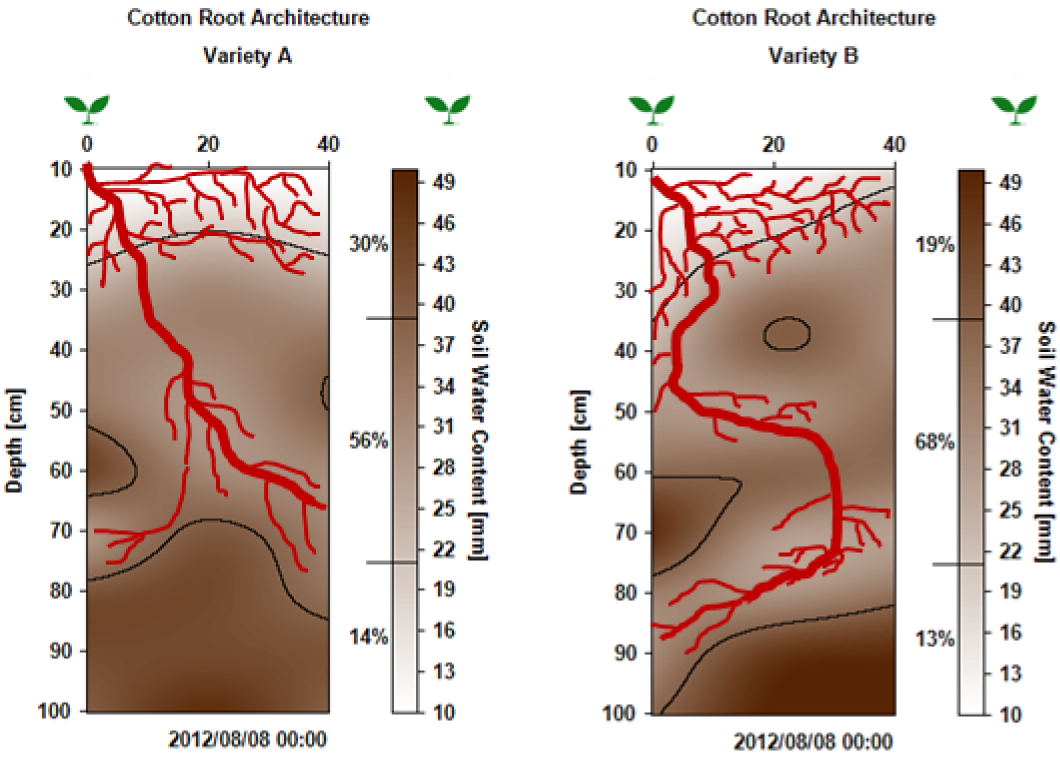

Figure 3: Cotton: Root architecture differences between varieties.

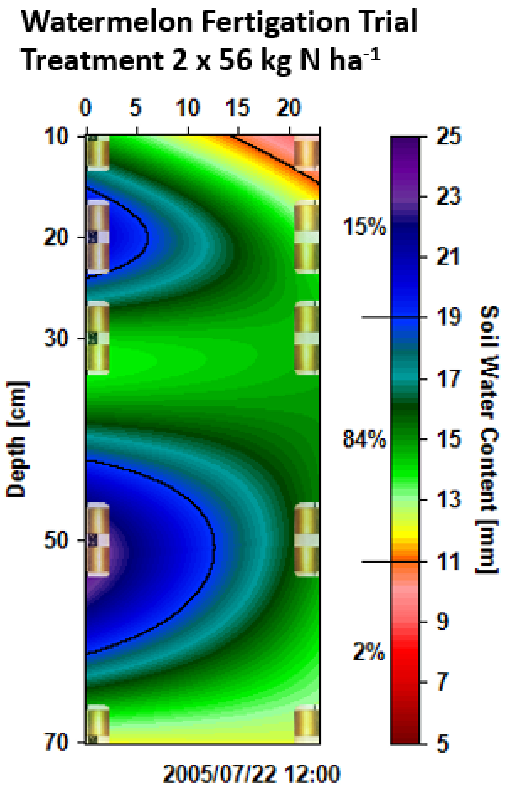

Figure 4: Watermelon: Volumetric Water Content (VWC) in soil profile. Data source: Starr *et al.*, personal communication, USDA.

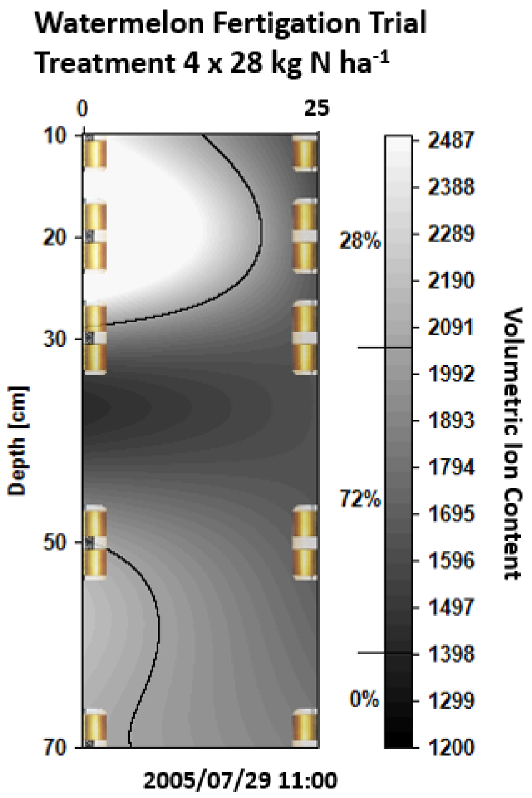

Figure 5: Watermelon: Volumetric Ion Content (VIC) in soil profile. Data source: Starr *et al.*, personal communication, USDA.

APPLICATIONS, PAPER 2.2

Improved Water Supply Forecasts Using Soil Moisture Data

[a]B. Keith Bellingham and [b]Jolyne Lea
[a]Stevens Water Monitoring Systems, Portland, OR 97220, USA.
[b]US Department of Agriculture. NRCS, National Water & Climate Center, Portland, OR 97232, USA

Abstract

Much of the water in the Western United States used for irrigation, municipal supplies and hydro-electric production originates as winter snow pack at higher elevations. Since the early 1900s, the correlation between stream flow and the snow water equivalent (SWE) has been used to forecast the available water for beneficial uses and assess flood potential. Currently the US Department of Agriculture, Natural Resources Conservation Service (NRCS) maintains a network of nearly 850 high elevation stations called SNOTEL to collect snow and climate data in addition to over 1100 manually measured snow courses used in the statistical based forecasting of streamflow. Because the soil under the snowpack represents a significant storage reservoir for snow melt water, soil sensors began to be installed at SNOTEL sites starting in the late 1990s. In this network, some of the longest records of soil moisture are at three Idaho SNOTEL sites. This study is to determine if 14 years of soil moisture data at 3 SNOTEL sites measured with the Stevens Hydra Probe could statistically improve the stream flow forecasts at a river gage operated by the US Geological Survey (USGS). A parameter call the Soil Moisture Deficit Index (θ_{di}) was calculated from the average soil moisture and the soil's water content at 333 hPa, was used as an attenuation coefficient in the stream flow forecasts. The forecasted stream flow was compared to the actual stream flow recorded by the USGS and a correlation faction (R) was developed to compare the accuracy of the forecasts. Preliminary work shows that soil moisture data improved the water supply forecast and showed a positive correlation between stream flow and soil moisture deficit index. The impetus for an improved forecast are many, as water resources continue to be limited, especially in light of increasing demand in an environment where there is evidence that climate change is changing seasonal snowpack and snowmelt timing.

Introduction

Water in the Western United States

Most of the water in the arid part of Western United States originates from as snowpack at higher elevations (Folliott, et al., 1989). The streamflow in most streams in the western US are fed from the springtime melting of the seasonal snowpack or fed from aquifers that are recharged by snowpack melt. In the western United State, about 80% of the water consumed is for irrigation (Kenny, 2005) since many crops grown in the west require irrigation. Another major use for water in the western United States is hydroelectric power. More than half of the electricity in the States of Oregon and Washington come from hydroelectric (US EIA). In recent years, climate change has been identified as a factor that could affect the snowpack in terms of the amount of available water and the timing of the runoff, and thus affect the availability of water. Monthly forecasts of the seasonal water supply from the snow pack are critical for water management decisions for irrigation, hydroelectric, and other water uses (emergencies, such as for flood mitigation).

SNOTEL and Snow Survey

The relationship between the snowpack characteristics and the available water throughout the year for specific watershed basins was first scientifically studied in the early 1900s by setting up snowpack observation reference points called snow courses (SNOTEL). The snow water equivalent (SWE) which is the amount of water the snowpack would yield if it were to melt was correlated statistically to volumetric streamflow at monitoring stations in the watershed (SNOTEL). The SNOTEL program emerged from the snow courses in the 1970s, when the snow courses were suplimented or replaced with a new automated station. Today, the US Department of Agriculture National Resources Conservation Service (NRCS) operates about 900 SNOTEL sites in 12 western States and provides seasonal streamflow forecasts for water management and decision making for many federal, state and local water users, and the general public (SNOTEL).

Streamflow Forecast Modeling

Statistical models are used to forecast water supplies using a spreadsheet approach developed by the NRCS. This model is based on a statistical principle component regression between the antecedent snow data from the SNOTEL network and the historical streamflow data measured at US Geological Survey measurement points. This regression analysis is a statistical technique restructuring a set of weighted inter-correlated variables to generate a new variable (principle component). The weights of inter-correlated variables used in the linear combinations are from eigenvectors of the correlation matrix. The output variable, principle component, is an eigenvalue represented by a percentage of a total variance (Garen, 1992). This allows the modeler to use several interrelated variables to produce a robust regression equation. The input variables in the water supply forecast, using the model, are parameters such as snow water equivalent (SWE), antecedent precipitation, and observed streamflow. The statistical measure used to determine the accuracy of the forecast is correlation coefficient, R, (sometimes called the skill of the forecast) between the actual stream flow and the model produced forecasted streamflow values. The closer the R value is to 1, the stronger the correlation between the predicted and measured data and the better the accuracy of the forecast.

Soil Moisture Deficit Index

The soil under the snow pack represents a large reservoir capable of holding large amounts of water in a watershed and the soil moisture is an important factor in forecasting streamflow. Preliminary work (Lea and Harms, 2011) suggests that soil moisture data could significantly improve streamflow forecast. They indicated that the use of the data was provisionally an important parameter in improving water supply forecasts. With the additional years of data and using the full soil moisture deficit of the soil column, there is an improved correlation to streamflow, and the accuracy of streamflow forecasts is also improved. Soil moisture historically has not been used in the water supply forecasts because soil moisture data were not available, and hydraulic properties of the soil were scarce. Monthly precipitation has been used as a surrogate of soil moisture, as well as groundwater well data, when available. Starting in the late 1990s, SNOTEL stations began to include the Stevens Hydra Probe Soil Sensor and now many SNOTEL stations have been equipped with Hydra Probe Soil Sensors. The Hydra Probe soil sensors are installed at standard depths of 5, 10, 20.3, 51 and 102 cm. Sensors at multiple depths capture the distribution and the variation of water content gradient throughout the soil column as it changes throughout the year. At some SNOTEL sites, the deeper probes may not be installed if there is shallow bedrock. The SNOTEL station evaluated here, Bogus Basis, Jackson Peak, and Atlanta Summit, have the four soils sensors at the standard depths but do not have a soil sensors at 102 inches.

The available water held in the soil at a given point in time is the difference between the field capacity, θ_{fc} and the soil moisture at that point in time, θ (m^3m^{-3}). The available water holding capacity of the soil is defined as the soil moisture deficit index, $\theta_{di:}$

$$\theta_{di} = \overline{\theta} - \theta_{fc} \qquad [1]$$

where $\overline{\theta}$ is the average soil moisture throughout the column for a time step. The field capacity, θ_{fc} , is the upper limit of soil moisture where the soil's capillary forces can no longer suspend water. If the soil moisture is above field capacity, the soil is near saturation and water can be pulled downward by gravity or run off. If the soil moisture is below field capacity, the water is held in the soil by capillary forces. In this study, the soil moisture deficit index is a parameter that describes how much more water the soil can retain during the spring melting period and theoretically is positively correlated to stream flow. It will be a negative value if the moisture content is below field capacity, equal to zero at field capacity and a positive number above field capacity.

The purpose of this work is to quantify the improvements to the streamflow forecasts by incorporating the soil moisture deficit index on monthly time steps into the principle component statistical model along with the SWE and precipitation data.

Methods

Site Descriptions

Three SNOTEL sites in Idaho, namely, Bogus Basin, Atlanta Summit, and Jackson Peak were used in this study to forecast the streamflow at the USGS monitoring point on the Boise River near Twin Springs site ID 13185000. Each of these SNOTEL sites contains the standard complements of sensors, such as snow pillows for measuring SWE, a large cumulative "rocket gage" for measuring total precipitation, as well as meteorological sensors to measure parameters such as wind speed and direction, air temperature, relative humidity, and barometric pressure. In addition to the standard sensors, these SNOTEL sites also have four to five Hydra Probe Soil Sensors at 5, 10, 20.3, and 51cm and are among the first soil probes installed in the SNOTEL network. Hourly data are reported and transmitted via Meteor-burst telemetry to telemetry ground receive sites and stored on an NRCS server. The data are available from the NRCS web site http://www.wcc.nrcs.usda.gov/snow/.

Soil Moisture Sensors

The soil sensors used are the Stevens Hydra Probe Soil Sensor. The Hydra Probe is an impedance based dielectric sensor that contains a fractal model that separates out the real from the imaginary dielectric permittivity (Campbell, 1990, Logsdon, 2005). Dielectric permittivity is a complex number containing both a real and imaginary component and is dependent on the frequency, temperature, and the properties of the material. This can be expressed by,

$$\kappa^* = \varepsilon_r - j\varepsilon_i \qquad [2]$$

where K* is complex dialectic permittivity, ε_r is the real dielectric permittivity, ε_i is the imaginary dielectric permittivity and $j = \sqrt{-1}$ (et al. Topp, 1980). The soil moisture is determined from the real component due to the strong rotational dipole moment that water has in relation to soil from 1 to 1000 MHZ. A general calibration based on a dielectric mixing model was used and is expressed in equation [3] (et al. Seyfried, 2005).

$$\theta = A\sqrt{\varepsilon_r} + B \qquad [3]$$

where "A" and "B" are empirical coefficients fitted from 20 different soil samples representing a variety of soil textures and morphologies (et al. Seyfried, 2005).

Regression Modeling

The inputs to the model in monthly time steps from October 1997 to March 2014 are snowpack SWE value on the first of the month and total accumulated monthly precipitation (snow and rain) are used every month. The hourly soil moisture values collected at each depth were averaged across depth for the whole month. The field capacity was physically measured and determined by the volumetric water content at a potential of 333 hPa (1/3 bar). The soils data is exhibited in table [1] and the soil moisture deficit was calculated using equation [1].

Table 1, Soil survey data including the water content at 333 hPa (Lea and Harms 2011)

SNOTEL Site	Horizon	Top depth (cm)	Bottom Depth (cm)	Water content at 333 hPa
Atlanta Summit	A	2.00	5.00	12.79
	Bw1	5.00	23.00	24.24
	Bw2	23.00	36.00	21.44
	C	36.00	58.00	20.45
Bogus	A1	0.00	5.00	21.62
	A2	5.00	18.00	21.11
	A3	18.00	38.00	25.60
	Bw1	38.00	63.00	12.59
	Bw2	63.00	91.00	14.50
	Bw3	91.00	119.00	16.42
Jackson	A	0.00	13.00	28.36
	B1	13.00	25.00	24.53
	B2	25.00	43.00	19.00

Figure 1. Soil moisture deficit index and average soil moisture from October 1997 through March of 2014.

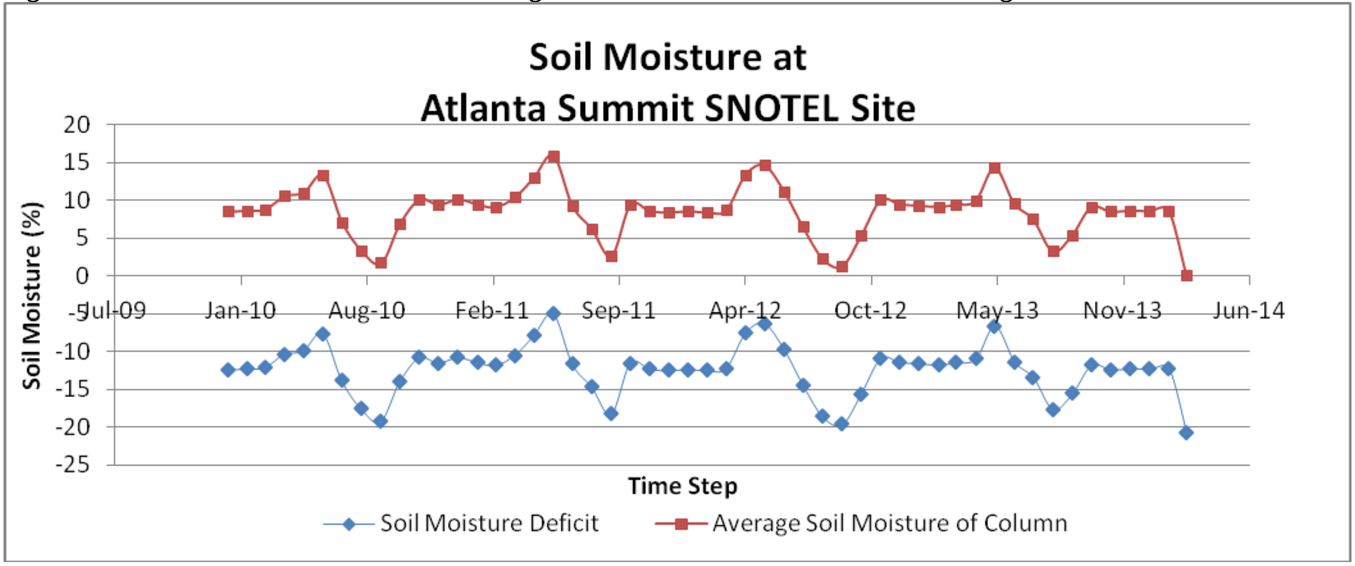

Figure 1 shows that there is strong correlation between the average soil moisture and the soil moisture deficit. Distinct seasonal trends can be observed. Both the soil moisture and the deficit index reach a low point in late summer when the soil is the driest and reach a maximum in spring when the snow begins to melt. The monthly seasonal soil moisture pattern is consistant with seasonal precipitation in this region with higher values in the spring during the melting period and lower values in the summer during the drier parts of the year. Soil moisture deficit index will theoretically be a better predictor of streamflow than the average soil moisture because it takes into consideration the soil textural differences in the ability to hold and retain water.

The average monthly soil moisture deficit was used as a parameter in the regression equation to assess if it could be correlated enough to be used in the water supply forecast. Each station's soil moisture deficit index was an input as a monthly time step and the best fit for the forecast was the soil moisture deficit from the previous summer. This is logical assuming that the winter precipitation and snowpack would melt filling the soil pores combining with the residual soil water from the previous summer before the streamflow runoff would occur.

Results and Discussion

Adding the average monthly soil moisture deficit for each station into the regression model produced the following correlation results:

Table 2. Regression correlation for each station soil moisture deficit to the Boise River at Twin Springs April-July 2013 streamflow.

	Atlanta Summit SNOTEL	Bogus Basin SNOTEL	Jackson Peak SNOTEL	3 Stations
	Previous May-September	Previous Mar-September	Previous Mar-September	
Correlation coefficient(r)	0.361	0.429	0.405	0.484
Years of data	14	13	15	13

When the soil moisture deficits for all stations are combined in a variable in the forecast model, the correlation is 0.484. Using it as the sole predictor in the model of streamflow produces relatively good results that roughly follow the streamflow volumes of high and low years [Figure 2]. When θ_{di} was used in conjunction with the traditional snow and precipitation parameters, the forecast showed significant improvement over the model based on snow and precipitation alone. As shown in Figure 2, the flow simulation is closer to the actual flows for the model that included the soil data with the precipitation parameter than the simulation that include the precipitation parameter alone (Historical Forecast) from 2001 to 2013.

Figure 2. Boise River Flow vs. year. Historical forecast, modeled with soil moisture deficit only, and modeled with snow and soil moisture deficit.

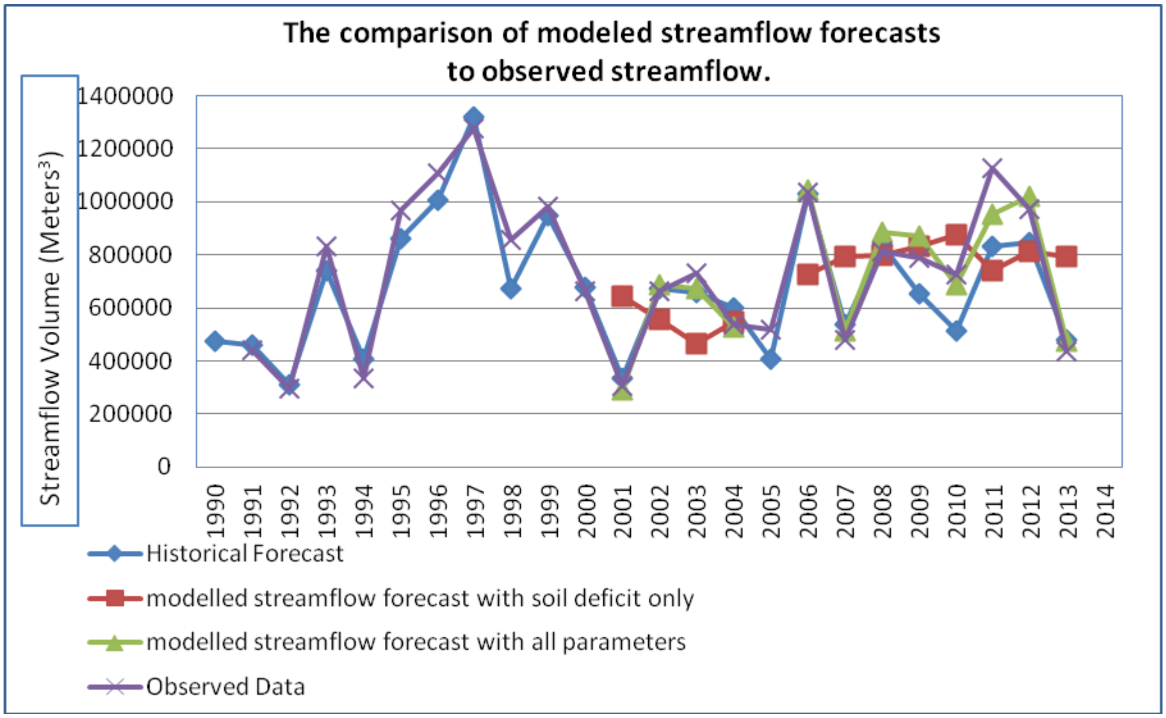

Figure 3 indicates the absolute errors from 2001 to 2013 between the model simulations and the actual stream flow. Streamflow forecasts that include the soil moisture deficit index have less absolute error than those forecasts that is used as a parameter in the forecast.

Figure 3. Historical Forecast, the new model with soil moisture and the observed streamflow, Volume/year vs. year.

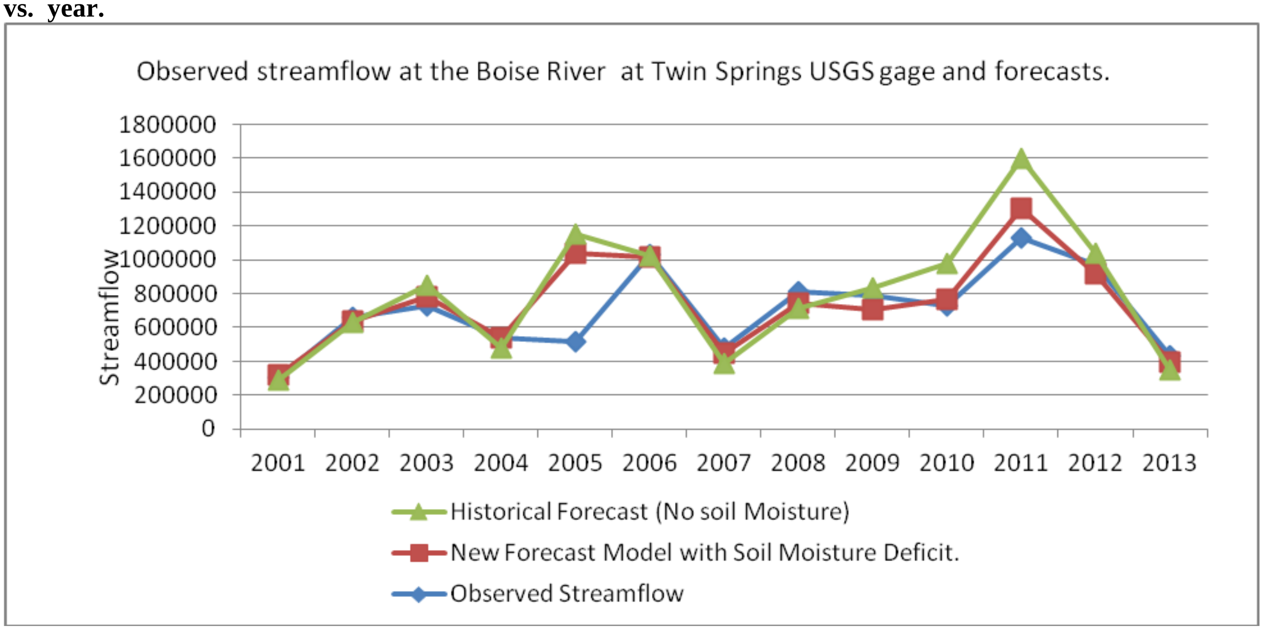

Each of the parameters in the forecast provides a percentage of the total to provide the best statistical model of the streamflow volume. The average monthly soil moisture deficit accounts for 13% of the total forecast model. Each station accounts for a portion of the total (table 3.). All the April 1 snow (SWE) combines to a weighted value of 59%, while the combined weighted march precipitation accounts for 28% of the forecast total.

Table 3. The monthly average soil moisture deficit accounts for a percentage of the total modeled forecast equation for the Boise River at Twin Springs Idaho April-July volume.

	Atlanta Summit SNOTEL	Bogus Basin SNOTEL	Jackson Peak SNOTEL	3 Station total
Percentage of the total forecast accounted for by the soil moisture deficit for each station.	3%	5%	5%	13%

Conclusion

Using soil moisture measurements directly can improve the water supply forecasts to provide a more accurate model and assessment of water supplies. The soil moisture deficit also provides early information before the winter season about the water needed to fill the deficit and its effect on the snowmelt streamflow runoff. As the years of data increase for the soil moisture sensors at the NRCS stations, the data will be able to be used in more models across the West. The NRCS SCAN (Soil Climate Analysis Network) also has soil moisture sensors and that data can be used in other applications across the country.

Disclaimer:

The USDA NRCS does not endorse any source or product in our climate and snowpack measurement system.

References

Campbell, J.E., 1990. Dielectric properties and influence of conductivity in soils at one to fifty Mega Hertz. Soil Science Society of America Journal. 54:332–341

Folliott, P. F., Gottfried, G. J. and Baker, M.B., Jr, 1989. Water yield from forest snowpack management: research findings in Arizona and New Mexico. Water Resources Research. 25: 1999–2007.

Garen, D. ,1992. Improved Techniques in Regression-Based Streamflow Volume Forecasting, ASCE Journal of Water Resources Planning and Management, 118 (6).

Kenny, J.F., Barber, N.L., Hutson, S.S., Linsey, K.S., Lovelace, J.K., and Maupin, M.A., 2009, Estimated use of water in the United States in 2005. U.S. Geological Survey Circular 1344

Lea, J. and Harm, D.,2011.. Developing NRCS SNOTEL and SCAN Soil Moisture Parameters for Water Supply Forecasting Application, Western Snow Conference 2011 Proceedings.

Logsdon, S.D. 2005. Soil dielectric spectra from vector network analyzer data. Soil Science Society of America Journal 69:983–989.

Seyfried, M.S., Grant, L. E., Du, E, and Humes, K., 2005. Dielectric loss and Calibration of the Hydra Probe Soil Water Sensor. Vadose Zone Journal 4:1070-1079.

SNOTEL, US Department of Agriculture, National Resources Conservation Service, http://www.wcc.nrcs.usda.gov/snow/

Topp, G. C.. Davis, J. L, Annan, A. P.,1980. Electromagnetic Determination of Soil Water Content; Measurements in a Coaxial Transmission Lines. Water Resources Research, 16(3): 574-582.

US EIA, State Renewable Electricity Profiles, 2012. US Energy Information Administration http://www.eia.gov/

NEW DEVELOPMENTS, PAPER 3.1

Multi-GHz Monitoring of Cement Hydration using Time Domain Reflectometry Dielectric Spectroscopy

N. E. Hager III,[1,2] R.C. Domszy,[1,2] and M. R. Tofighi[3]

[1]Dept of Physics and Engineering, Elizabethtown College, Elizabethtown, PA, 17022, USA
[2]Material Sensing & Instrumentation, Inc., 772 Dorsea Rd. Lancaster, PA 17601, USA
[3]Electrical Engineering, The Pennsylvania State University at Harrisburg, Middletown, PA, 17057, USA

Abstract

The compressive strength of concrete is directly related to the degree of hydration in the cement paste. Our prior work demonstrated a continuous monitoring of the physical state of water in hydrating cement paste from around 10 kHz to several GHz throughout the cure process. The broadband complex permittivity was monitored as a function of cure time using Time-Domain-Reflectometry (TDR) Dielectric Spectroscopy and an embedded capacitance sensor. Current work now focuses on extending the frequency range to around 12-15 GHz, to more fully capture the free-water relaxation occurring in this range and separate it from the bound-water relaxation occurring at lower frequencies. New methods being developed include a TDR Smith chart, which displays the TDR transient in a complex reflection-coefficient plane, accentuating differences between expected sensor loading and unwanted signal artifacts. Such artifacts may include reflections from sample boundaries, resonance in the sensing pin, reflections from shielding arrangements, and errors in numerical transforms. Other methods include improved calibration using reference liquids which closely match the real and imaginary permittivity of hydrating cement at various stages of cure. In fresh cement paste, where water-loading and ion conductivity is high, a mixture of saline and Poly(methyl methacrylate) (PMMA) powder

provides a reference with a relaxation time similar to pure water, but at a reduced permittivity and increased conductivity comparable to fresh cement paste. At longer cure times, where water-loading and ion conductivity are minimal, references such as tetrahydrofuran with added electrolyte provide a comparable relaxation reference and reduced conductivity comparable to cured paste. These two references set a high and low "calibration window" through which the real and imaginary permittivity can be monitored over a wide range in cure. To verify dispersion in the captured TDR transient directly, transients are compared in the time domain with constant-permittivity references to ensure expected stretched exponential behavior is present. Methods should have broad applications in a variety of inorganic/organic materials and aqueous systems of interest in groundwater characterization.

Introduction

The setting of ordinary portland cement (OPC) is caused by the formation of calcium silicate hydrate (C-S-H)[i] by a dissolution-precipitation process[ii] that occurs when calcium silicates react with water. The ultimate properties of concrete such as compressive strength and pore structure are governed by these hydration reactions, and hence the service life of concrete is largely controlled by cure conditions.

Techniques to characterize the nature of the water reactions include Nuclear Magnetic Resonance (NMR) relaxation measurements,[iii,ii] solid-state ^{1}H NMR experiments[iv] and quasi-elastic neutron scattering (QENS).[v,vi] A variety of electrical methods can also be used including low frequency methods, which follow dissolved alkali ions in percolative channels, and high-frequency methods, which monitor the ability of the water molecule to reorient in an applied electric field. Pervious work in our laboratory[vii] demonstrated a Time Domain Reflectometry (TDR) method for monitoring of the dielectric relaxation spectrum in hydrating cement paste, over the frequency range 10 kHz to several GHz from initial mixing to several weeks cure.

A limitation has been obtaining reliable information over 10 GHz where the free-water relaxation occurs.[viii] Information in this range is desirable, as it more clearly separates the free-water relaxation occurring around 18 GHz from the bound-water relaxation occurring below 1 GHz. We have recently developed a TDR Smith chart technique[ix] to isolate small instrument artifacts captured in the reflected signal from dielectric response, which become accentuated by Laplace transform and differential methods used in processing and calibration. The focus here is to apply this and other calibration methods to obtain complex permittivity spectra in cement paste to around 15 GHz, continuously as a function of cure time.

Background[9]

The expressions governing TDR Dielectric Spectroscopy are described in the literature.[x] An incident voltage pulse $v_i(t)$ propagating along a transmission line of characteristic admittance G_c encounters a terminating capacitive sensor of admittance Y producing a reflected pulse $v_r(t)$. The terminating admittance is the total current-to-voltage ratio $G_c(v_i - v_r)/(v_i + v_r)$, where v_i and v_r are the Laplace transforms of the incident and reflected pulses. The terminating admittance is related to sample permittivity ε by $Y = i\omega\varepsilon C_o$, so the permittivity is written as:

$$\varepsilon(\omega) = \frac{G_c}{i\omega C_o}\frac{v_i - v_r}{v_i + v_r}$$ **Equation 1**

where C_o is the geometric capacitance of the open terminated sensor.

To establish a common time reference, the incident voltage is substituted by the empty sensor reflection, by writing Equation 1 for both empty sensor and sample reflections and manipulating the two equations to eliminate v_i. The result is a relative *reflection function* ρ(ω) of similar form:

$$\rho(\omega) = \frac{G_c}{i\omega C_o}\frac{v_{r,r} - v_{r,x}}{v_{r,r} + v_{r,x}}$$ **Equation 2**

where $v_{r,r}$ and $v_{r,x}$ are the reflected pulse's Laplace transforms for the empty sensor and sample reflections.

Alternatively, the reflection function ρ(ω) can be written in terms of a relative *reflection coefficient* Γ_{rel}

$$\rho(\omega) = \frac{G_c}{i\omega C_o}\frac{1 - \Gamma_{rel}}{1 + \Gamma_{rel}}$$ **Equation 3**

where $\Gamma_{rel} = v_{r,x}/v_{r,r}$ is the *reflection coefficient* of the unknown signal relative to the empty-sensor signal.

The complex permittivity is then obtained from a differential expression:

$$\varepsilon(\omega) = \frac{\rho + 1}{1 - (\omega C_o/G_c)^2\rho}$$ **Equation 4**

where the denominator represents the offset between the incident pulse and the empty sensor reflection at the measurement plane. The complex permittivity can also be written in bilinear form, to remove transmission line effects:

$$\varepsilon = \frac{(1 + A)\rho + C}{1 - B\rho}$$ **Equation 5**

where complex parameters A, B, and C are determined using calibration with known reference standards.

A key step is displaying the initially transformed data in the complex plane as a relative reflection coefficient, thus providing a simple Smith chart as a diagnostic for unwanted signal artifacts. The relative reflection coefficient approximates the absolute reflection coefficient $\Gamma_x = v_{r,x}/v_i$, provided the empty-sensor capacitance is small and empty-sensor reflection approximates the incident pulse. Real and imaginary components are plotted on the lower capacitive half of the Smith chart as a function of frequency, with the approximate sensor admittance read from the susceptance and conductance circles. Since Γ_{rel} is referenced to the empty-sensor, reflection losses in the transmission line do not appear, and losses appearing on the Smith chart are due to sample losses. An increasing real permittivity produces an increasing sensor susceptance, following a path around the lower perimeter of the Smith chart, while an increasing sample loss produces an increasing sensor conductance, following a path which spirals inward on the Smith chart. Artifacts in acquisition or Laplace transform appear as deviations from this expected behavior; these may include resonance of the sensing pin, reflections within the sample boundaries, resonance of the sensing pin, or improper Laplace transform settings. The TDR Smith chart thus provides a quick method for assessing sensor response and material characteristics in the multi-GHz range, which requires no calibration and is only one computational step removed from the direct TDR transient.

Procedures

Measurements are made in Portland cement paste mixed in a water-to-cement ratio of 0.35. The fresh paste is placed in a styrofoam cup with the sensor immersed and cup sealed to prevent evaporation. The sensor is a 20-30 cm length of 3.5 mm semi-rigid coaxial line (MicroCoax UT-141) in which one end is ground mechanically flat. This provides a terminating capacitance of around 20 fF into the sample material, as determined by calculating the reflection function ρ (Equation 3) matching to a known permittivity in the low-frequency limit, and working backwards to obtain the sensor capacitance C_o.

Calibration liquids are chosen to tightly straddle the range of permittivity and frequency response expected during cement cure. We assume the fresh cement paste contains a strong water-like relaxation, reduced in amplitude by the water/solids ratio.[xi,xii] We make no assumption for the cured cement, and choose a low-permittivity calibration which varies only slowly with frequency in permittivity and loss.

For the fresh cement paste, a mixture of saline and PMMA beads (Acros Organics, m.w. 35,000, diam. 50-150 μm) provides an 8.2 ps water-like relaxation at the reduced permittivity ($\varepsilon' \approx 40$) and water/solids ratio of fresh cement paste. The bulk PMMA relaxation is negligible[xiii], and the saline has a conductivity that matches the cement conductivity. To ensure uniformity, the mixture is stirred with a magnetic stirrer during measurement. At longer stages of cure, a low-permittivity solvent with a very high relaxation frequency provides a slowly deceasing real permittivity $\varepsilon'(\omega)$ and a slowly increasing imaginary permittivity $\varepsilon''(\omega)$ through the range. Solvents such as tetrahydrofuran[xiv] (THF) or dichloromethane[xv] work appropriately, with a small amount of electrolyte added[xvi,xvii] to increase low frequency conductivity. A finite conductivity is needed to keep calibration and empty-sensor signals resolvable from one another, so bilinear parameters can be generated over the entire frequency range.

Signals are acquired with an Agilent 54750 TDR oscilloscope with a 54754A differential plug-in, which has a 35-ps internal voltage step and a 20-GHz detection bandwidth. Reflected signals are captured non-uniformly on consecutive linear time segments[xviii], starting at 10 ps/cm and increasing to 500 μs/cm in an automated sequence. At the beginning of the sequence the incident pulse is captured and used as a timing reference, with a feedback algorithm adjusting the timing of all later segments to provide drift control. Small jitter between segments is further minimized by scanning the entire sequence repetitively and averaging, thus minimizing jitter between the incident and initial reflected pulses during sequencing. The incident and initial reflected pulses are captured at 2000 points to provide a timing resolution of 50 fs/point, with later segments gradually reduced to 200 points per segment. Other settings are typically 12 time segments, with 32x signal averaging for each segment, and 8 repetitions of the entire sequence for a total acquisition time of 3-4 minutes. Since the scope is AC-coupled, a vertical correction is applied to each segment to remove DC offsets from electrochemical effects and splice it smoothly with the preceding segment.

To reduce excessive computation and noise the linear segmented data is interpolated onto a logarithmic time scale prior to Laplace transform, using cubic-spline algorithms found in most math software. Each segment is first run through a median smoothing filter to minimize noise and provide additional signal averaging. Then the smoothed data is interpolated linearly up to the peak of the reflected transient, and logarithmically for all times thereafter. The linear interpolation is spaced at 5 ps per point, consistent with a 100 GHz Nyquist sampling frequency which is well above the 20 GHz bandwidth of the scope. The logarithmic interpolation starts at 5 ps per point and increases at a rate of around 50-60 points per decade.[xix] A numerical Laplace integration is performed over the interpolated data with the integration interval adjusted to the logarithmic data spacing. Further details are found in the references.[ix]

Results

Reflected transients are shown in Figure 1 for saline/PMMA high calibration, a THF/zinc nitrate low calibration, and hydrating cement paste at cure times of 0 h, 8 h, 24 h, and 72 h. In each case segment 1 is the timing reference, segment 2 is the initial reflected transient, and segments 3-12 are the continuation of the initial reflected transient on increasing time scales. The empty sensor returns a positive reflection indicating the open-circuit reference, while the liquids return an increasing negative reflection whose exponential decay is governed by the loaded sensor capacitance and the 50 Ω (0.02 S) line impedance. The negative peak reflection amplitude decreases with increasing permittivity, and the stretched-exponential decay follows the changing permittivity and loss with frequency. In TDR measurements of calibration samples and cement paste, the stretched-exponential decay spans many decades due to ionic conduction and electrode polarization. The high calibration uses approximately 0.5 M saline in PMMA, and the low calibration uses approximately 0.4 M $(Zn(NO_3)_2 \cdot 6H_2O)$ in THF.

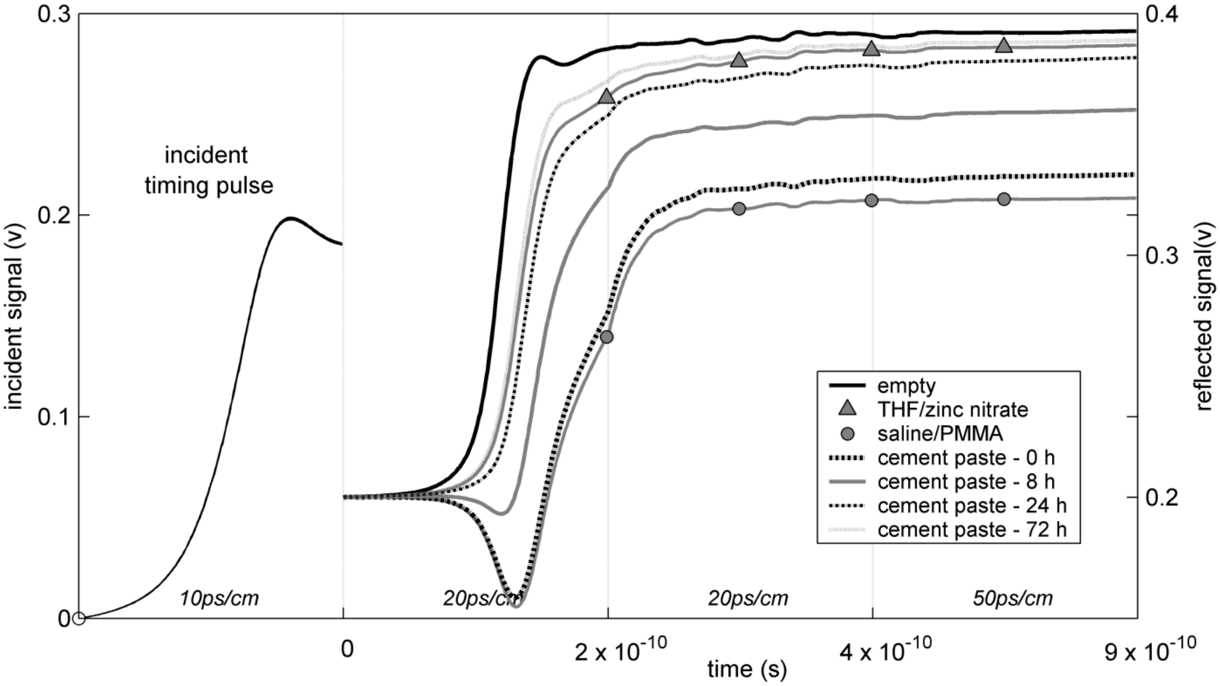

Figure 1 - Segmented transient acquisition for calibration liquids and cement paste with 3.5-mm flat termination (4 of 12 segments shown).

The corresponding Smith charts for the reflected transients are shown in Figure 2. The figure uses an admittance Smith chart, with susceptance/conductance circles originating from the left, displaying the terminating admittance (proportional to permittivity) in the standard manner as a parallel combination of capacitance and conductance. Circles of constant susceptance and constant conductance are labeled, normalized to the 0.02 S (50 Ω) line admittance. For each transient, the Smith chart shows the load susceptance $\varepsilon'\omega C_o$ increasing with frequency, crossing lines of constant susceptance and tracing an arc around the lower perimeter of the chart. Selected frequency points are labeled, starting at 2 GHz on the right and continuing to 16 GHz on the left.

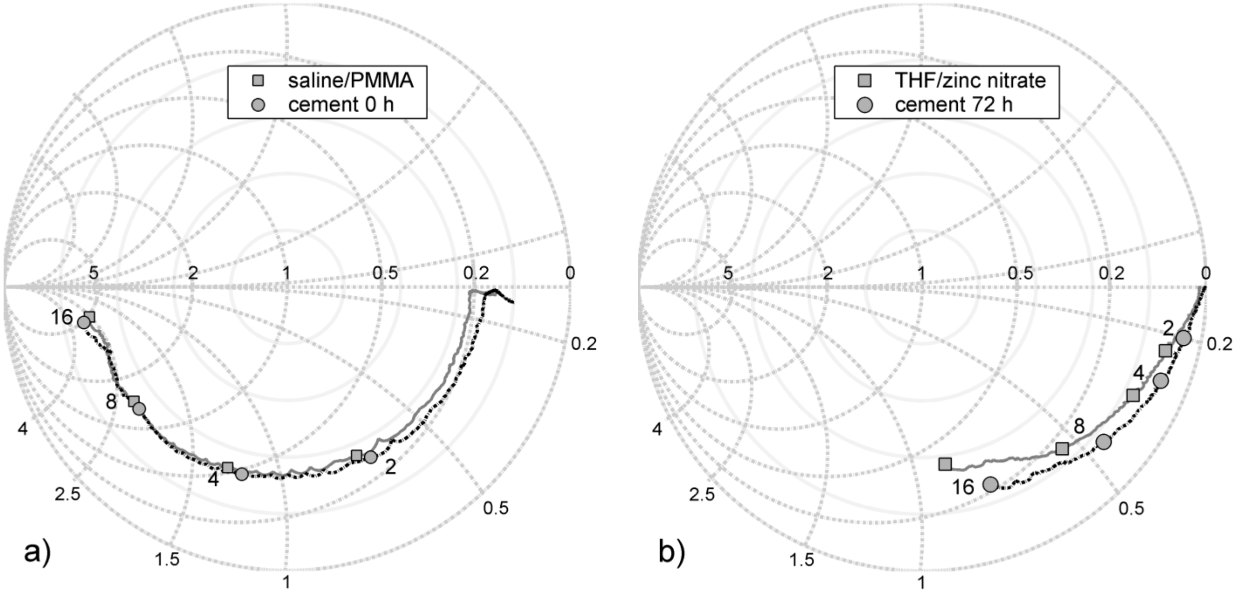

Figure 2 - TDR Smith charts for calibration liquids and cement paste at 0 h and 72 h cure. Frequency markers are shown in GHz.

Figure 2 shows the relative reflection coefficient Γ_{rel} for two different cure levels. Figure 2a shows the fresh cement paste signal at 0 h compared with the saline/PMMA reference. The two signals follow a smooth circle around the lower interior of the complex plane, showing a rapid increase in susceptance with frequency and following a circle of constant conductance. No large deviations due to sample boundary reflections[9] or Laplace transform artifacts are seen. The susceptance approaches resonance at around 16 GHz (negative real axis) where the absolute reflection coefficient Γ_x crosses into the inductive region. Fig 2b shows the cement signal at 72 h compared with the THF/zinc nitrate reference. The permittivity is now reduced at the lower free-water loading, and Γ_{rel} traces a shorter path around the lower perimeter of the diagram. The conductivity has also decreased, as Γ_{rel} at low frequencies moves to the outer perimeter of the diagram. Γ_{rel} spirals inward with increasing frequency, indicating an increasing loss factor ε''(ω). The Smith chart thus provides a quick way showing the data is behaving as expected and is free of unwanted artifacts, before proceeding to the next step of calibration.

Figure 3 shows the reflection function ρ(ω) for the 2 calibration liquids. Real and imaginary parts are shown as a function of frequency, and overlaid with dielectric models for the expected behavior for both calibrations. ρ'' is multiplied by $\varepsilon_0\omega$ to display the conductivity, thus removing the ω^{-1} dependence at low frequencies and displaying as a deviation from constant conductivity (displayed on a log scale). For the THF/zinc nitrate calibration, the model includes a 4 ps solvent relaxation (Debye), a 200 ps solute relaxation (Cole- Davidson β= 0.8), a solvent relaxation magnitude of 8, a solute relaxation magnitude of 9, and a 0.11 S/m ion conductivity. For the saline/PMMA calibration, the model includes an 8.2 ps free-water relaxation (Debye), an adjustable free-water relaxation magnitude, and a 1.9 S/m ion conductivity. Complex bilinear parameters A(ω) and B(ω) are generated by solving Equation 5 for 2 calibration references, and separating real and imaginary parts into 4 simultaneous equations. Details are given in the references.[ix]

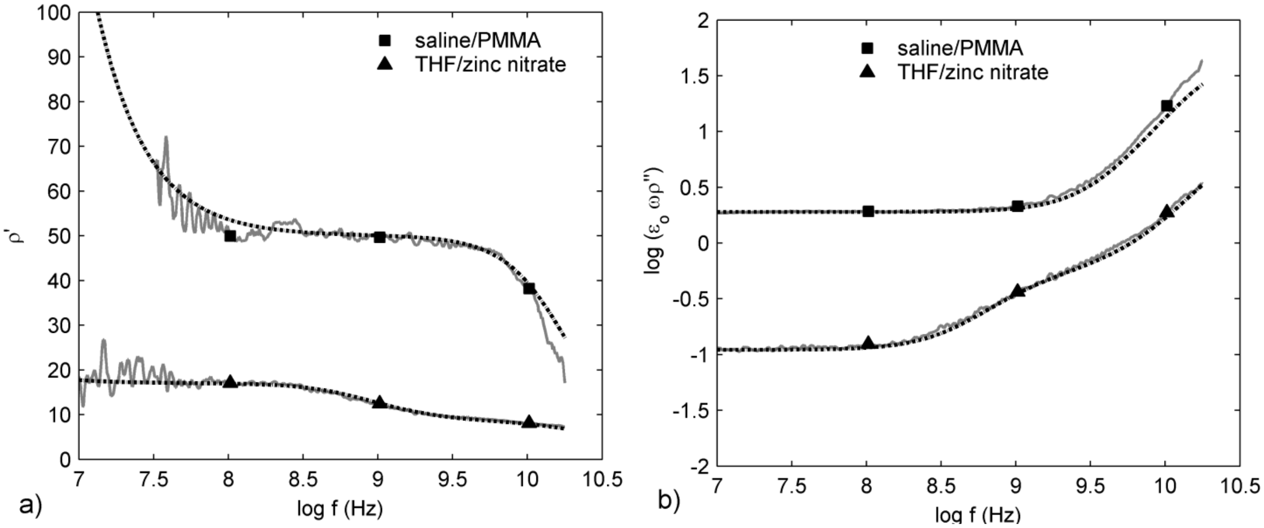

Figure 3 – Reflection function ρ' and $\varepsilon_o\omega\rho''$ for calibration liquids and model fit for THF/zinc nitrate and saline/PMMA.

Figure 4 shows the calibrated cement permittivity for the data in Figure 1, calibrated using the bilinear parameters obtained from Figure 3. The data is valid to around 15 GHz, and shows that at around 10 GHz the permittivity ε' starts decreasing and the conductivity $\varepsilon_o\omega\varepsilon''$ starts increasing. As cure proceeds both the magnitude ε' over the range decreases as well as the magnitude of the 10 GHz transition. Simultaneously, the magnitude of the conductivity $\varepsilon_o\omega\varepsilon''$ (displayed on a log scale) decreases over the range as well as the magnitude of the 10 GHz peak transition. A broad feature appears around 100 -1000 MHz in the conductivity, which should be due to the bound water signal observed previously.

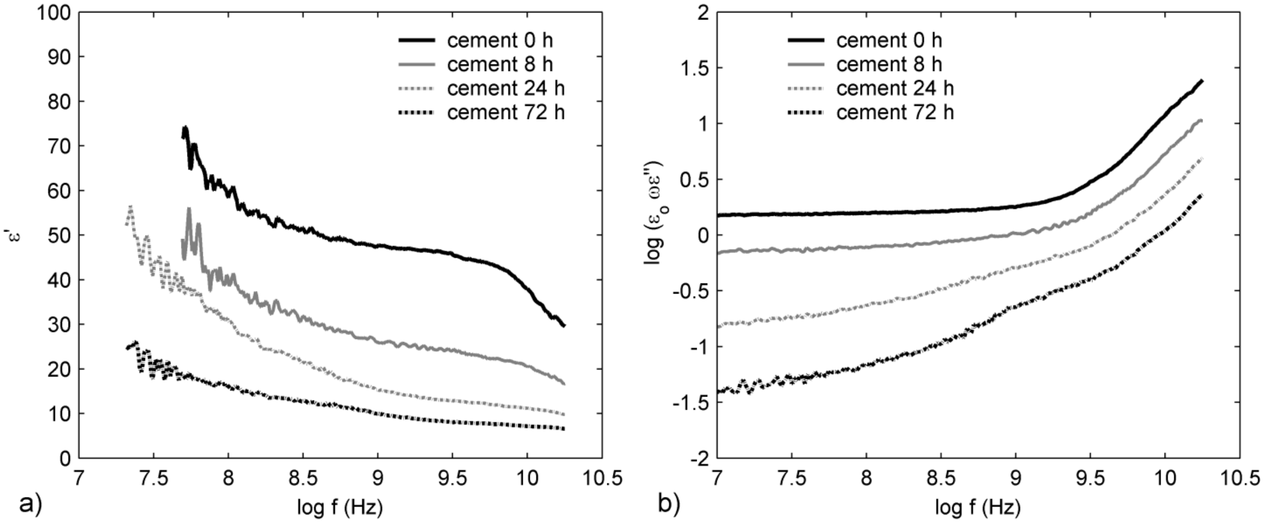

Figure 4 – Calibrated real permittivity ε' and conductivity $\varepsilon_o\omega\varepsilon''$ during cement cure.

The entire signal evolution remains within the calibration "window" defined in Figure 3 for both real and imaginary components. The relaxation amplitude decreases in both permittivity and conductivity as cure proceeds, as water is consumed in reaction. Sensitivity is gained in the 10-15 GHz range, critical to resolving free-water behavior, but lost below 100 MHz due to the lower sensor capacitance. (20 fF). It would seem reasonable that data could be captured over the entire range 10 kHz to 15 GHz, using the current sensor with a flat termination (20 fF) and the previous sensor with protruding pin (100 fF) running in tandem.

Discussion

We have demonstrated the monitoring of complex permittivity of hydrating cement paste in the 100 MHz to 15 GHz range continuously as a function of cure time. This bandwidth is sufficient to observe details of 18 GHz free-water relaxation, and separate it from the bound-water relaxation occurring below 1 GHz. This bandwidth is achieved through the use of Smith chart analysis, to control small unwanted artifacts, and the use of calibration standards which tightly define a calibration "window" for the range of frequency and cure state.

Future work should include a low-calibration model system with a similar permittivity and conductivity, but with a lower or negligible solute relaxation. A candidate for this could be dichloromethane with perchlorate salts.[xv,xvi] Additional work will involve using a complex model fit to fully separate free- and bound-water components as a function of cure time. Additional components would be included in the model, such as a limiting high-frequency permittivity ε_∞ to better fit the $\varepsilon'(\omega)$ roll-off.

Acknowledgement

This work was supported in part by the National Science Foundation under grant number 0700699.

---

[i] Cement chemistry notation: C = CaO, S = SiO_2, H = H_2O, A = Al_2O3.

[ii] H. F. W. Taylor, Cement Chemistry, 2nd ed. (Thomas Telford Publishing, London, 1997).

[iii] R. J. Wittebort, M. G. Usha, D. J. Ruben, D. E. Wemmer, and A. J Pines, J. Am. Chem. Soc, **110**, 5668 (1988).

[iv] R. Rassem, H. Zannitheveneau, D. Heidemann, and A. Grimmer, Cement and Concrete Research, **23**, 169- (1993)

[v] S. A. FitzGerald, D. A. Neumann, J. J. Rush, D. P. Bentz, and R. A. Livingston, Chem. Mater. **10**, 397 (1998).

[vi] J. J. Thomas, S. A. FitzGerald, D. A. Neumann, and Richard A. Livingston, J. Am. Ceram. Soc. **84** (8), 1811 (2001).

[vii] N. E. Hager III and R. C. Domszy, J. Appl. Phys. **96**, 5117-5128 (2004).

[viii] U. Kaatze, J. Molecular Liquids, **56**, 95 (1993).

[ix] N.E. Hager III, R.C. Domszy, M.R. Tofighi, Rev. Sci. Instrum. 83, 025108 (2012).

[x] R. H. Cole, J. G. Berberian, S. Mashimo, G. Chryssikos, A. Burns, E. Tombari, J. Appl. Phys. **66**, 793 (1989).

[xi] D.A. Robinson, S.P. Friedman, J. Non-Crystalline Solids 305, 261 (2002).

[xii] S. B. Jones, S. P. Friedman, Water Resources Research, 36 (10), 2821c (Oct 2000).

[xiii] S. Mashimo, H. Nakamura, A. Chiba, J. Chem. Phys, 76, 6342 (1982).

[xiv] A. C. Khumbharkhane, et al, Pramana J. Phys., Vol. **46** (2), 91 (Feb 1996).

[xv] J. Hunger, A. Stoppa, A.Thoman, M. Walther, R. Buchner, Chem. Phys. Lett. **471**, 85 (2009).

[xvi] B. Gestblom, J. Songstad, Acta Chemica Scandinavica, **B41**, 396 (1987).

[xvii] H. Farber, J. Petrucci, J. Phys. Chem., **79(**12) 1221 (1975).

[xviii] N.E. Hager III, Rev. Sci. Instrum. **65**, 887 (1994).

[xix] F. I. Mopsik, Rev. Sci. Instrum. **55**, 79 (1985).

TRANSACTIONS OF THE FOURTH INTERNATIONAL SYMPOSIUM ON SOIL WATER
MEASUREMENT USING CAPACITANCE, IMPEDANCE AND TDT
MONTREAL, CANADA, JULY 16 – 18, 2014

NEW DEVELOPMENTS, PAPER 3.2

Development of a Capacitance-Based Sensor for On-the-Go Soil Moisture Measurements

Maria Mastorakos[1*,] Viacheslav Adamchuk[1**], Frédéric Réne-Laforest[1], Charles Hemplemen[2]

[1]Bioresource Engineering Department, McGill University, Ste-Anne-de-Bellevue, Quebec, Canada

[2]Retrokool, Inc., Berkeley, California, USA

Abstract

Mapping the heterogeneity of soil water content within an agricultural field can be advantageous when optimizing crop management in response to local soil conditions. Capacitance-based soil sensors have been a popular means of *in-situ* quantification of soil water content. However, current commercial sensors have been used only for point-based measurement and temporary monitoring when placed in a stationary position. This limits their ability to obtain a thorough representation of soil water conditions with high spatial resolution at an economically feasible cost. The sensor system presented in this paper was developed for on-the-go measurement of soil water content. The sensor operates at a maximum depth of 10 cm below the soil surface. The sensor is small in size (20 cm in length, 5 cm high and wide), is simple to operate and relatively inexpensive. The measurements obtained from this sensor can be used for

---

[*] Presenter (maria.mastorakos@mail.mcgill.ca)

[**] Corresponding author (viacheslav.adamchuk@mcgill.ca)

constructing soil moisture maps to be employed in the follow-up decision making process and/or to control the parameters of a specific field operation, such as planting depth, in real time. Preliminary laboratory evaluation of the latest sensor prototype has revealed lower than 8% soil water content prediction errors (both gravimetric and volumetric) while testing soils with a broad range of particle size distributions.

Keywords: soil moisture, on-the-go sensors, capacitance, precision agriculture

Introduction

One of the technological limitations affecting the adoption of precision agriculture is lack of real-time information regarding spatially variable soil water content (Andrade *et al*. 2004). Monitoring soil moisture on-the-go allows farm machinery operators to tailor the application of seed, fertilizer or other inputs according to specific local needs. Currently, there are four strategies for measuring soil water content: 1) laboratory analysis of soil samples, 2) point-based *in-situ* measurements using stationary sensors, 3) on-the-go sensing, and 4) indirect predictions using remote sensing data. Many studies utilize laboratory analysis as a reference method even though point-based measurement systems offer various benefits including faster data collection and the ability for temporal monitoring of water content in a given location. Solid-state electrical resistivity granular matrix sensing, gamma-ray attenuation, time-domain reflectrometry, and neutron thermalization are examples of point-based sensing systems (Topp 1993). However, point-based systems have major shortcomings since they do not map the true heterogeneity of soil water content across large areas, such as farm fields. As a result, researchers began exploring the possibility of developing on-the-go sensing systems. Similarly to remote sensing, on-the-go soil sensors allow for obtaining relatively high data density at a low cost. However, in most cases these measurements are more directly linked to subsurface soil water content than those obtained from aerial or satellite platforms.

The dielectric constant of water (ε = 80) is much greater than that of soil (ε = 3 to 5) and air (ε = 1). It is therefore possible to estimate soil water content by measuring indirectly the dielectric constant of wet soils (Thomas 1966; Campbell 1990; Sun *et al*. 2005). Due to the high magnitude of differences between the dielectric constants of water vs. soil and air, the use of capacitance based sensors for sensing of moisture has been seen as an attractive option (Dean *et al.* 1987; Eller and Denoth 1995; Gaudu *et al.* 1994). Also, the capacitance-based sensors have been indicated as a viable choice for dynamic soil moisture sensing (Whalley *et al.* 1992). In addition to providing accurate field maps of soil moisture content variability, on-the-go soil sensing systems could be implemented into other field operations. For instance, information gathered in real-time from an on-the-go soil moisture sensor could be coupled with a control system that changes seed planting depth (deep seeding in relatively dry soil and surface seeding in wet areas). Alternatively, the sensor could be used to map field drainage infrastructure and identify poorly drained areas.

Mouazen *et al.* (2004) developed an on-line soil moisture sensor using a near-infrared spectrophotometer. The need for soil-specific calibration and a relatively high cost are the main disadvantages of optical soil moisture sensing. Based on the original work by Andrade *et al.* (2004), Adamchuk *et al*. (2004) developed a three-electrode capacitance sensor operated in a vertical configuration to measure soil water content using one side of the slot to cut in soil. The same approach was used for the second prototype (Adamchuk *et al.* 2009), which allowed measurements to be made from both sides of the slot. One disadvantage of the first two sensor designs was a requirement for a relatively deep slot and poorly controlled depths of measurement. The ***objective*** of this project was to develop a capacitance-based on-line soil sensor capable of detecting subsurface soil water content at a predefined depth for real-time applications.

Materials and Method

The sensor shown in Figure 1 consisted of a plastic encasing with two stainless steel electrodes. To ensure contact between the soil and the electrodes, the electrodes were mounted at an angle. Both electrodes were connected to a coaxial cable (one electrode to the inner copper wire and the other to the woven copper shield). The two electrodes were mounted to the plastic casing using nylon screws. As in previous studies, a proprietary electric circuit was constructed by Retrokool, Inc. (Berkeley, California, USA) providing voltage output related to dielectric constant of soil in contact with the two electrodes.

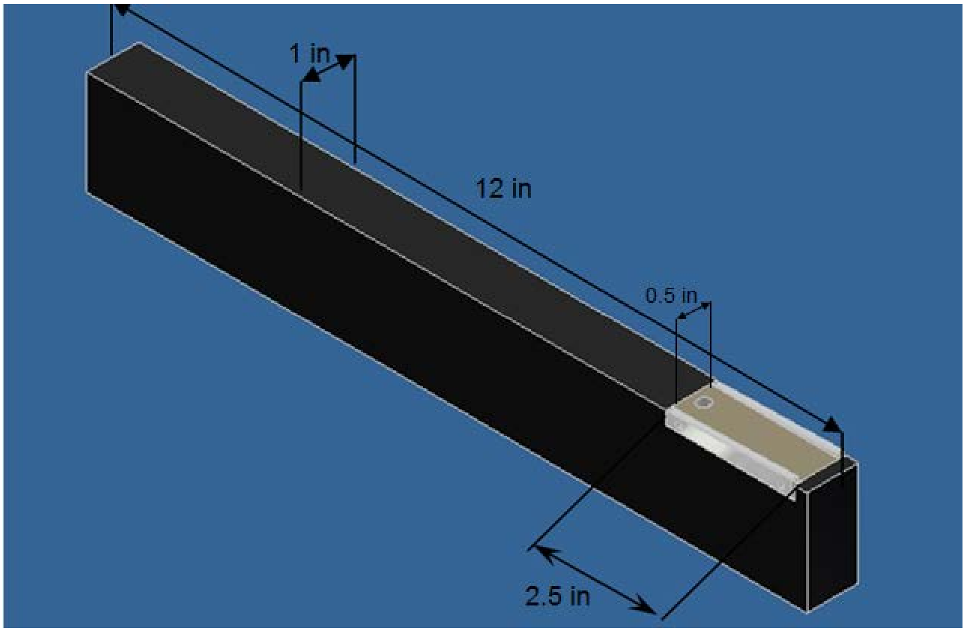

Figure 1. Prototype capacitance soil moisture sensor.

A data acquisition application was developed using LabView software and NI myDAQ card (National Instruments, Corp., Austin, Texas, USA) to enable pairing soil moisture sensor voltage output and geographic coordinates obtained using a GNSS receiver. An applicator knife with a coulter was used to mount the sensor for field mapping as shown in Figure 2.

Figure 2. An applicator knife equipped with the prototype soil moisture sensor.

The sensor was calibrated in the laboratory using five different soils with 3-5 differing amounts of added water. Soil types ranging from clay loam to sandy loam were used with water content ranging from air-dried soil to a near-saturated amount of moisture, not-exceeding 50% volumetric soil moisture content. Each soil-water content combination was replicated three times. Each replication was measured by the sensor and through the laboratory technique. Both gravimetric and volumetric soil water contents were determined using the oven-dry method (Gardner 1987) for each soil and for every amount of added soil water. For each measurement, 50-s average of 1 kHz data output was calculated when sensor was in contact with the soil and a 10-s average when the sensor was held in the air before the measurement.

Recording the sensor's output held in the air was performed to account for any potential drift during multiple days of testing. Due to the non-linear sensor response to the water content increase observed in this test, the following calibration equations were applied:

$$w = \alpha_0 - \alpha_1 \log(V_{air} - V_{soil}) \tag{1}$$

$$\theta = \beta_0 - \beta_1 \log(V_{air} - V_{soil}) \tag{2}$$

where w = gravimetric soil water content (g/g), θ = volumetric soil water content (%), V_{air} = voltage output of the sensor suspended in the air (V), V_{soil} = voltage output of the sensor while measuring soil.

Results and Discussion

Figures 3 and 4 show the relationship between soil water sensor index (SWSI) estimated as $log(V_{air}-V_{soil})$ and the corresponding laboratory measurements. Using a simple linear regression method, the following equations were found:

$$w = 0.61 - 0.21\log(V_{air} - V_{soil}) \tag{3}$$

$$\theta = 65.4 - 22.3\log(V_{air} - V_{soil}) \tag{4}$$

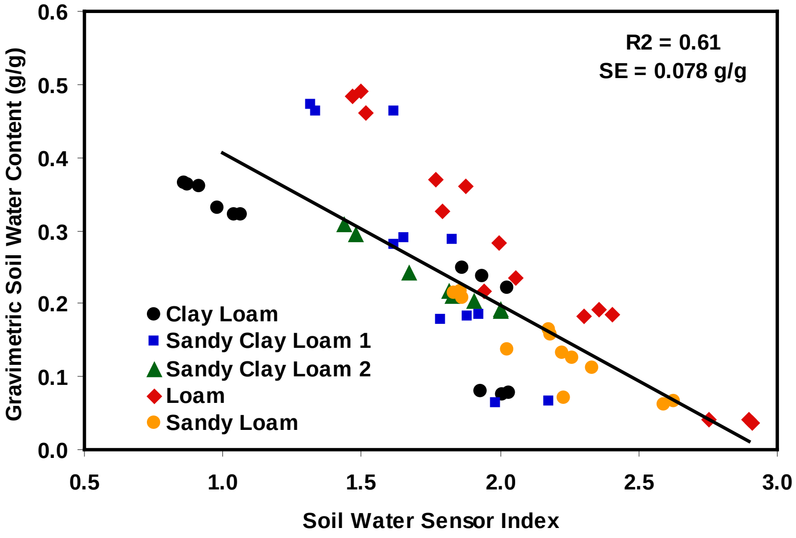

Figure 3. Sensor calibration using gravimetric water content.

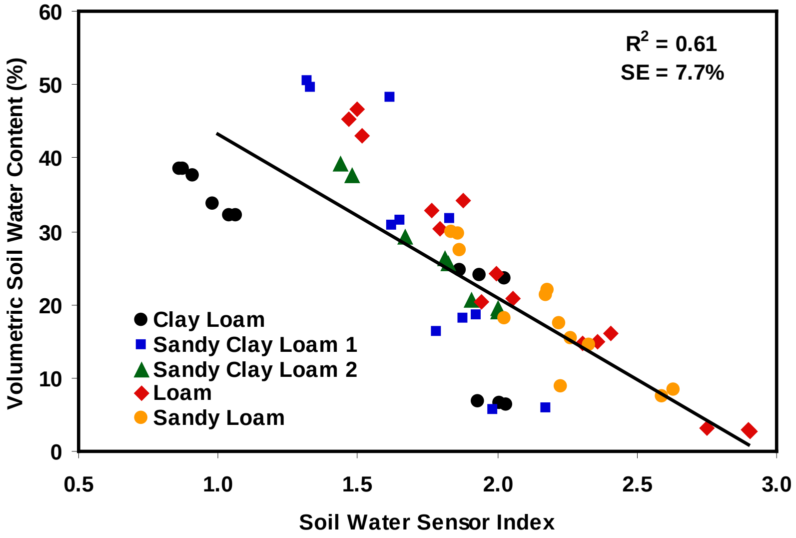

Figure 4. Sensor calibration using volumetric water content.

Based on these results, SWSI was linearly correlated with soil water content with the coefficient of determination R^2 = 0.61. The standard error was near 8 g/g and 8% when predicting gravimetric and volumetric water content, respectively. In previous prototypes, these estimates were around 3 g/g and 4% (Adamchuk *et al.* 2004). This discrepancy could be due to differences among the soils used in this experiment. Table 1 summarizes calibration results for each soil individually. For soil-specific calibrations, standard error varied between 0.025 and 0.059 g/g gravimetric water content as well as between 2.0% and 6.5% volumetric water content. In both volumetric and gravimetric moisture contents, the clay loam soil presented the highest standard errors.

The next step in this research project will be to map the volumetric soil water content and fine-tune calibration equations 3 and 4 for local conditions using a recognized reference method. A portable sensor, such as a time-domain reflectometry (TDR) probe, could be a suitable instrument to use for a field-specific calibration.

Table 1: Soil-Specific Sensor Calibration

Soil type	Equation	R^2	SE
Gravimetric Water Content, g/g			
Clay Loam	$w = 0..52 - 0.19\log(V_{air} - V_{soil})$	0.76	0.059
Sandy Clay Loam 1	$w = 1.16 - 0.53\log(V_{air} - V_{soil})$	0.96	0.033
Sandy Clay Loam 2	$w = 0.62 - 0.22\log(V_{air} - V_{soil})$	0.96	0.045
Loam	$w = 0.91 - 0.31\log(V_{air} - V_{soil})$	0.95	0.038
Sandy Loam	$w = 0.56 - 0.19\log(V_{air} - V_{soil})$	0.82	0.025
Volumetric Water Content, %			
Clay Loam	$\theta = 55.11 - 20.35\log(V_{air} - V_{soil})$	0.75	6.53
Sandy Clay Loam 1	$\theta = 126.05 - 58.83\log(V_{air} - V_{soil})$	0.96	3.54
Sandy Clay Loam 2	$\theta = 92.69 - 36.97\log(V_{air} - V_{soil})$	0.98	2.02
Loam	$\theta = 86.19 - 29.83\log(V_{air} - V_{soil})$	0.94	3.53
Sandy Loam	$\theta = 78.92 - 27.73\log(V_{air} - V_{soil})$	0.82	3.52

Conclusions

The sensor developed in this study was capable of detecting differences in soil water content at a specific depth below the soil surface. Although preliminary laboratory calibration revealed 8% soil water content prediction error, it is expected to be capable of distinguishing field areas with different soil water content. Examining the individual calibration curves, it was clear that certain soils (such as clay) require their own calibration procedure. On-going field mapping activities will provide the actual estimates of soil water content prediction errors when mapping a single agricultural field.

References

Adamchuk, V.I., Hummel J.W., Morgan M.T., and Upadhyaya S.K. 2004. On-the-go soil sensors for precision agriculture. Computers and Electronics in Agriculture 44(1): 71-91.

Adamchuk, V.I., Hempleman C.R., and Jahraus D.G. 2009. On-the-go capacitance sensing of soil water content. 2009 ASABE Mid-Central Conference; 2009 Apr 4-5. St. Joseph, Michigan: ASABE.

Andrade P., Upadhyaya S.K., Aguera-Vega J., Jenkings B.M. 2004. Evaluation of a capacitance-based soil moisture sensor for real-time applications. Transactions of the ASAE 47(4): 1281-1287.

Andrade P., Upadhyaya S.K., Jenkins B.M., Plouffe C., Poutre B. 2004.Field evaluation of the improved version of the UC-Davis compaction profile sensor (UCD-CPS). 2004 ASAE/CSAE Annual International Meeting; 2004 Aug 1-4. Ottawa, Ontario: ASABE.

Campbell J.E. 1990. Dielectric properties and influence of conductivity in soils at one to fifty megahertz. Soil Science Society of America Journal 54 (2): 332–341.

Dean T.J., Bell J.P., Baty J.B. 1987. Soil moisture measurement by an improved capacitance technique, part I.:Sensor design and performance. Journal of Hydrology 93: 67-78.

Gardner, W.H. 1987. Water content. In: Klute, A., editor. Methods of Soil Analysis. 2nd edition. Madison, Wisconsin: America Society of Agronomists. p. 493.

Gaudu J., Mathieu J.M., Fumanal J.C., Bruckler L.,Chanzy A., Bertuzzi P., Stengel P., Guennelon R. 1993. Mesure de l’humidité des sols par une méthode capacitive :analyse des facteurs influençant la mesure. Agronomic 13 : 57-73.

Eller H., Denoth A. 1996. A capacitive soil moisture sensor. Journal of Hydrology 185: 137–146.

Mouazen A.M., De Baerdemaeker J., Ramon H. 2004. Towards development of on-line moisture content sensor using a fibre-type NIR spectrophotometer. Soil & Tillage Research 80: 171-183.

Thomas A.M.1966. *In situ* measurement of moisture in soil and similar substances by fringe capacitance. Journal of Science Instrumentation 3(1): 21–27.

Topp, G.C. 1993. Soil water content. In: Carter, M.R., editor. Soil Sampling and Methods of Analysis. Boca Raton, Florida: Lewis Publishers. p. 541-557.

Sun Y., MA D., Lin J., Lammers P.S., Damerow L. 2005. An improved frequency domain technique for determining soil water content. Pedosphere 15(6): 1–8.

Whalley, W.R., Dean, T.J., Izzard, P. 1992. Evaluation of the capacitance technique as a method for dynamically measuring soil water content. Journal of Agricultural Engineering Research 52: 47–155.

NEW DEVELOPMENTS FORUM, ABSTRACT 3.3

Capacitive Sensing of Water Potential

Leonardo D. Rivera, Douglas R. Cobos, Colin S. Campbell, Gaylon S. Campbell

Decagon Devices, Inc. 2365 NE Hopkins Court, Pullman, WA 99163

ABSTRACT

Since well before the initial development of the field tensiometer by L.A. Richards in the early 1920s, engineers, hydrologists, and soil and plant scientists have desired a maintenance-free sensor for continuous *in situ* monitoring of water potential. Subsequent sensor development efforts by university and private sector researchers have produced several generations of new sensors, but each still has limitations in range of measurement, field robustness, and/or measurement accuracy. After more than a dozen years of continuous development effort, and three separate generations of porous matrix sensors, we now have a sensor that more closely approaches the ideal than previously possible. This presentation will discuss a new, automated calibration procedure allowing individual calibration of large batches of sensors simultaneously. The accuracy resulting from the new calibration procedure will be discussed, as will other *in situ* measurement considerations including robustness, maintenance requirements, range of measurement, soil type dependence, and hysteresis, among others.

NEW DEVELOPMENTS FORUM, ABSTRACT 3.4

IRROmesh Radio Network for Soil Moisture Monitoring

Tom Penning - IRROMETER Company, Inc., Riverside, CA 92507-1600, USA, TomP@Irrometer.com

ABSTRACT

This will be a description of the features and operation of IRROMETER Company's new mesh radio data logging system for soil moisture monitoring.

NEW DEVELOPMENTS FORUM, ABSTRACT 3.5

Enhanced Portable Soil Sensor from Advances in Electronics and Cloud Computing

B. K. Bellingham, Stevens Water Monitoring Systems, Inc., Portland, OR 97220, USA

ABSTRACT

Advances in computer science, and data acquisition engineering were employed in the development of an enhanced portable soil sensor platform called the Stevens POGO.

A Hydra Probe Soil Sensor that has an RS485 half duplex output has been interfaced with a new generation of micro controllers that can convert the RS485 protocol into Wi-Fi making the communication of soil data wireless and compatible with smart phones such as Androids and I-Phones. A patch antenna attached to the RS485/Wi-Fi Module provides low power wireless communication for up to 30 meters. A micro RS485 GPS module was also connected to the Wi/Fi Module providing location data. Smart phone APPs called Turf Pro and HydraMON, were written to retrieve the soil data and the GPS data via an Ad Hoc Wi-Fi connection. The user can instantaneously view data in the field with a smart phone and can then archive the data in the cloud server. The date set includes soil moisture, soil bulk electrical conductivity, temperature, a time stamp and location data. The data can be analyzed by the user or have algorithms perform computations. Cloud based algorithms that can calculate parameters such as sprinkler distribution uniformity, and other predictive modeling methods. Applications include turf management, precision irrigation, hydrological research and other related applications.

NEW DEVELOPMENTS FORUM, ABSTRACT 3.6

"CS650-Series Water Content Reflectometers"

Jason Ritter - Campbell Scientific Inc., Logan, UT 84321, USA

ABSTRACT

The newest generation of water content reflectometers are multi-parameter smart sensors that use innovative techniques to monitor soil volumetric water content, bulk electrical conductivity, and temperature. The factory calibration may be improved by applying a soil-specific linear correction to the square root of reported dielectric permittivity or to the reported volumetric water content. Model CS655 is shown to operate over a wider range of soils with better overall accuracy than model CS650.

NEW DEVELOPMENTS FORUM, ABSTRACT 3.7

New arrivals: the ALL-IN-ONE and Drill & Drop probes at Sentek

Dalton, M., Buss, P., Portmann, M. and Luca, J.

Sentek Pty. Ltd., 77 Magill Road, Stepney, Adelaide, South Australia, 5069, Australia.

ABSTRACT

Sentek has recently released two new capacitance probes to add to its product range: the ALL-IN-ONE™ and the Drill & Drop™. As the name suggests, the ALL-IN-ONE is a complete stand-alone probe solution (figure 1). It consists of a standard 56mm diameter probe with customisable configured sensors, a modem and a battery power source. Under normal operation the lithium-ion battery is projected to last 18 months before depletion. The probe is fully serviceable, access being gained from an above-ground screw top cap. Remote communications can be facilitated using a small mobile phone antenna or a standard 7 dB whip antenna placed on an adjacent pole for areas of lesser quality mobile phone coverage. Blue Tooth functionality allows for direct mobile phone access to the data and to facilitate probe configuration setup without wired connections.

The Drill & Drop probe is a revolutionary solid encapsulated probe of slim design (2.5cm – 3.0cm in diameter and either 60cm or 120cm in length) (figure 2). The probe itself has a sensor every 10cm starting from 5cm depth and is tapered from top to bottom. It is installed in minutes using a similarly tapered auger attached to an electric or unpowered drill. A rigid installation tripod is used to control the accuracy of the auger drilling. Minor air gaps in the soil are sealed by pushing the conical probe into the augered hole firmly. No slurry, which may cause preferential path flow, is required in most soil types. A 5m cable connects to a Sentek logger system or to a range of commercially available data loggers. The probe can be installed flush with the soil surface or buried at the required depth.

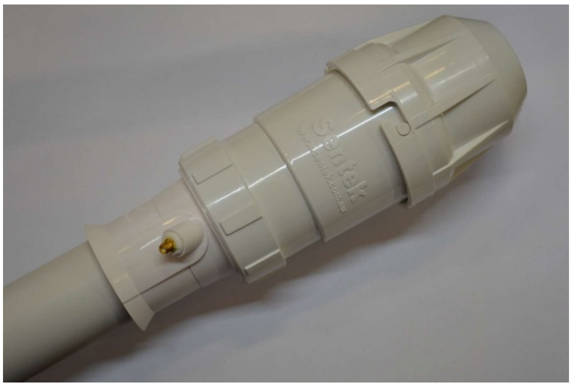

Figure 1: The ALL-IN-ONE probe.

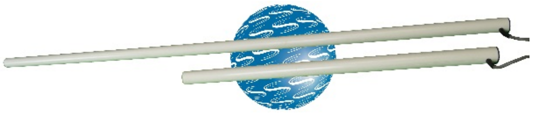

Figure 2: The Drill & Drop probe.

POSTER 4.1

Evaluation of Eight Electromagnetic Sensors for Measuring Water Content and Electrical Conductivity in Mineral, Organic, and Saline Soils

Carlos M. P. Vaz[1], Scott B. Jones[2], Mercer Meding[3] and Markus Tuller[3]

1 Embrapa Agricultural Instrumentation, São Carlos, 13560-970, P. O. Box 741, Brazil, carlos.vaz@embrapa.br

2 Department of Plants, Soils and Climate, Utah State University, Logan, UT 84322

3 The University of Arizona, Department of Soil, Water and Environmental Science, Tucson, AZ, 85721

ABSTRACT

In the present work the performance of eight commercially available electromagnetic (EM) sensors (TDR 100, CS616, Theta Probe, Hydra Probe, Wet-2, 5TE, SM300 and 10HS) are evaluated for different soil textures consisting of five mineral soils, one organic, and a mineral soil with high electrical conductivity (EC). The objective was to evaluate sensor performance under well-defined conditions in terms of soil water content (θ) and soil bulk electrical conductivity (EC_b), and to test the validity of factory supplied-calibration equations for θ. Results indicate that the factory-supplied calibration relationships for groups of mineral and organic soils, in general, were acceptable, but some inconsistences were identified and suggestions for improvements are presented. The performed experiments allowed the evaluation of several aspects of the factory-supplied calibration relationships such as goodness of fit and the influence of the soil properties on sensor response. Soil-specific calibrations from this study yielded accuracies of about 0.015 $m^3 m^{-3}$ for 10HS, SM300, and Theta Probe, while lower accuracies of about 0.025 $m^3 m^{-3}$ were found for TDR100, CS616, Wet2, 5TE and the Hydra Probe. In terms of EC_b the Hydra Probe, 5TE and Wet-2 sensors responded similarly to the TDR100. Good estimates were obtained for EC_b up to 2 dS m^{-1} with

best response for the Wet-2 (RMSD=0.11 dS m^{-1}), followed by the 5TE (RMSD=0.14 dS m^{-1}) and the Hydra Probe (RMSD=0.18 dS m^{-1}).

POSTER 4.2

Evaluation of EM Sensors Using Acetic Acid-Water Mixtures

Carlos M. P. Vaz[1], Scott Jones[2], and Markus Tuller[3]

1 Embrapa Agricultural Instrumentation, P.O. Box 741, São Carlos, SP, 13560-970, Brazil, carlos.vaz@embrapa.br

2 Department of Plants, Soils and Climate, Utah State University, Logan, UT 84322, USA

3 The University of Arizona, Department of Soil, Water and Environmental Science, Tucson, AZ, 85721, USA

ABSTRACT

Reference liquids and mixtures have been widely used to calibrate and evaluate electromagnetic (EM) soil moisture sensors. The main advantages of liquids, compared to other materials such as powders and granular media, are the intimate contact between probe and medium (absence of air gaps), excellent sample homogeneity, and the possibility to reproduce experiments in different laboratories utilizing essentially identical samples. It was previously proposed to use dioxane/water mixtures or 2-isoprooxyethanol/water mixtures as reference liquids. However, dioxane is highly volatile and a carcinogenic chemical and requires careful handling. Other water miscible liquids such as ethanol, methanol, propanol, butanol and isopropanol have also been used, pure or mixed with water, to calibrate different EM sensors. However, their relatively high dielectric permittivity only covers the wet range of soil moisture conditions. In this study, acetic acid/water mixtures were used to evaluate the response of EM sensors. Pure acetic acid (AcOH) exhibits a low dielectric constant ($\varepsilon = 6.2$) and electrical conductivity close to zero. As acetic acid is diluted with water ($\varepsilon = 80$), the dielectric permittivity of the mixture (ε_{mix}) increases, producing equivalent permittivity of porous medium ranging from dry to saturation. Measurements were conducted with 8 commercially available EM sensors (i.e. CS616, Acclima, TDT, Hydra Probe, Theta Probe, SM200, 5TE and TDR100) and dielectric mixtures, ranging from pure acidic acid to pure deionized water. Results are discussed in terms of sensor output and dielectric constant measured with the TDR100 as reference. For ε_{mix} up to about 40 (70% AcOH) sensor output increases linearly with ε_{mix}, but for ε_{mix} higher than 40 and mainly close to 80, a singular behavior is observed (a limiting response and a sharp decrease) for sensors CS616, 5TE, SM200 and Theta Probe. Frequency dependent permittivity measurements of AcOH/water mixtures showed relaxation effects for frequencies at same order of the operating frequencies of some EM sensors tested, limiting its use for calibration of some EM sensors. However, due to the complex relaxing and conducting behavior such AcOH/water mixtures provide interesting media for testing equivalent conducting or non-conducting and relaxing and non-relaxing soil media, depending on the operating frequency of each EM sensor.

POSTER 4.3

A New Calibration Equation for Diviner2000 Capacitance Probe Accounting for Soil Shrinkage Characteristic Curve and Estimation of Parameters on the Basis of Soil Physical Properties

Giovanni Rallo[1], Giuseppe Provenzano[1], Ioan Caton Paltineanu[2]

1. Dipartimento Scienze Agrarie e Forestali, Università degli Studi di Palermo, Viale delle Scienze 12, 90128 Palermo, Italy. Corresponding Author: giovanni.rallo@unipa.it

2. PALTIN International Inc., 6309 Sandy St., Laurel, Maryland 20707, USA.

ABSTRACT

Real-time measurements of soil water status are quite often used for irrigation scheduling and particularly in precision irrigation, in order to identify the exact timing and amount to supply to crops according to their water requirements.

Diviner2000 capacitance probes, measuring the apparent soil dielectric permittivity, have been extensively used in the last decade. Several studies have shown that, for different soils, there is a relationship between the volumetric soil water content (θv) and the scaled frequency (*SF*) measured by the sensor.

However, for swelling/shrinking clay soils, for which bulk density changes with soil water content, there is a lack of knowledge on how these variations influences the soil apparent dielectric permittivity and therefore the sensor calibration relationship, as a consequence of different contributions that soil solids, water and air, have on the *SF*. These contributions can be quantified on the basis of the so-called soil shrinkage characteristic curve, representing the relationship between the soil bulk density (ρ_b) or specific volume (ν) and the gravimetric water content *(U)*.

The main objectives of this research are i) to propose a new calibration equation for Diviner2000 capacitance probe, taking into consideration the soil shrinkage characteristic curve as well as ii) to suggest an indirect procedure to estimate the parameters of the sensor calibration relationship by means of easily-measurable soil physical properties.

Experiments were carried out at the University of Palermo, Italy, on nine different soils collected in agricultural area of SW Sicily for which, the textural analysis showed that the clay content ranged between 9% and 45%. Soil samples were sieved and compacted, using a standard method and a Proctor hammer, in containers (25 cm diameter and 25 cm height), to reach two different bulk densities (ρ_{b_min}, ρ_{b_max}). The soil shrinkage characteristic curve, $\rho_b(U)$, and the *U(SF)* relationships were contextually determined during a drying process, in order to develop a new model, represented by an implicit $U(SF,\rho_b(U))$ function. In order to validate the proposed model, the same procedure was used for undisturbed soil monoliths having identical dimensions of the sieved soil samples.

Considering that the calibration equation parameters were recognized to depend only on the soil clay percentage, new empirical relationships for their indirect estimation were proposed and then validated on the basis of the independent measurements obtained on undisturbed soil samples, as well as by considering other experimental data collected in the published literature.

POSTER 4.4

Design and Application of Frozen Soil Depth Sensor

Ye Linmao[1], Wang Yanbin[2], Niu Sujun[2], Zhang Guangzhou[1], Chen Tao[2], Chen Haibo[1], Li Peng[2], Jiang Shan[1], Shi Likui[1]

1. Henan Institute of Meteorological Science /Key Laboratory of Agrometeorological Safeguard and Applied Technique, CMA, Zhengzhou 450003, China; 2. Zhongyuan Photoelectric Control Technology Company, Zhengzhou 450045, China

ABSTRACT

Frozen and unfrozen soils are significantly different in dielectric coefficient, temperature and other physical parameters. In the measurement of frozen soil depth, a temperature and soil dielectric sensor (normalized frequency) were combined to form a automatic frozen soil depth sensor utilizing the temperature-dielectric coefficient method. We have developed and evaluated prototypes and established three automatic observation stations of frozen soil depth. The accuracy of this approach was determined from manual frozen soil depth measurements compared to the reported prototype frozen soil depth measurements. The correlation coefficient of sensor and manual measurements is above 0.99, with a mean absolute error below 2.5 cm. The instrument can continuously and automatically observe the freezing and thawing conditions of frozen soils, the ground temperature and the water content in soils. The instrument can meet the technical requirements of frozen soil depth measurement and can replace manual observation of frozen soil depth.

Key words: Frozen Soil, Capacitance Sensor, Soil Water Content

POSTER 4.5

The Design and Application of an Automatic Soil Water Monitoring System in Henan Province

Zhang Guangzhou[1], Wang Yanbin[2], Ye Linmao[1], Niu Sujun[2], Chen Haibo[1], Li Peng[2], Shi Likui[1]

1. Henan Institute of Meteorological Science /Key Laboratory of Agrometeorological Safeguard and Applied Technique, CMA, Zhengzhou 450003, China; 2. Zhongyuan Photoelectric Control Technology Company, Zhengzhou 450045, China.

ABSTRACT

The automatic soil water monitoring system is composed of three parts, namely, the automatic soil water stations, central server, and the Soil Water Analysis and Processing Software (SWAPS). Each station is equipped with a GStar-I type soil water meter based on the Frequency Domain Reflection (FDR) principle and carries out data collection, coding, and sending data through the GPRS (General Packet Radio Service) wireless network to the central server. To minimize measurement error of the soil water sensor and meet operational requirements for accuracy, a FDR-based "four-step calibration" process for soil water observation is established. The calibration includes factory calibration, field calibration, running calibration, and operation calibration via acquiring instrument calibration parameters of different soil textures from a large number of experiments.

The central server software obtains soil water data from the automatic observatory stations. It collects and unpacks data, checks format, processes, performs quality control checks, as well as standardizing warehousing data.. Data backup, and hence data safety is completed by the data storage management modules according to time strategies..

The Soil Water Analysis and Processing Software can visually browse the automatic soil water database. It can access the real-time or historical soil water information on the central database via the Henan Meteorological Bureau broadband network and visually show the status of soil water distribution according to drought/flood classification standards. Thereby, one can acquire information and analyze soil water changes in the province in real-time, so as to provide a means for the agro-meteorology personnel to access current and historical conditions.

Key words: Soil Water, Monitoring System, FDR, Calibration

LIST OF PARTICIPANTS

Australia:

Mr. Michael Dalton
Sentek Sensor Technologies
Stepney, SA 5069, Australia
mdalton@sentek.com.au

Brazil:

Dr. Carlos M. P. Vaz**,**
Embrapa Agricultural Instrumentation
São Carlos, Brazil
carlos.vaz@embrapa.br

Canada:

Dr. Chandra A. Madramootoo
James McGill Professor and Dean
Faculty of Agricultural and Environmental Sciences
McGill University
Macdonald Campus
Sainte-Anne-de-Bellevue Quebec, Canada
chandra.madramootoo@mcgill.ca

Mr. Eduardo Ganem Cuenca
Project Manager
McGill University
Faculty of Agricultural and Environmental Sciences
Sainte-Anne-de-Bellevue, Quebec, Canada
eduardo.ganemcuenca@mcgill.ca

Ms. Maria Mastorakos, Ph.D.
Graduate Student
Bioresource Engineering Department
McGill University
Macdonald Campus
Sainte-Anne-de-Bellevue Quebec, Canada
maria.mastorakos@mail.mcgill.ca

Mr. René Parisé
Vp Ventes et Marketing
GENEQ Inc.
Montréal, (Québec), H1J 1S5, Canada
rparise@geneq.com

China:

Dr. Linmao Ye
Henan Institute of Meteorological Science /Key Laboratory of Agrometeorological Safeguard and Applied Technique, CMA
Zhengzhou 450003, China
yjx819@163.com

Mr. Guangzhou Zhang
Henan Institute of Meteorological Science /Key Laboratory of Agrometeorological Safeguard and Applied Technique, CMA,
Zhengzhou 450003, China
hnzgz@163.com

Mr. Yanbin Wang
Zhongyuan Photoelectric Control Technology Company
Zhengzhou 450045, China
wngynbn@sohu.com

Mr. Sujun Niu,
Zhongyuan Photoelectric Control Technology Company
Zhengzhou 450045, China
nsjun@qq.com

France:

Dr. Arnaud Mialon CESBIO
Toulouse, France
arnaud.mialon@cesbio.cnes.fr

Dr. Simone Bircher
Centre d’Etudes Spatiales de la Biosphère
Toulouse, France
birchers@cesbio.cnes.fr

USA:

Dr. Ioan C. Paltineanu
President, PALTIN International Inc.
Laurel, Maryland, USA
ioan@paltin.com

Dr. Jeffrey E. Campbell
Senior Vice President
Sensor Development
UgMO Technologies
King of Prussia, PA, USA
jcampbell@ugmo.com

Mr. Tom Penning
President
IRROMETER Company Inc.
Riverside, CA 92507-1600, USA
tomp@irrometer.com

Dr. Nathaniel Hager III
President and PI
Material Sensing and Instrumentation
Lancaster, PA, USA
nehager@msi-sensing.com

Mr. Brad Rathje
Manager AquaCheck USA
Perry, IA, USA
brad.rathje@vanwall.com

Mr. Stephen P. Farrington
Chief Scientist
Transcend Engineering and Technlogy LLC
Gaysville, VT, USA
SFARRINGTON@TRANSCENDEV.COM

Dr. Jason Ritter
Soil Scientist
Research Department
Campbell Scientific Inc.
Logan, Utah, USA
jritter@campbellsci.com

Mr. Keith Bellingham
Soil Scientist
Stevens Water Monitoring Systems
Portland, OR, USA
kbellingham@stevenswater.com

Mr. Michael Swanson
Project Manager-Soil & Nutrient Mgmt
Spectrum Technologies, Inc.
Aurora, IL, 60504 USA

Mr. Nabil Mohamed
Water and Energy Resource Engineer
GreenWood Resources BTF,
Boardman, Oregon, USA
nabil.mohamed@gwrglobal.com,

Dr. Leonardo D. Rivera
Decagon Devices, Inc.
Pullman, WA 99163, USA
leo@decagon.com